Uncertainty modeling of thermoluminescence glow curve and development of deconvolution technique to resolve TL peak

By
Manish K. Sahai

PHYS01201604010

Bhabha Atomic Research Centre, Mumbai

A thesis submitted to the

Board of Studies in Physical Sciences

In partial fulfillment of requirements

for the Degree of

DOCTOR OF PHILOSOPHY

of

HOMI BHABHA NATIONAL INSTITUTE

February 2021

Homi Bhabha National Institute[1]

Recommendations of the Viva Voce Committee

As members of the Viva Voce Committee, we certify that we have read the dissertation prepared by Manish Kumar Sahai entitled 'Uncertainty modeling of thermoluminescence glow curve and development of deconvolution technique to resolve TL peak' and recommend that it may be accepted as fulfilling the thesis requirement for the award of Degree of Doctor of Philosophy.

Chairman – Dr. Saibal Basu	5/2/2021
Guide / Convener – Dr. D. Datta	ddatta 5/2/2021
Co-guide - Name & Signature with date (if any)	No Co-guide
Examiner - Dr. Rashmi Bhardwaj	Rbhardwaj 5/2/2021
Member 1- Dr. D. K. Koul	5/2/2021
Member 2- Dr. Indranil Mukhopadhyay	05/02/2021
Member 3- Dr. Devesh Mishra	05/2/2021.

Final approval and acceptance of this thesis is contingent upon the candidate's submission of the final copies of the thesis to HBNI.

I/We hereby certify that I/we have read this thesis prepared under my/our direction and recommend that it may be accepted as fulfilling the thesis requirement.

Date: 5/2/2021

Place: Mumbai

	ddatta
Signature	**Signature**
Co-guide (if any)	**Guide**

---

[1] This page is to be included only for final submission after successful completion of viva voce.

STATEMENT BY AUTHOR

This dissertation has been submitted in partial fulfillment of requirements for an advanced degree at Homi Bhabha National Institute (HBNI) and is deposited in the Library to be made available to borrowers under rules of the HBNI.

Brief quotations from this dissertation are allowable without special permission, provided that accurate acknowledgement of source is made. Requests for permission for extended quotation from or reproduction of this manuscript in whole or in part may be granted by the Competent Authority of HBNI when in his or her judgment the proposed use of the material is in the interests of scholarship. In all other instances, however, permission must be obtained from the author.

MSahai

(Manish K. Sahai)

DECLARATION

I, hereby declare that the investigation presented in the thesis has been carried out by me. The work is original and has not been submitted earlier as a whole or in part for a degree / diploma at this or any other Institution / University.

Msahai

(Manish K. Sahai)

List of Publications arising from the thesis

Journal

1. Study of Residual TL of CaSO4: Dy based Thermoluminescence Dosemeter, Manish K. Sahai, S. M. Pradhan, A. K. Bakshi and D. Datta *Radiation Protection Dosimetry*, 177 (2017) 342.

2. Revisit to power law decay of luminescence, Manish K. Sahai, A. K. Bakshi and D. Datta, *Journal of Luminescence* 195 (2018) 240

3. Anomalous fading correction for dosimetry at small time scales, *Radiation Physics and Chemistry*, Manish K. Sahai, A. K. Bakshi and D. Datta, 158 (2019) 137

Conferences

1. Relative contribution of various traps to residual TL in $CaSO_4$:Dy based dosimeter using hot gas TLD badge reader, Manish K. Sahai, A. K. Bakshi, C. Sneha and D. Datta, 21st National Symposium on Radiation Physics (NSRP-21) held at RRCAT Indore, MP, India during 5-7 March, 2018.

2. How uncertainty goes with order of kinetics of thermoluminescence, Manish K. Sahai. C. Sneha, A. K. Bakshi and D. Datta, 6th International Conference on luminescence and its applications (ICLA-2019) held at Raipur, Chhattisgarh, India during 7-10 January, 2019.

Msahai

(Manish K. Sahai)

To my Teachers and my family

ACKNOWLEDGEMENTS

It has taken years of hard work and sincere effort to develop the contents of this dissertation. Finally, I am putting together my ideas and achievements in this thesis. Many people have given their efforts and encouragement during this journey. Hence, I take the opportunity to express my gratitude to all of them.

To begin with, I am thankful to my guide Dr. D. Datta for his wonderful ideas and concepts he gave me during the period of my work. Many a times his capability of connecting different subjects and his ability of reproducing concepts at any point of time really mesmerized me. I am also thankful for the freedom he gave me to pursue my ideas. Interactions with him have always given new directions to the work.

I am fortunate to have my chairman, Dr. S. Basu, committee members Dr. D. K. Koul, Dr. D. R. Mishra, Dr. I. Mukhopadhyay and my technical advisor Shri S. M. Pradhan, who gave their valuable time as and when required for gathering for review of work during various meetings of Doctoral Committee. Their constructive and valuable suggestions have given this thesis the shape it has.

I am greatly indebted to Prof. S. Mukhopadhyay, Shri N. N. Mishra and Shri K. Soni for wonderful discussions whenever I visited IIT Mumbai.

I am also thankful to my section head Dr. A. K. Bakshi, who continuously helped in development of the manuscripts. Discussions with Shri. M. S. Pathan and Dr. G. S. Sahoo were always enlightening.

And finally I would like to express my gratitude to my mother and wife for their support and encouragement during this long journey. Last but not the least I would like to show my love to my daughter, Lavanya, for the refreshing moments she added to stressful Ph. D life.

CONTENTS

Page No.

SUMMARY i

LIST OF FIGURES iii

LIST OF TABLES ix

ABEREVIATIONS xi

SYMBOLS xiii

CHAPTER I. INTRODUCTION

1.1 Preamble 1

1.2 Introduction 2

1.3 Basic Terminology used in TL phenomenon 3

1.4 Few applications of thermoluminescence 8

1.5 Phosphor important for PMS in India: $CaSO_4$: Dy 12

1.6 Computerized glow curve deconvolution 17

  1.6.1 Need of deconvolution 17

  1.6.2 Basics of deconvolution (Mathematical background) 21

  1.6.3 Conclusions 24

  1.6.4 Chronological Development of Computational techniques in deconvolution 25

  1.6.5 Few Recent Contributions 27

1.7 A brief note on athermal fading 30

1.8 Research objective and gap areas 32

1.9 Organisation of thesis 33

1.10 Scope of thesis 37

1.11 Milestones in thesis period 38

CHAPTER II. Basic TL models and estimation of glow curve

2.1 Traditional Approach 41

 2.1.1 Rate equations 41

 2.1.2 Quasi equilibrium condition 43

 2.1.3 First order kinetics 44

 2.1.4 Second order kinetics 46

 2.1.5 General order kinetics 50

 2.1.6 Mixed order kinetics 52

 2.1.7 Some more realistic models 54

 2.1.8 Localised transition models 57

2.2 Master Equation Approach 60

 2.2.1 Analytical Solution of GOT / OTOR model 60

 2.2.2 Analytical Solution of mixed order kinetics (MOK) model 66

 2.2.3 Analytical Solution of NMTS model 68

 2.2.4 Analytical Solution of simple localized transition (SLT) model 70

 2.2.5 Analytical solution of Tunnelling localized transition (TLT) model 72

2.3 Conclusions 74

CHAPTER III. Deviations in TL intensity from model estimated glow curve: Sources of uncertainty

3.1 Fading 76

 3.1.1 Thermal fading 76

 3.1.2 Anomalous fading (or Athermal fading) 77

  3.1.2.1 Anomalous fading and power law decay 78

  3.1.2.2 Non linearity is general feature of after glow 89

 3.1.3 Thermally assisted fading 97

3.2 Finite life time in conduction band 97

3.3 NIK approximation 97

3.4 Temperature dependence of parameters 99

3.5 Uncertainty in parameters 100

3.6 Re absorption 100

3.7 Quenching effects 101

  3.7.1 Thermal quenching 101

  3.7.2 Concentration quenching 102

  3.7.3 Impurity quenching 103

3.8 Residual TL 103

3.9 Non linear response of TL dosimeter 110

3.10 Other factors 113

3.11 Conclusions 115

CHAPTER IV. Parametric uncertainty analysis of basic TL models

4.1 Monte Carlo (MC) approach for uncertainty propagation 117

  4.1.1 Algorithm for uncertainty propagation using MC 118

  4.1.2 Simulation results 120

    4.1.2.1 First order kinetics 121

    4.1.2.2 General order kinetics 127

  4.1.3 Discussions 130

4.2 Fuzzy set theory approach for uncertainty propagation 130

  4.2.1 Basics of Fuzzy set theory for uncertainty analysis 131

  4.2.2 Algorithm for estimation of uncertainty using α cut method 132

  4.2.3 Simulation Results 135

    4.2.3.1 First order kinetics 135

4.2.3.2 General order kinetics 137

4.2.4 Discussions 137

4.3 Polynomial Chaos Expansion (PCE) for uncertainty analysis 139

4.3.1 Basics of PCE 139

4.3.2 Algorithm for uncertainty propagation using PCE 139

4.3.3 Simulation results 141

4.3.3.1 First order kinetics 141

4.3.3.2 Second order kinetics 141

4.4 Conclusions 143

CHAPTER V. Deconvolution of TL glow curve

5.1 Conditional probability 145

5.2 Bayes' theorem 145

5.3 Posterior probability 145

5.4 Maximum likelihood 146

5.5 Expectation Maximization (EM) algorithm 147

5.6 Mathematical background of Mixture Model (MM) for deconvolution of TL glow curve 149

5.6.1 For Gaussian peaks 154

5.6.2 For first order kinetics peaks 155

5.6.3 For general order kinetics peaks 156

5.7 Algorithm for MM based CGCD 157

5.8 Validation with simulated glow curve 158

5.9 Deconvolution of experimental glow curve 165

5.10 Comparison with Synthetic glow curve of GLOCANIN Project 167

5.11 Advantage and disadvantage of MM based CGCD over other CGCD techniques 169

5.12 Conclusions 169

CHAPTER VI. Summary and future plans 171

References 180

LIST OF FIGURES

Figure 1.1 $CaSO_4$: Dy glow curve [Souza et. al., 1993]

Figure 2.1 Schematic diagram for rate equations assuming only electron to be freed by the thermal stimulus.

Figure 2.2 Electron transition involving localised energy levels.

Figure3.1 Illustration of wave functions and boundaries

Figure 3.2 Shape of potential barrier in region II.

Figure 3.3 Z of equation (3.19) as a function of radial distance (A) for different potential barrier shape and (B) for different time.

Figure 3.4 Log (I) with Log (st) for different values of recombination center concentration

Figure 3.5 Log(I) vs log (st) graph with change in potential barrier shape

Figure 3.6 (A) Normalized plot of time dependent (G_2) and time independent (G_1) component of Z. (B) Normalized plot of Z for shown value of G_1 and G_2.

Figure 3.7 Temporal behaviors of the components of integrand Z

Figure 3.8 Effect of starting time of observation on log (I) vs. log (st) curve for two values of times.

Figure 3.9 Effect of observation period on curvature of log(I) vs log(st) graph. Initial time of observation is 1 milliseconds

Figure 3.10 Effect of recombination centre concentration on advent of non linearity

Figure 3.11 Effect of shape of potential barrier on advent of non linearity.

Figure 3.12 Log (I) vs log(st) graph for different RC concentrations. The curve are fitted with $y = -p_3x^2 + p_4x + p_5$

Figure 3.13 Log(I) vs log(st) graph with different RC concentrations (same as figure 3.12) fitted to $(x - p_6)^2 + (y - p_7)^2 = {p_8}^2$

Figure 3.14 Experimental first, second read out glow curves and hot gas temperature profile.

Figure 3.15 Characteristic shape differences in first and second readouts for same dose

Figure 3.16 Simulated temperature profile of disc and experimental hot gas temperature profile.

Figure 3.17 First readout glow curve from different types of traps. Overall TL (a) is a summation of TL from shallow (b), dosemetric (c) and deeper (d, e) traps.

Figure 3.18 Experimental first (a), second (b) readouts and simulated (c) and second (d) readouts.

Figure 4.1 Algorithm for uncertainty propagation using MC technique

Figure 4.2 Optimisation of sample size

Figure 4.3 Output thermoluminescence intensity with its 1σ values on both side.

Figure 4.4 Positive and negative residue as a function of temperature for first order kinetics (RW model) of thermoluminescence

Figure 4.5 CDFs for mentioned values of temperature for first order kinetics of thermoluminescence.

Figure 4.6 2.5th and 97.5th percentile plot for half range of temperature

Figure 4.7 Glow curve for two certain (σ_D=0.0) values of trap depth (D).

Figure 4.8 Modulus of differentiation of themoluminescence (TL) output as a function of temperature.

Figure 4.9 Positive and negative residue as a function of temperature for b=2

Figure 4.10 Positive and negative residue as a function of temperature for b=1.8.

Figure 4.11 The CDFs for mentioned values of temperature for b=2 of general order kinetics

Figure 4.12 CDFs at five representative temperatures for b=1.8 of general order kinetics

Figure 4.13 Triangular membership function

Figure 4.14 Flow chart of α cut method for estimating uncertainty profile of single TL peak.

Figure 4.15 Triangular membership function is best approximation of Gaussian PDF

Figure 4.16 Triangular membership function is a reasonable approximation for trap parameters.

Figure 4.17 Membership function graph of output TL intensity at T=500 °K for 1st order kinetics.

Figure 4.18 DOU with temperature for full range of temperature under consideration for 1st order kinetics.

Figure 4.19 Membership function graph of output TL intensity at T=500 °K for general order kinetics at b=1.8.

Figure 4.20 DOU with temperature for full range of temperature under consideration for general order kinetics with b=1.8.

Figure 4.21 CDFs at five representative temperatures generated using PCE for first order kinetics model.

Figure 4.22 CDFs at five representative temperatures generated using PCE for second order kinetics model.

Figure 5.1 Convolved glow curve which is to be deconvolved using MM formalism.

Figure 5.2 Plot of equation (5.53) with its independent variable i.e. trap depth for the three types of traps considered

Figure 5.3 Figure show variation of 2nd derivative of convolved glow curve data with variation in temperature

Figure 5.4 Deconvolution process at different iteration steps.

Figure5.5 Original convolved graph (1), deconvolved glow peaks (2,3,4) and superposition of the deconvolved glow peaks (5) at concluding iteration step

Figure 5.6 Figure of merit (FOM) during the iteration process

Figure 5.7 Experimental glow curve of $CaSO_4$: Dy for a dose of 3.00 gray and heating rate of 1 °K/sec [Souza et. al., 1993].

Figure 5.8 The deconvoluted graph of Figure 5.7 glow curve

Figure 5.9 Deconvolution of Ref glow curve 002 of GLOCANIN Project

Figure 5.10 FOM with iteration step for Ref glow curve 002 of GLOCANIN Project

LIST OF TABLES

Table1.1 Trap parameters of CaSO4: Dy [Oliveri, 1978]

Table 1.2 Trap parameters for CaSO4: Dy [Souza et al., 1993]

Table 1.3 Chronological Development of Computational techniques in deconvolution

Table 3.1 Location and height of integrand of equation (3.19) with changing shape of NRPB

Table 3.2 Location and height of Integrand of equation (3.19) at different times for a fixed shape of NRPB.

Table 3.3 Slopes for different values of RC concentration for curves of Figure 3.4.

Table 3.4 Slopes for different shape parameters for curves of Figure 3.5.

Table 3.5 Fitting parameters for the curves of Figure 3.12 with $y = -p_3 x^2 + p_4 x + p_5$

Table 3.6 Fitting parameters for the curves of Figure 3.13 with $(x-p_6)^2+(y-p_7)^2={p_8}^2$

Table 3.7 Least square fitting error with various functions

Table 4.1 Mean value and standard deviation of PDFs of trap parameters

Table 5.1 Actual value of parameters trap depth (D), frequency factor (f), initial concentration (C_0) and values obtained from simulation for three trap types (indicated by subscript indices).

Table 5.2 Trap parameters obtained by MM algorithm for $CaSO_4$: Dy

Table 5.3 Comparision of FOM of our algorithm with result of Sature et al, 2017 and those of programs of GLOCANIN Project

CHAPTER I

Introduction

1.1 Preamble

It has always been a point of interest for us to probe the microscopic properties of matter. Many experimental tools have been developed with time for this purpose like diffraction of X-ray by the crystal (XRD), technique of scanning the surface by focussed beam of electrons (SEM), energy dispersive X-ray spectroscopy (EDXS) and many more. Thermoluminescence (TL) emission, which opens a window to look into defect generated trap centres for the charge carriers (electrons and holes), is also one of the techniques to probe microscopic properties of condensed matter.

TL is emitted by thermally exciting pre-irradiated sample. Activation of trap centres depends on the temperature range used to stimulate the sample. The characteristic of sample is investigated through analysing the glow curve which is superposition of TL emission from many stimulated trap centres inside the material. The TL emission from each type of trap centres has information regarding the characteristic parameters (termed as trap parameters) of the particular defect type. Hence, it is necessary to deconvolve the glow curve for investigating the trap parameters of a particular defect centre.

Numerical value of trap parameters of defect centres, found by any experimental or theoretical methodology, is always reported in literature with associated uncertainty. These trap parameters are model parameters of various models proposed for TL phenomenon. Hence, uncertainty in model parameters will propagate to final assessment end point of these models, i.e. TL emission. Hence, it is of interest to carry out the parametric uncertainty analysis of various models (like Randall Wilkins model, Garlick Gibson model and May

Partridge model) proposed for TL phenomenon. Propagation of error through theoretical models of TL phenomena due to variability of trap parameters will reveal insight on TL emission and associated glow curve.

In this research work, various aspects of deconvolution of TL glow curve, error propagation methodologies through theoretical models on TL emission phenomenon are explored.

1.2 Introduction

Thermoluminescence is the release of light from a pre irradiated sample due to thermal stimulation. In case of TL the source of energy is the excitation by an ionising radiation. This energy stored can be released whenever the material gets a stimulus. In the case of TL, the stimulus is heat. Hence, a more appropriately coined term can be thermally stimulated luminescence (TSL), more precisely. Heat is just an stimulating agent and not the source of energy released in form of luminescence. Hence, TL is radiation induced thermally stimulated emission of optical energy.

Further, it is necessary to distinguish between TL and incandescence emitted from material when heated. Incandescence emissivity has maxima where absortivity of the material under investigation is maximum. Whereas, mostly TL luminescence is in a temperature range where material is non absorbing. Though there are exceptions.

It is also important to differentiate between fluorescence and TL. This differentiation is made on the basis of characteristic life time (τ^*) between absorption of ionising radiation and emission of luminescence. If $\tau^* < 10^{-8}$ seconds, the phenomenon is known as fluorescence. Otherwise it is called phosphorescence. More importantly, the temperature dependence of phosphorescence is the fact that is practically used to differentiate between the two closely related phenomenon. If temperature is not fixed at a particular point, rather changes with any time dependent profile, the phenomenon is called TL. Normally used temperature profile is linear, where temperature increases linearly with time. This temperature profile is normally used as linear temperature profile stimulates various traps present in the material one by one, depending on their trap depths. So investigation of the material becomes easier. But other profiles are also in practice, like hyperbolic profile, which have their own benefits.

The phenomenon of TL is well documented by various authors [Nambi, 1977; Chen and Mckeever, 1997; Mckeever, 1983; Horowitz, 2000]. Handbook on TL [Furetta, 2003] provides compilation of terms in an alphabetical order. Hence, it is very useful for fluid consultation. Numerical approach towards various aspects of TL is given by Pagonis and co-authors [Pagonis et al, 2006]. There are exhaustive review articles by various authors on TL specific to materials like Calcium sulphate doped with rare earth materials ($CaSO_4$: RE) [Laxmanan, 1999]. There are review articles on deconvolution domain of TL [Horowitz and Yossian, 1995]. There is a recent review article by Kitis et al [Kitis et al, 2019] explaining stimulated phenomenon using Master equation. Recent article by Peng et al [Peng et al, 2021] is also worth mentioning. In addition to this there is a plethora of research articles on different domains of TL like phosphor synthesis, application of TL in various domains and many more. This list is growing at a very fast rate. References of research articles are not being given because it is next to impossible to give an exhaustive list because of very large number.

1.3 Basic Terminology used in TL phenomenon

In order to understand the applications of TL a basic knowledge of terminology used in explaining properties of TL phenomenon is required. Hence, brief note on it is given. Some of the terminologies used in discussing properties of TL materials are listed briefly under their respective headings.

Dose response

Ideally speaking there should be straight line graph between thermoluminescence output and dose. This behaviour is the ideal condition for quantifying the dose (dosimetry). Dosimeter can be calibrated at a given dose and the unknown dose can be found by comparing the TL responses at the calibration dose and unknown dose. However linearity is mostly exhibited by most of TL material at low doses. At high doses most of TL material show non linear effects in graph of TL output and dose imparted.

Though non linearity, in general, is not a very serious constrain to dosimetry. It is possible to have a calibration curve and dosimetry can be done with non linear response function as well.

Mathematical representation of response of TL material to imparted dose, response function or supralinearity index $\{\chi\ (d)\}$, is done in following way [Chen and Mckeever, 1994].

$$\chi\ (d) = \frac{(\zeta(d) - \zeta_0)/d}{(\zeta(d_l) - \zeta_0)/d_l} \tag{1.1}$$

$\zeta(d)$= TL intensity value at dose d.

$\zeta(d_l)$= TL intensity value at dose d_l.

d= Dose at which investigation is being done.

d_l= Dose at which linearity exist.

ζ_0= Intercept on TL axis, actually it is the response of dosimeter at zero dose.

The concept of linearity, sublinearity or supralinearity is defined by $\chi\ (d)$.

If $\chi\ (d)$= 1 then linearity persists at dose d

If $\chi\ (d) < 1$ then dosimeter has Sublinear response at dose d.

If $\chi\ (d) > 1$ then dosimeter has Supralinear response at dose d.

The main problem with dose response function is that it is not a function of dose only, rather it is a functional, i.e. the actual value of $\chi\ (d)$ not only depends on dose but also on thermal history, type and energy of radiation, heating methodology for exciting the sample, linear energy transfer (LET) of ionising field etc.

Hence a careful calibration process (considering radiation type, LET, energy response etc.) and proper annealing procedure is required to use TL material in dosimetric applications.

It is worth to mention at this point that dose response curve should be independent of dose rate effect. Though, the dose rate effect is not a serious problem for most of the phosphors.

In addition to sublinearity, supralinearity and linearity observed in TL vs. dose profile, dosimeters also exhibit a phenomenon of saturation. Saturation is a serious problem in high dose applications.

Sensitivity

Another important term is sensitivity. Sensitivity is thermoluminescence emission per unit absorbed dose. For dosimetry, sensitivity of the TL material should be sufficiently high (especially for low dose applications like personnel monitoring) so that TL emission can be detected properly and is not masked by background effects like instrumental noise etc.

There are difficulties in defining absolute sensitivity as TL output is affected by readout system, filters used and method of measurement (glow curve area between two temperatures / height of particular TL peak). Hence, a term is coined "relative sensitivity". Relative sensitivity {RS (d)} is defined by equation (1.2)

$$\mathrm{RS}\ (d) = \frac{[\zeta(d)]_{material}}{[\zeta(d)]_{TLD-100}} \tag{1.2}$$

where

$[\zeta(d)]_{material}$= TL intensity value at dose d for the material.

$[\zeta(d)]_{TLD-100}$= TL intensity value at dose d for TLD-100.

Since $\zeta(d)$ of material under investigation and TLD-100 will have different non linearity, $RS\,(d)$ will be dose dependent. TL dose response function is a functional of various parameters like LET of ionizing radiation, heating rate etc., as explained previously. Obviously, relative sensitivity will also be affected by all those factors.

Literature survey further reveals that there exists a term known as Minimum measurable dose (MMD) which is closely related to sensitivity. Hence, it is pertinent at this point to explain the difference between the two. MMD is defined for not only the material but for whole TL system, including material, sample shape, sample size, construction of badge, readout instrumentation, filters, algorithm and analysis routine.

Energy Response

Energy Response is defined as variation of TL intensity output with energy of incident radiation, for a given value of dose.

Energy response {ER(E)} for photons is defined as

$$\mathrm{ER(E)} = \frac{[\frac{\mu(E)}{\rho}]_{material}}{[\frac{\mu(E)}{\rho}]_{air}} \tag{1.3}$$

where

$\frac{\mu(E)}{\rho}$ = mass energy absorption coefficient

We should also define Relative energy response {RER (E)} of material. With respect to 1.25 MeV gamma radiation from ^{60}Co source it is defined by equation (1.4).

$$\mathrm{RER(E)} = \frac{ER\ (E)}{ER\ (1.25\ Mev\ )\ Co{-}60} \tag{1.4}$$

If RER(E) of TLD material coincides with RER(E) of human tissue, this is termed as tissue equivalence. It is important in applications like personnel monitoring and dosimetry in medical field. Since we are interested in dose delivered to human tissue and we assess it based on response of TLD material, if energy response of TLD material and human tissue are different the dose calculated from TLD material will not be correct estimation of dose delivered to human tissue. Hence tissue equivalent energy response of TLD material is important in such applications.

In this context an important term is effective atomic number Z_{eff}. It affects the energy absorbed by a material provided radiation is incident on the material. Z_{eff} of human tissue is 7.4.

For a higher value of Z_{eff} and lower energy of incident radiation, higher is the response of TLD material. This happens because energy loss in a material takes place by three mechanism, namely, photoelectric effect, Compton scattering and pair production. In general, they have following dependencies on Z_{eff}.

Photoelectric Effect: ${Z_{eff}}^3$

Compton Scattering: Z_{eff}/M, M is molar mass of material

Pair Production: ${Z_{eff}}^2$

Generally photo electric effect is dominant at low values of energy and pair production is dominant for energy greater than 1.02 MeV. Compton Scattering is dominant between these two.

Fading

Fading is loss of signal during storage. The stability of signal in the environment where it is stored and operated is an important parameter for the performance of dosimeter. The loss of signal may happen due to light (optical fading), environmental temperature (thermally assisted fading/ thermal fading) or due to pure tunnelling (anomalous fading). This topic has been dealt with in further section (section 1.7) and will be further discussed in chapter two and three.

1.4 Few applications of thermoluminescence

TL has very wide range of applications. Few will be discussed in brief. It is worth mentioning that the list is in no way exhaustive.

It was observed long back that few materials have high sensitivity, i.e. they have property of emitting TL signal on giving thermal stimulus if a small dose is previously given to the sample. For the range of applied dose relevant to applications like personnel monitoring etc., the TL signal is proportional to applied dose. As a result if a calibration curve is generated (between imparted dose and TL output), unknown doses can be estimated by measuring the TL signal and using the calibration curve. This property gave these materials due importance in dosimetry. The pioneers of the field are Watanabe [Watanabe, 1951], Daniels and colleagues [Daniels et al, 1953] and later Cameron and colleagues [Cameron and Kenney, 1963]. First book was published on the topic in 1968 [Cameron et al, 1968].

Personnel Monitoring

An important application based on TL phenomenon is Personnel Monitoring Service (PMS). International bodies like ICRP, IAEA and Indian regulatory body AERB give their recommendations based on their studies for maximum dose that can be given to a radiation worker due to his/her occupational exposure. Personnel monitoring is the task of continuously monitoring the radiation worker during his/her service period for the dose delivered to him/her due to his/her work. People working in hospitals (in radiation therapy/ diagnostics) like X ray technicians etc., radiation based research institutions like BARC, naval person on nuclear power vessel etc. constitute the work force of “radiation workers”. Two important properties a TLD material should have for being used as personnel monitoring dosimeter are: tissue equivalence (for correct estimation of dose to human body) and high sensitivity (as doses involved are very small in personnel monitoring most of the time).

Environmental Dosimetry

Other than cosmic rays (which may be important for air crew and astronauts) environmental dosimetry mainly concerns estimating dose due to radioactive material release to environment due to human intervention like nuclear power plants (NPPs) [eg. Brinck et al., 1977; Oatley, 1981]. An environmental dosimeter is placed in air to detect dose due to environmental radioactivity. The doses to be measured in environmental dosimetry are very small; hence the dosimeter has to have high sensitivity, least fading (thermal and optical), and robustness to environment (moisture and chemicals). High sensitivity is due to small doses. Least fading (optical and thermal) so that signal is not lost during the exposure time itself. This is important because dosimeters are exposed for a long periods of time to get measurable dose. Robustness to environmental factors like moisture is again important because of long exposure periods. Suspending dosimeters ~1m above ground level is a normal practise. Piesh suggests calibration and measurement procedures for environmental dose assessment using TLD [Piesh (1981)].

Space Dosimetry

With progress in space expeditions, space dosimetry is becoming an important application of TLD material. Space dosimetry has many aspects like monitoring of astronauts during their expeditions and stay in space, assessment of background radioactivity in space and exposure of electronic components to discrete radiation events. Single event upset i.e. interaction of single particle with electronic circuits is becoming a serious concern because main component of galactic radiation are high energy protons and Heavy Charge Particles (HCP). TLDs are used in space expeditions for some of these purposes [Vana et al., 1996].

Medical Dosimetry

TL has important application in medical field as well. It is possible only with thermoluminescence dosimeters to be inserted in human body, adjacent to the point of application of radiation, before exposure of patient to radiation during any course of diagnosis or therapy. These thermoluminescence dosimeters are further analysed to assess dose to internal organs. Further medical treatments are planned based on these results. Properties of TLD material important for these applications are tissue equivalence, high sensitivity, small size and non toxicity.

High Dose applications

High dose applications of radiation include irradiation of food stuff for better shelf life, sterilization of medical gadgets like syringes etc. TLD has also found applications in dosimetry of this domain. Since the doses involved are very high, there are various limitations like supralinearity and saturation of TLD material. Due to the same reason of very high doses, some researchers have suggested use of reduction in sensitivity (radiation damage) as the parameter for measurement of dose rather than TL output.

TL dating

TL dating is another application of TL phenomenon. Aitken [Aitken, 1985] is the father of the technique. This technique is estimation of age of archaeological and geological samples using TL. While the sample is buried in the soil it is irradiated by natural radioactive materials like Potassium, Thorium and Uranium which are present everywhere in at least ppm level. Since the flux of these is almost constant, the age of the sample can be calculated from the time since it was set on fire by the ancient man. Setting on fire sets the TL clock to zero. In this technique the sample under investigation is heated and TL is estimated. In second heating the signal consists of only IR. The extra TL output during first readout is induced due to radioactivity. Sample used for investigation using TL dating should have linear dependence on dose, low fading (thermal and optical), no effect of dose rate and sensitization effects should be negligible. If these qualities are not there they have to be somehow compensated for. If these effects are compensated in some way then we may have a formula for TL dating.

$$\text{Age} = \frac{Thermoluminescence\ output}{\frac{TL}{dose}\ X\ annual\ surrounding\ dose} \tag{1.5}$$

Other applications

There is long list of applications of TL phenomenon. TL has application in Biology and biochemisty [Tatake V. G., 1975; Altekar W. et al., 1975]. It has applications in forensic science [Chandrasekharan, 1975; Ingham and Lawson, 1973]. Geology is the earliest discipline where TL technique is being used in a variety of applications like identification of minerals, radioactive trace estimation in rocks and many more [McDougall, 1968]. In principle TL based methods can be employed in quality control in many glass, ceramic and semi conductor products. TL can also be used in study of defect characterisation, as it gives the value of trap parameters (D and f) and TL output can be directly correlated to defect centres. TL has applications in retrospective dosimetry as well.

1.5 Phosphor important for PMS in India: $CaSO_4$: Dy

There is a long list of phosphors that are of practical importance in different dosimetry applications. Few of them are Lithium Flouride based phosphors, Calcium Fluoride doped with Mn, Dy or Tm, Aluminium oxide based (Al_2O_3: Mg, Y and Al_2O_3: C) and Calcium sulphate doped with Dy or Tm.

With calcium sulphate as host there are mainly many variants of TLD material namely $CaSO_4$: Dy, $CaSO_4$: Tm etc. Since $CaSO_4$: Dy is used in Indian personnel monitoring program, focus will be on it.

$CaSO_4$: Dy

Calcium sulphate has numerous crystallographic locations at which defect centres may be located. As an example oxygen interstitial may be located in many configurations with slight difference in its local environment. As a result quasi continuous trap distributions may be found. ESR and optical absorption have suggested rich variety of radicals (SO_4^- ,SO_2^-,SO_3^-,O_3^- and O^-). This makes the material complex from perspective of TL phenomenon. But still $CaSO_4$: Dy is accepted as TLD material for personnel monitoring program of India because of following reasons.

1. Low cost.
2. TL sensitivity is 40-50 times higher that TLD-100.

3. Inertness to heat treatment below 700ºC, unlike TLD-100.
4. Very small fading after stabilization, i.e. after fading of low temperature peak.
5. Robustness to environmental conditions like moisture.

There is extensive literature existing on various aspects of $CaSO_4$: RE. These include studies on dose response [Nambi et al., 1974; Lakshmanan et al., 1978; Srivastava and Supe, 1979], kinetics [Fiorella et al., 1976], specific ionisation density [Shinde and Shastry, 1979; Srivastava and Supe, 1980; Lakshmanan et al., 1981; Srivastava et al., 1991], activator and its concentration [Ayyangar et al., 1974; Chandra and Bhatt, 1979], grain size [Lakshmanan et al., 1988; Shinde et al., 1988], irradiation and thermal history [Lakshmanan, 1982; Bhatt et al.,1988], codopents [Bhatt et al., 1996; Lakshmanan et al., 1986; Srivastava et al., 1992; Atone et al., 1993; Chandra et al., 1987], energy transfer process [Draaai and Blasse, 1974; Lapraz et al., 1996], emission spectra, OA and ESR [Tomita and Tsutsumi, 1978; Morgan and Stoebe, 1989; Nambi and Bapat, 1980; Mathews and Stoebe, 1982; Danby et al., 1982; Gundu et al, 1993], TSC/TSEE [Murthy 1982].

Mechanism

First mechanism of TL in $CaSO_4$: Dy was suggested by Nambi [Nambi et al., 1974]. In this mechanism during irradiation an electron is detached from F^- or SO_4^{2-} leaving a hole presence in them. This electron is trapped at RE^{3+} ion site and converts it to RE^{2+}. When heated these trapped electrons get detached from their sites and convert RE^{2+} to RE^{3+}, leaving them in excited state. The excited ion emits radiation to come to ground state. This emission is the TL emission. This idea can be expressed in following reactions.

During irradiation

$$RE^{3+} + \text{------} + F^{-} + \text{------} \longrightarrow RE^{2+} + \text{--------} + F^{o}$$

$$RE^{3+} + \text{------} + 2F^{-} + \text{------} \longrightarrow RE^{2+} + \text{--------} + F_2^{-}$$

etc.

During heating

$$\begin{tikzcd} RE^{2+} + \text{--------} + F^{o} + \text{-------} \arrow[r] & {[RE^{3+}]^{*} + \text{------} + F^{-} + \text{------}} \arrow[d, "TL"'] \\ & RE^{3+} \end{tikzcd}$$

$$\begin{tikzcd} RE^{2+} + \text{--------} + F_2^{-} + \text{-------} \arrow[r] & {[RE^{3+}]^{*} + \text{------} + 2F^{-} + \text{------}} \arrow[d, "TL"'] \\ & RE^{3+} \end{tikzcd}$$

etc.

But this mechanism has been criticized on various aspects [Stoebe and Morgan, 1984]. Another mechanism was suggested by Huzimura et al. [Huzimura et al., 1980]. Another mechanism was also suggested by Stoebe [Stoebe and Morgan, 1984].

Glow Curve

The $CaSO_4$: Dy glow curve structure is affected by the time after which glow curve is recorded since exposure, as the low temperature peaks fade. But after some time (say a week) glow curve becomes stable. Another factor is the dose at which glow curve is recorded, as on high temperature side new peaks evolve at high doses [Souza et. al., 1993].

Figure 1.1 represents the glow curve of $CaSO_4$: Dy at a delivered dose of 3.00 Gray and heating rate 1°Kelvin/second. A typical $CaSO_4$: Dy glow curve has a main dosimetric peak with small satellite peaks on both sides of main dosemetric peak. The main dosimetic peak is at 220°C in case of powder of $CaSO_4$: Dy and at 230°C in case of TLD discs are made out of phosphor by mixing them with Teflon binder in ratio of 1:3.

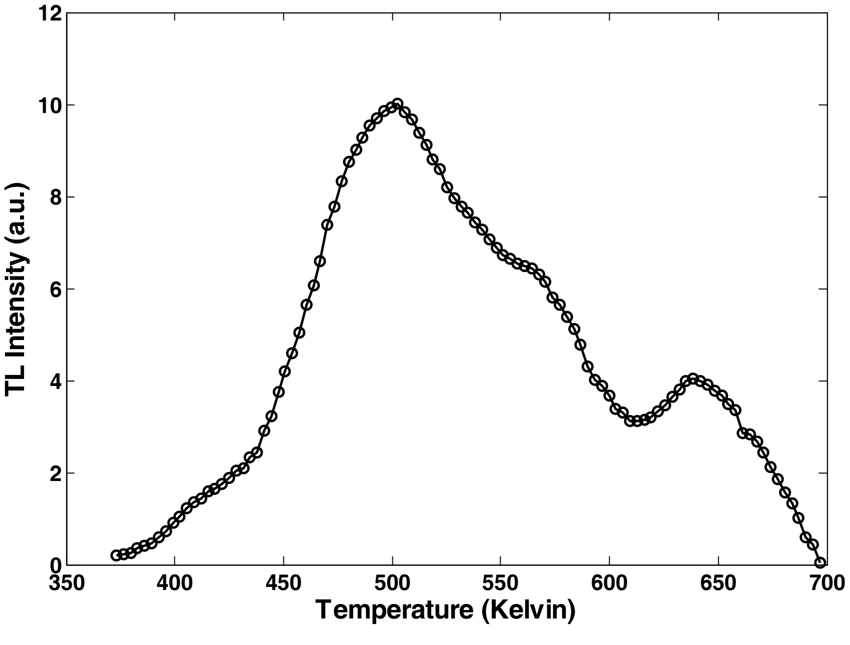

Figure 1.1 $CaSO_4$: Dy glow curve [Souza et. al., 1993]

Brief literature survey on Trap Parameters

Different authors have arrived at different set of model parameters for $CaSO_4$: Dy.

In one model [Fiorella et. al., 1976] it is proposed that results of experiments could be associated with an explanation by associating the main glow peak with more than one Gaussian distribution of trap depths with the mean values (D_j) and full width at half maxima (σ_j) as in Table 1.1.

Table1.1 Trap parameters of CaSO4: Dy [Oliveri, 1978]

No. of Gaussian	Mean energy value	σ_j
1	1.28 eV	0.033 eV
2	1.38 eV	0.043 eV
3	1.50 eV	0.025 eV
4	1.62 eV	0.021 eV

Attempt to escape frequency 3 X 10^{12} sec^{-1}.

Souza's model associates with glow curve of $CaSO_4$: Dy ten traps of trap depth and pre exponential factors as tabulated in Table 1.2.

Table 1.2 Trap parameters for CaSO4: Dy [Souza et al., 1993]

Peak No.	Tmax (°C)	D (eV)	f (sec^{-1})
1	128	1.15	2.3 X 10^{13}
2	143	1.25	1.2 X 10^{14}
3	170	1.16	1.2 X 10^{12}
4	198	1.09	2.6 X 10^{10}

5	222	1.10	8.3 X 10^{9}
6	248	1.22	3.6 X 10^{10}
7	274	0.98	4 X 10^{7}
8	306	1.19	9.2 X 10^{8}
9	360	1.70	1.7 X 10^{12}
10	387	1.47	7 X 109

Srivastava and Supe's model associates a quasi continous distribution of trap depths with a range of activation energy from 1.15 eV to 2.39 eV for a temperature range 340-740 °K with the glow curve of $CaSO_4$: Dy [Srivastava and Supe, 1983].

Dose response

The dose response of $CaSO_4$: Dy has straight line behaviour up to 30 Gy [Lakshmanan, 1999]

1.6 Computerized glow curve deconvolution

Deconvolution of TL glow curve using computational techniques is called computerized glow curve deconvolution (CGCD). For various reasons it becomes mandatory to deconvolute the signal into individual glow peaks. Few benefits are discussed below.

1.6.1 Need of deconvolution

Increment in precision and reducing MMD

Pla and Podgorsak followed by Moscovitch et al. and Horowitch et al. demonstrated deconvolution based dosimetry as an application of CGCD for TLD-100 [Pla and Podgorsak, 1983, Moscovitch et al., 1984; and Horowitch et al., 1986]. In this application, full blown deconvolution after subtracting the background signal is to be done and the dosemetric standards based on single peak (or a part of glow curve) are to be developed. This significantly reduces MMD and increases precision. This effect has also been examined by various authors on other TLD material like α Al_2O_3: C [Moscovitch et al., 1993] and CaF_2: Tm [Ben Shachar and Horowitz, 1988]. CGCD has also been applied to glow curve obtained from hot gas readers which have non linear heating profile [Van Dijk and Julius, 1993; Gomez Ros et al., 1993]. Gomez Ros et al. explored the possibility of applying CGCD to hot gas readers for improvement of precision and lowering of MMD [Gomez Ros et al., 1993]. Encouraging results were found. Recent work in domain of TL from hot gas reader has been done by Kitis et al [Kitis et al, 2006a6; Kitis et al, 2006b].

Dose re-estimation

CGCD has importance in dose re-estimation as well. Dose re estimation is of administrative importance; hence it has been extensively studied for TLD-100. PTTL technique of dose re-estimation is based on the fact that during normal readout the high temperature peaks are not fully depleted. When exposed to proper wavelength either at room temperature or at elevated temperature, transfer of charge takes place from high temperature peaks to dosimetrically important peaks. These peaks can be deconvolved using CGCD and dose re-estimation can be done using second readout of the dosimeter. Charles illustrated the use of 250nm radiation for this purpose in TLD-100 [Charles, 1983]. Many other authors have also studied the subject in detail [McKinlay et al., 1980; Budd et al., 1979]. Delgado et al. studied the subject with focus on application of CGCD and UV induced background [Delgado et al., 1992].

Estimation of elapsed time since irradiation

Time passed since an accidental exposure is important in planning medical treatment of a patient [ICRP, 1978]. It has also been claimed that estimation of time that has passed since exposure has importance in space experiments [Sidran, 1969]. Since different peaks have different fading rates, different peaks fade to different extent as a function of time. Hence, relative intensities of different peaks can be measured to estimate the time since exposure. Though it has complications, like

- Temperature profile of the place where TLD was stored after exposure should be known.
- Fading properties are dependent on dose.
- If the constant background exposure is over and above the accidental exposure, there would be further complications. This has been dealt with by Furetta [Furetta, 1988].
- Glow curve shape and estimated time may be affected by energy of irradiating radiation and presence of neutron.

Various authors have studied the topic in context of $CaSO_4$: Dy [Bacci et al., 1983; Wang et al., 1987], CaF_2: Tm and CaF_2: Dy [Furetta, 1988], TLD-100 [Moscovitch, 1986].

High Dose dosimetry

CGCD has importance in high dose dosimetry as well. Still the technology of high dose dosimetry is not saturated. Measuring doses of the range 10^2-10^6 Gray are needed in high dose applications like food processing, radiation sterilization and many others. Though few techniques have been developed to some extent [Holm and Berry, 1970; IAEA, 1973; Matthews, 1982]. But the techniques are costly and difficult. Barthe et al. have investigated several TLD material (Al_2O_3, $CaSO_4$: Dy, SiO_2: Ce, and YPO_4: C2) using various readers in this context [Barthe et al., 1993]. The supralinear dose response and complexity of high temperature peaks have made TLD-100 a low contender for high dose dosimetry. The biggest disadvantage on the side of TLD based techniques in context of high dose applications is radiation damage that occurs at high dose levels in TLD material.

Fading and sensitivity correction

Fading and sensitivity correction is an important application of CGCD, as many TLD materials like $CaSO_4$: Dy (used in personnel monitoring program of India) have low temperature peaks that fade rapidly. Fading is usually referred to leakage of charge from traps during the period of use or storage. This can have many reasons to it; like, interaction between occupied and unoccupied traps which may lead to sensitivity change. A separate problem is fading due to ambient temperature (thermally assisted fading/thermal fading). The problem and its various aspects is summarized in editorial [Horowitz, 1990]. Application of CGCD to this domain is an upcoming field, lot of work is being done and much more is required to be done.

Mixed field dosimetry

In most of the practised cases mixed field dosimetry is carried out without the use of CGCD. Ben Shachar and Horowitz studied the importance of CGCD to mixed field dosimetry [Ben Shachar and Horowitz, 1988]. Inaccurate separation of neutron sensitive peaks and gamma sensitive glow peaks is major source of error in mixed field dosimetry [Horowitz and Yossian, 1995].

Understanding mechanism of TL in TLD material

CGCD is necessary for understanding mechanism of TL in TLD material. Each TL peak has different origin in terms of defect centres from which they originate. Hence, obviously they will have different mechanisms. Unless we deconvolve the composite glow curve of TL material it is not possible to say anything about the origin and mechanism of TL in the material. So use of CGCD is vital in this context.

Other applications

There are other applications also like, optimizing annealing procedures and in quality control. They are not being discussed in detail, not because they are less important but because of time and space constrain. But they are discussed in detail in review article by Horowitz and Yossian [Horowitz and Yossian, 1995].

Because of above mentioned applications it is of interest to look into techniques of deconvolution which is elaborated further.

1.6.2 The basics of deconvolution (Mathematical background)

Glow curve is a function of trap parameters, trap depth (D), frequency factor (f) and initial concentration of charge carriers (C_{t0}). Alternatively it can be derived as a function of peak temperature (T_{max}), peak intensity (I_{max}) and width of peak (FWHM) or some other shape parameter.

Chi-square method

If the composite glow curve has r number of glow peaks then the number of unknown parameters will be $3r$. Since mostly, background is fitted by $l\exp(\frac{T}{m}) + n$, hence the number of known parameters become $3r + 3$. A chi-squared minimization, by defining a chi-squared merit function, can provide best fit values of parameters.

Let us assume M number of experimental data $\{x_i, y_i\}$ $i = 1, 2 \dots, M$ in a glow curve having r number of parameters.

Mathematically we have,

$$y = g\ (x, a_1, a_2, \dots, a_r) = g\ (x, \boldsymbol{a}) \qquad (1.6)$$

As per ordinary least square method , merit of system is addressed by the Chi-square merit function is defined by equation (1.7)

$$Q\ (\boldsymbol{a}) = \sum_{i=1}^{M}[\, y_i - g\ (x_i, \boldsymbol{a})]^2 \qquad (1.7)$$

In order to estimate the parameter set $\boldsymbol{a}$, the function $(Q\ (\boldsymbol{a}))$ can be differentiated with respect to $a_i \ \ i = 1, 2, \dots, M$ to obtain set of r differential equations.

$$\Psi_j\ (\boldsymbol{a}) = \sum_{i=1}^{M}[y_i - g\ (x_i, \boldsymbol{a})]\ \frac{\partial g\ (x_i, \boldsymbol{a})}{\partial a_j} = 0 \qquad j = 1,2, \dots, r \qquad (1.8)$$

Close to minima the condition given by equation (1.9) is obtained [Chen and Mckeever, 1997]

$$\partial a_k = [\frac{\partial \Psi_j(\boldsymbol{a})}{\partial a_k}]^{-1}\Psi_j\ (a) = H_{jk}^{-1}\ \Psi_j\ (\boldsymbol{a}) \qquad j = 1,2, \dots, r \qquad (1.9)$$

NRM & SGM

By differentiating $Q\ (\boldsymbol{a})$ with respect to $a_j\, j = 1, 2, \dots, r$ we arrive at a set of r non linear equations. This set of r non linear equations can be solved to get the correct value of parameter set $\boldsymbol{a}$**.** It is known that NRM for solving set of differential equations is suitable only if initial guess is close to optimal value.

On the other hand Chi-squared 'steepest decent method' known as SGM is preferred if initial guesses are far off. But it is limited by very slow convergence.

The merging of the two techniques is LMM. It gives excellent results.

LMM

The Marquardt method [Marquardt, 1963] is based on earlier suggestion from Levenberg [Levenberg, 1944]

A new parameter is defined

$$H'_{jk} = H_{jk} \quad j \neq k \tag{1.10}$$

$$H'_{jk} = H_{jk}(1 + \lambda) \quad j = k \tag{1.11}$$

Steps of algorithm of LMM is presented as follows

- Calculate $Q\ (\boldsymbol{a})$
- Initial guess λ=.001
- Calculate $\partial\mathbf{a}$ and $Q\ (\boldsymbol{a} + \partial\mathbf{a})$
- If $Q\ (\boldsymbol{a} + \partial\mathbf{a}) > Q\ (\boldsymbol{a})$ » $\lambda_{new} = 10\lambda_{old}$ and repeat with step 3
- If $Q\ (\boldsymbol{a} + \partial\mathbf{a}) < Q\ (\boldsymbol{a})$ » $\lambda_{new} = \frac{\lambda_{old}}{10}$ and replace $\boldsymbol{a}$ by $\boldsymbol{a} + \partial\mathbf{a}$

But the difficulty is that this method guarantees only convergence to local minima. Other methods like simulated annealing [van Laarhoven and Aarts, 1987] tabusearch [Glover, 1994] and genetic algorithm [Koza, 1992] are being tried in search of global minima.

In GLOCANIN [Bos et al., 1993] program in which a total of 13 CGCD codes were compared, LMM was the highest scorer.

FOM (Figure Of merit)

Finally it is required to define goodness of fit. FOM [Misra and Eddy, 1979] is a very good criteria.

$$\text{FOM}=\sum_{i_{Initial}}^{i_{Final}} \frac{100\ (|g\ (x_i, a^*) - y_i|)}{\text{⌂}} \tag{1.12}$$

Where

⌂= Area under the curve.

a^*= Fitted set of parameters.

y_i= Experimental data points

g= Function to which data points are to be fitted.

It is pertinent to mention at this point that for fitting purpose one has to generate the glow curve with desired set of parameters, in which differential equation is to be solved. For this purpose variety of numerical methods exists like Runge Kutta Method (RKM), Predictor Corrector Method (PCM) and Richardson extrapolation leading to Bolirsch Stoer Method (BSM) [Horowitz and Yossian, 1995].

1.6.3 Conclusions

Since last five decades non linear least square fitting methods for deconvolution are in use [Horowitz et al., 1986; Shenker and Chen, 1971; Mohan and Chen, (1970)] and is still in use, though solution of set of non linear equations is optimized to use of Marquardt Levenberg algorithm [Peng et al., 2016].

One important milestone in the domain of deconvolution is; Kitis [Kitis et al.,1998] converted equation of glow curve, which a function of trap parameters to a function of experimentally known parameters peak temperature (Tm), peak intensity (Im) and one more (shape) parameters. Many other such examples exist. A plethora of literature on glow curve deconvolution exists in literature [Furetta et al., 2000; Kitis, 2012; Gorkum, 1980; Pagonis et al., 2001; Harvey, 2011; Degado and Gomez Ros, 2001; Llamas and Tapia, 2013]. It is pertinent to mention at this point that above list is not exhaustive as amount of literature is very huge.

At one point of time there was an international inter comparison of various codes developed by different countries also took place [Bos et al, 1993; Bos et al, 1994]. There are detailed review articles on the topic [Horowitz and Yossian, 1995; Horowitz and Moscovitch, 2013].

But if we analyse all the literature in detail, attempts have been mainly in following directions.

- Developing new expressions for TL kinetics and fitting them with experimental glow curve like Sadek et al. [Sadek et al., 2015].
- Converting the parameters to experimentally known parameters like Kitis et al. [Kitis et al., 1998].
- Using rate equations for fitting an attempting reducing number of parameters like Sakurai [Sakurai, 1995].
- Increasing ease of execution and availability to community like Afouxenidis [Afouxenidis, 2012].
- New directions like use of genetic algorithm [Adamiec, 2006]
- Attempts in search of global minima; like simulated annealing [van Laarhoven and Aarts, 1987] and tabusearch [Glover, 1994]

It is worth mentioning at this point that the references given in above points are only for example and not exhaustive.

1.6.4 Chronological Development of Computational techniques in deconvolution

The chronological order of published or cited programs for TL glow curve deconvolution is provided by Peng et al [Peng et al, 2021].

Table 1.3 Chronological Development of Computational techniques in deconvolution

S. No.	Model/Expression	Platform	Reference
1.	First Order	---	Horowitz and Mosowitch (1986)
2.	First Order	---	Delgado and Gomez-Ros (1990,

			2001)
3.	First Order / General Order	---	Bos et al (1993, 1994)
4.	First Order	Window	Sprunck et al. (1996)
5.	First order/Second order/General order	MINUIT	Kities et al.(1998)
6.	First order	----	Gomez –Ros et al.(1999)
7.	Mixed order	MINUIT	Kitis and Gomez –Ros (2000)
8.	First order/Second order/General order	Peak-Fit	Pagonis and kitis (2002)
9.	First order/Second order/general order/mixed order/general approximation/Full iteration	Window XP/C#	Chung et.al (2005)
10.	First order	Window/C++	Puchalska and Bilski (2006)
11.	General Order	Window/Micrpsoft Excel	Van Dijk (2006)
12.	First Order	Window/Microsoft Excel	Chaseet.al. (2008)
13.	General Order/Mixed Order	Window/Microsoft Excel	Afouxenidis et.al (2012)
14.	First order/Second order/general order/mixed order/general approximation	Mathcad	Kiisk (2013)
15.	General Order	Peakfit	Singh et al.(2011)
16.	First Order	MATLAB	El-Hafezet.al. (2011)
17.	First Order	MATLAB	Harvey et.al. (2011)
18.	One Trap-one Recombination	Windows/visual Basic	Singh and Gartia (2014)
19.	General Order/ One Trap-one Recombination	Fortran, R	Peng et al.(2016)
20.	First order/Second order/general order	Fortran	Sature et.al. (2017)
21.	First order	Window/Microsoft Excel	Stadtmann and Wilding (2017)
22.	First Order/ General Order	Window/Microsoft Excel	Duran-Munozet.al. (2018)
23.	First Order/ General Order	Windows/Fortran,Visual Studio	Benavente et.al. (2019)
24.	One Trap-one Recombination	MATLAB	El-Kinaway et. al. (2019)
25.	General Order/Mixed Order	Window/Microsoft Excel	Kazakis (2019)

Few recent works are revolutionary in the domain so specific attention is being given to them in subsequent paragraph.

1.6.5 Few recent contributions

Using Lambert –W function

Section (2.2.1.1) may be referred to for detail discussion on analytical solution of OTOR model using Lambert –W function. Here the final transformed equations relevant for deconvolution is being documented.

Case I

$B = \frac{B_t}{B_{tr}} < 1$

Sadek et al. [2015] has done this transformation for first master equation from $L\ (C_{t0}, D, f, B, T)$ to $L\ (L_m, D, T_m, B, T)$ using the general procedure (as explained by Kitis et al. [2019])

The final expression is

$$L = L_m \exp(\frac{D\ (T-T_m)}{K\ T\ T_m})\ [\frac{W\ [e^{z1m}]+W\ [e^{z1m}]^2}{W\ [e^{z1}]+\ W\ [e^{z1}]^2} \qquad (1.13)$$

Where

$$z1 = \frac{1}{c} - \ln(c) + \frac{D \exp(\frac{D}{KT_m})}{K\ T_m^2}\ \frac{F\ (T,D)}{1-1.05\ B^{1.26}} \qquad (1.14)$$

Where $z1m = z1$ at $T = T_m$ and $F\ (T, D) = \int_{T0}^{T} \exp(-\frac{D}{KT})$

Case II

$B = \frac{B_t}{B_{tr}} > 1.$

It can be presented in a transformed form by using the procedure explained by Kitis et al. [2019]. The final result as developed by Sadek et al. [2015] is

$$L = L_m \exp(\frac{D\,(T-T_m)}{K\,T\,T_m})\ [\frac{W\,[-1,-e^{-z2m}]+W\,[-1,-e^{-z2m}]^2}{W\,[-1,-e^{-z2}]+W\,[-1,-e^{-z2}]^2} \qquad (1.15)$$

Where

$$z2 = \frac{1}{|c|} - \ln(|c|) + \frac{D\exp(\frac{D}{KT_m})}{K\,T_m^2}\ \frac{F\,(T,D)}{2.963-3.24\,B^{-0.74}} \qquad (1.16)$$

Where $z2m = z2$ at $T = T_m$ and $F\,(T,D) = \int_{T0}^{T} \exp(-\frac{D}{KT})$

The TL expression, equation (1.13) and equation (1.15) can be used for deconvolution of glow curve with linear heating profile. Fitting process can be performed using “Trust Region” algorithm of MATLAB package. The frequency factor may be obtained using the maxima condition [Kitis and Vlachos, 2013].

$$\frac{\beta D}{KT_m^2} = \left(\frac{1}{1-B}\,\frac{1+2W[\exp(z_m)]}{1+W[\exp(z_m)]^2}\right) fexp(-\frac{D}{KT_m}) \qquad (1.17)$$

The benefits of using these expressions for deconvolution are as follows.

1. The model has physical basis where as general order kinetics expressions are totally empirical.
2. The expression can fit any glow curve even if sample dose is in saturation range.

Contribution of Lovedy Singh et al (Hybrid Algorithm)

Lovedy Singh et al [Singh et al, 2014] has made a vital contribution to the domain of deconvolution by making use of hybrid genetic algorithm.

Set of coupled differential equation was proposed by Halperin and Braner [1960] for modeling of TL phenomenon. These are very difficult to solve and attempt to solve them is rather impractical. Due to this reason Lovedy Singh et al. introduced simplified version of

General One Trap (GOT) equation for glow curve derived from OTOR model. The expression covers first order kinetics for α=0.0001 and general order kinetics for α=0.99999.

The hybrid algorithm is a combination of genetic algorithm and simulated annealing. It is quite suitable for TL glow curve fitting as it is efficient and fast. In order to understand benefits of algorithm, short note on advantages and limitations of genetic algorithm and simulated annealing is given below.

Genetic algorithm has many advantages e.g.

1. It requires only evaluation of function values and not the derivatives of it.
2. It has higher probability of finding global minima.
3. It allows mix of continuous and discrete variables.
4. It provides a set of optimal solutions instead of single solution.

But it has a disadvantage that it slows down once the region of optimal solution is arrived. Simulated annealing [Kirkpatrick, 1983] based on analogy between statistical mechanics and combinatorial optimization. It is simply a technique of iterative improvement in which initial solution is repeatedly improved by making small local perturbation until no further improvement is found.

However it has some limitations, algorithm is almost a local optimizer and get and get trapped in the basin of attraction in which it begin if annealing temperature is reduced too quickly. If temperature is not lowered quickly enough computations become too time consuming.

Few other important contributions

Pagonis made use of Weibull distribution and Logistic distribution function for 1st and 2nd order kinetics respectively [Pagonis et al, 2001; Pagonis and Kitis, 2001]. He also explored possibilities of using commercial software packages for thermoluminescence glow curve analysis [Pagonis and Kitis, 2002]. His work on semi localized transition model is also worth mentioning [Pagonis, 2005].

R Package for deconvolution

A self consistent code of thermoluminescence glow curve deconvolution in R, namely “tgcd” package is developed [Peng et al, 2016; Peng et al. 2021]. This is an open source package in accordance with various transformed analytical equation of first, second and general order kinetics [Kitis, 1998], mixed order kinetics [Kitis and Gomez-Ros, 2000; Gomez-Ros and Kitis, 2002] as well semi analytic expression based on OTOR model utilizing Lambert –W function or Wright Omega function [Sadek et al, 2014; Sadek et al, 2015; Singh and Gartia, 2015]

The code is comprehensive, flexible, convenient and openly assessable.

1.7 A brief note on athermal fading

Till now the phenomenon of TL is presented where recombination of trapped charge carrier with respective recombination centre is routed through delocalized bands (conduction band and valence bands). In contrast to this tunneling of charge carrier from trapping sites to respective recombination centre may also be route of charge transfer. These are called tunneling localized model.

Halperin and Braner [1960] developed a model which is generally referred as localized recombination model for recombination via route of tunneling. Many authors [e.g. Land, 1969; Chen, 1976; Bull et al, 1989; Sunta et al, 2006; Pagonis 2005 etc.] have referred to this work in their respective works,

The mechanism of localized tunneling model has been employed to more involved models [e.g. Mandowski, 2005], where localized transition in a defect complex is combined with delocalized transition across complexes. Such models are referred to as semi localized models. Both models localized and semi localized transition models have been studied in detail by various authors [Chen and Mckeever, 1997; Kumar et al, 2006; Sunta et al, 2006].

All the above models consider a fixed tunneling probability. This is true if donor acceptor (d-a) distance is fixed, which is not always the case. In many cases power law decay is observed. Power law decay has been documented in many materials like feldspar [Visocekas et al, 1994], irradiated glasses [Kieffer et al, 1971], KCl [Delbecq et al, 1974] and several other materials.

Theoretical explanation has come from considering a distribution of donor acceptor distance instead of a fixed separation between donor and acceptor. This is theoretically addressed by few authors [Tachiya and Mazumdar, 1975; Huntley, 2006]. Their approach could explain only partial range of exponent of power law decay [i.e. slope of plot of ln(afterglow) vs. ln (st)] given in review article of Jonscher and Polignac [Jonscher and Polignac, 1984].

Recently Jain et al [2012] developed Halperin and Braner [1960] model further for material in which random distribution of defects exist. Nearest neighbor donor acceptor recombination and tunneling via the excited state of electron trapping centers are the features of models proposed by Jain et al [2012].

But none of above models considered the non rectangular shape of potential barrier between trap and recombination center. Due to above lacuna no one could explain full range of exponent of power law decay [Jonscher and Polignac, 1984]. This aspect is addressed in our publication presented in this dissertation and we could explain full range of exponent of power law decay given by Jonscher and Polignac [Jonscher and Polignac, 1984].

1.8 Research objectives and gap areas

As detailed before thermoluminescence (TL) is the phenomenon of emission of energy in optical form when thermal stimulus is given to a pre exposed sample. Charge carriers are generated due to irradiation and while translating in the material they get trapped at defect centres. When thermal stimulus is given they get excited to conduction band and further recombine with opposite charge carriers at recombination centres [Chen and Mckeever, 1997].

Hence, from the explained mechanism it is obvious that the overall signal obtained on giving thermal stimulus will be superposition of thermoluminescence signal emitted from various trapping sites. Thus, it is necessary to deconvolve the overall signal (glow curve) to infer any information regarding the defect centres.

Though, topic of deconvolution of TL glow curves has been investigated by a plethora of authors [Shenker and Chen, 1971; Mohan and Chen, 1970; Furetta et al, 2000; Horowitz and Moscovitch, 1986; Chung et al, 2012; Chung et al, 2007; Afouxenidis et al, 2012; Sakurai, 1995 and many more], mostly it boils down to a curve fitting procedure. Some authors have tried genetic algorithm as well for finding trap parameters [Adamiec, 2006].

But literature lacks any formulation which gives explicit algebraic expression for the trapping parameters. In present work an explicit expression for the trapping parameters (trap depth and frequency factor) is developed, which is to be solved iteratively.

Once the glow curve is deconvolved, the TL signal from each trap is obtained separately. There exist various model in literature for predicting the TL signal from a trap given its trap parameters like Randall Wilkins model [Randall and Wilkins, 1945a; Randall and Wilkins, 1945b], Garlick Gibson model [Garlick and Gibson 1948], May Partridge model [May and Partridge, 1964] and many more. But there also exist various sources (theoretical as well as experimental] that lead to deviation from a theoretically predicted glow curve from a set of trap parameters. Few of the many reasons may be instrumentation dependent effect (like dark current of PMT etc.), dosimeter dependent effects (like Residual TL etc.), and loss of signal during the storage i.e. fading. There are also field dependent effects (like angular incidence etc.) Residual TL which is left over TL after 1st readout is another factor. Most of these have got sufficient attention in existing literature. But origin of Residual signal was a gray area. This domain is investigated in our work [Sahai et al, 2017]. Fading has also got due attention experimentally, but its theoretical explanation is an area where addition is expected by present work [Sahai et al, 2018; Sahai et al, 2019].

As mentioned earlier various models have been developed to simulate TL glow curve from trap parameters. But parametric uncertainty analysis of these models is an area which is totally untouched. Hence, it has been our point of interest in present work with a focus on Randall Wilkins model [Randall and Wilkins, 1945a; Randall and Wilkins, 1945b], Garlick Gibson model [Garlick and Gibson 1948] and May Partridge model [May and Partridge, 1964].

1.9 Organisation of thesis

This dissertation is organised into six chapters. The brief context of each chapter is discussed here.

Chapter 1. Introduction

This chapter is dedicated to introduction and literature survey. It starts with discussing the basic phenomenon of TL.

Further, the applications of TL phenomenon are discussed. Main focus is on PMS, environmental monitoring, medical applications, TL dating and high dose applications.

Subsequently TL material important for personnel monitoring in Indian context namely, $CaSO_4$: Dy has been discussed. In this context its mechanism, typical glow curve and typical trap parameters are discussed.

Further the focus is on the deconvolution of the glow curves. In further section the necessity of deconvolution, its basics and literature survey on deconvolution is presented. Chronological order of development of deconvolution codes is presented, followed by some recent contributions.

One section is added on athermal fading.

Then the chapter concludes with motivation of study, organisation of thesis and scope of thesis.

Chapter 2. TL Models and estimation of glow curve

This chapter is divided into two subsections. Firstly, Traditional Approach to TL phenomenon and secondly, Master equation approach to stimulated phenomenon with focus on TL.

In first section, rate equations of TL kinetics are discussed and RW, GG and MP models are derived from the rate equation with suitable approximations like quasi equilibrium etc. Further, extensions of RW, GG and MP models under heading ‘more realistic delocalized models', are discussed. This chapter also includes mixed order kinetics model and localized transition models.

The later section discusses Five master equation for stimulated phenomenon with focus on TL.

Chapter 3. Deviations in TL intensiy from model estimated glow curve: Sources of Uncertainty

Various models like RW, GG and MP are presented in this chapter. Given the trap parameters the glow curve can be simulated using these models. But, there are various reasons due to which the experimental glow curves will deviate from the glow curves predicted by these models. This chapter is dedicated to this subject. Mainly the theoretical reasons are elaborated. This includes discussion on parametric uncertainty, quasi equilibrium approximation, non interactive kinetics, temperature dependence of parameters, fading, re-absorption, thermal and concentration quenching. *In this chapter our contribution in the domain of afterglow which is important for quantification of fading loss of TL signal is also presented*. Residual TL is the TL left over in the dosimeter after first readout. It is also a contributor to deviation from model predicted TL values. Theoretical explanation of origin of Residual TL did not exist in literature. *Hence, our contribution to origin of residual TL is also made a section of this chapter.* Non linear response of dosimeter is also discussed.

Chapter 4. Parametric Uncertainty analysis of basic Thermoluminescence Models

This chapter is dedicated to uncertainty in the TL emission intensity predicted by models like RW, GG and MP due to uncertainty in trap parameters (trap depth and attempt to escape frequency). Attempt to escape frequency is number of times trapped charge carrier attempts to escape from the trap per second. This chapter is divided into three sections based on the technique that is adopted for the uncertainty analysis.

First section is devoted to Monte Carlo technique. In this section assuming the probability density functions (PDFs) of input parameters, the PDF of output TL was generated and uncertainty (5th and 95th percentile difference) at a given temperature was obtained from the cumulative density function (CDF). Repeating this procedure for different temperatures within full range of temperature under consideration, the CDF's and uncertainty at different temperatures has been obtained.

Next section is based on fuzzy set theory. The membership function graph of output TL emission intensity is generated assuming the triangular membership function graph for input parameters at one temperature. From this membership function of TL intensity uncertainty was calculated. Repeating the process for different temperatures effect of temperature on uncertainty could be studied.

Last section is devoted to polynomial chaos technique. Based on this technique PDF (and corresponding CDF) of output TL is generated and corresponding visualization representing uncertainty is produced. Repetition at different temperatures in experimentally relevant range of temperature is done.

A manuscript has been communicated based on findings of this chapter.

Chapter 5. Deconvolution of TL glow curve

In this chapter after discussing the prerequisites like conditional probability, Baye's theorem, Posterior probability, Maximum likelihood estimation (MLE), and Expectation Maximization (EM), our algorithm developed for deconvolution is presented. Further we discuss mathematical aspects for following three cases.

1. Gaussian Glow peaks: In this case each individual TL peak is assumed to be Gaussian and corresponding values of the parameters, mean and standard deviation are calculated using EM algorithm.
2. First order peaks: Assuming each peak (normalised with respect to area) to be of first order kinetics, there are two parameters in the expression of TL intensity predicted by RW model, trap depth and pre exponential factor. These are related by a formula which involves peak temperature and heating rate. Pre exponential factor has been eliminated from RW equation using the mentioned formula. Hence, a TL intensity equation in only one variable i.e. trap depth is obtained. Its value is obtained by our algorithm using a computer program.
3. General order peaks: Each peak is assumed to be of general order kinetics and the parameters of each peak, trap depth, modified pre exponential factor and order of kinetics are estimated for each peak.

Second order peaks case is not discussed as it comes under preview of general order case.

Further results are validated with simulated glow curves. Following this, a fully fledged deconvolution of experimental glow curve of $CaSO_4$: Dy has been done. Comprision with simulated glow curve of GLOCANIN project is also there.

Chapter 6. Summary and future directions

The thesis concludes with summary of each chapter and probable future directions.

1.10 Scope of the thesis

This dissertation is limited to photon (including high and low energy) irradiation, beta and neutron irradiation are kept out of context. Another point which is worth to mention at this point is main focus is on RW, GG and MP models of TL kinetics and more realistic delocalised models, which are basically extensions of these models. The discussion on mixed order kinetics is very limited. Also, the discussion on localised transition models is only limited to the context of fading.

1.11 Milestones in thesis period

Five major achievements during the period of thesis are documented.

Origin of Residual TL

The origin of Residual TL, which is one of the sources of deviation from true dose in TL based dosimetry, has been investigated. Results of theoretical model and experiments are matching to a reasonable extent.

Theoretical explanation of experimental facts of fading

Afterglow from thermoluminescent material was mostly investigated experimentally. Theoretical explanation of experimental findings has been one of the achievements of this dissertation.

Non linearity is general nature of afterglow

It has been established that non linearity is general feature of afterglow.

Novel technique for deconvolution

A novel methodology of deconvolution of TL signal based on EM and MLE has been developed. It has been validated with simulated glow curve, and deconvolution of experimental glow curve of $CaSO_4$: Dy has been carried out.

Parametric uncertainty analysis of RW, GG and MP models

A Monte Carlo, fuzzy set theory and Polynomial chaos expansion based study for parametric uncertainty analysis of RW, GG and MP models has been conducted.

A manuscript is communicated based on findings of this chapter.

CHAPTER II

Basic TL Models and estimation of Glow Curve

When the thermoluminescent material (known as phosphor) is exposed to ionising radiation, electrons and holes are generated. The electrons translate through the crystal in conduction band and holes in valence band. While translating they get trapped in trap centres. The origin of these trap centres are defect centres in the material. With these charge carriers trapped in defect centres the system (material under investigation) goes to a metastable state. The material can stay in this metastable state for fairly a long period (years) unless the charge carriers get sufficient energy (thermal stimulus) to get into respective energy bands, where they are relatively free.

The rate of excitation from trap centres is given by Arrhenius law which is based on general account of conditions given by Gibbs [Gibbs, 1972].

Arrhenius law is given by equation (2.1)

$$R = f \exp(-\frac{D}{KT}) \tag{2.1}$$

Where

R is rate of excitation per unit time from trap.

D is trap depth

f is attempt to escape frequency. Physically it reflects number of attempts charge carrier make per unit time to escape from the trap.

T is Temperature in degree Kelvin.

K is Boltzmann constant

2.1 Traditional Approach

In this approach the rate equations are written at during stimulation (section 2.1.1) and are further analysed using quasi equilibrium approximation (2.1.2) to arrive at general one trap model (GOT) / One trap one recombination centre model (OTOR). The obtained equation is further analysed in different approximations and modifications.

2.1.1 Rate Equations

The phenomenon of themoluminescence can be modelled using rate equation. Rates equation gives the rate of change of charge carriers in various energy levels. These equations can be further solved with certain approximations to arrive at various expression of TL.

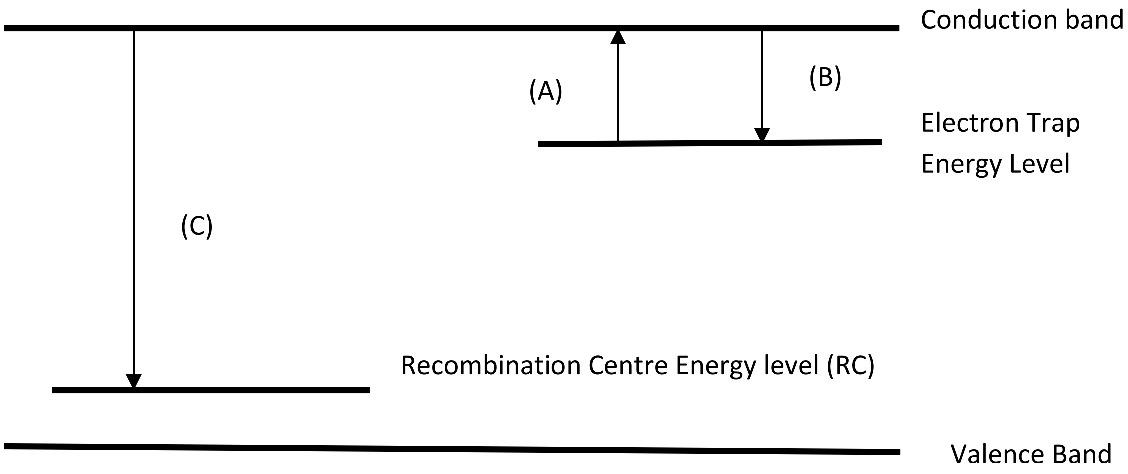

Figure 2.1 Schematic diagram for rate equations assuming only electron to be freed by the thermal stimulus. (A) Excitation from trap (B) Re-trapping (C) Radiative Recombination

Assuming only electrons to be freed by the thermal stimulus, the rate equations when the material is thermally stimulated can be written as

$$\frac{dC_c}{dt} = C_t R - C_c \left(C_T - C_t \right) B_t - C_c C_r B_{tr} \tag{2.2}$$

$$\frac{dC_v}{dt} = 0 \tag{2.3}$$

$$\frac{dC_t}{dt} = C_c\,(C_T - C_t)\,B_t - C_t\,R \tag{2.4}$$

$$\frac{dC_r}{dt} = -\,C_c\,C_r\,B_{tr} \tag{2.5}$$

It can be seen from equation (2.2) to equation (2.5) that

$$\frac{dC_c}{dt} = \frac{dC_r}{dt} - \frac{dC_t}{dt} \tag{2.6}$$

Applying charge neutrality we have

$$C_c + C_t = C_r \tag{2.7}$$

The TL luminescence is given by

$$L = -\frac{dC_r}{dt} \tag{2.8}$$

Where

C_t = Concentration trapped electron at time t (m^{-3})

C_r = Concentration of recombination centre at time t (m^{-3})

C_c = Concentration of electron in conduction band at time t (m^{-3})

C_T = Concentration of total number of electron traps (m^{-3})

B_{tr}= Coefficient for probability of electron recombining with holes in RC (m^3/s)

B_t= Coefficient for probability of electron re-trapping in electron traps (m^3/s)

L = Luminescence intensity

t = Time in seconds

2.1.2 Quasi Equilibrium Condition

Quasi equilibrium (QE) approximation says that the rate of change of charge carrier concentration in conduction band is very small as compared to rate of change of charge carrier concentration in electron traps or RC. Mathematically it can be framed as

$$\left|\frac{dC_c}{dt}\right| \ll \left|\frac{dC_r}{dt}\right| , \quad \left|\frac{dC_t}{dt}\right| \tag{2.9}$$

When combined with the initial condition

$$C_c\,(t = 0) = 0 \tag{2.10}$$

It gives

$$C_c \sim 0 \tag{2.11}$$

This physically means that in conduction band there is no accumulation of charge carriers. In other words charge carrier concentration in conduction band is quasi stationary. Or in other words we can say as many charge carriers are going into the conduction band per unit time, nearly same number is coming out of the conduction band per unit time.

Using quasi equilibrium condition we can simplify the rate equations.

Using equation (2.2) and equation (2.9) we can write

$$0 = C_t\,R - C_c\,(C_T - C_t)\,B_t - C_c\,C_r\,B_{tr} \tag{2.12}$$

$$\Longmapsto C_c = \frac{C_t\,R}{(C_T - C_t)\,B_t + C_r\,B_{tr}} \tag{2.13}$$

Putting the result of equation (2.13) into equation (2.5) we get

$$\frac{dC_r}{dt} = -\frac{C_t\,R}{(C_T - C_t)\,B_t + C_r\,B_{tr}}\,C_r\,B_{tr} \tag{2.14}$$

Using equation (2.8) we get

$$L = \frac{C_t\, R C_r\, B_{tr}}{(\, C_T - C_t)\, B_t + \, C_r\, B_{tr}} \tag{2.15}$$

This can be rewritten as

$$L = C_t\, R[\, 1 - \frac{(\, C_T - C_t)\, B_t}{(\, C_T - C_t)\, B_t + \, C_r\, B_{tr}}\,] \tag{2.16}$$

Equation (2.15) and equation (2.16) is known as general one trap one recombination centre (OTOR) model [Levy, 1985; Levy 1991].

2.1.3 First Order Kinetics

The approximation of first order kinetics

The equation (2.15) can be simplified further [Randall and Wilkins, 1945a; Randall and Wilkins, 1945b] with an approximation

$$C_r\, B_{tr} \gg (\, C_T - C_t)\, B_t \tag{2.17}$$

This physically means that the probability of re-trapping in an electron trap is very small as compared to the probability of recombination at a recombination cite for an electron translating in conduction band. It may be kept in mind that till present discussion we have assumed that only electrons are freed by the thermal stimulus and not the holes.

First Order Phosphorescence decay

In this approximation equation (2.15) boils down to

$$L = C_t\, R \tag{2.18}$$

We may arrive at equation (2.19) using equation (2.6), (2.8) and (2.9)

$$L \sim -\frac{dC_t}{dt} \qquad (2.19)$$

Using equation (2.18) and equation (2.19) we get

$$-\frac{dC_t}{dt} = C_t R \qquad (2.20)$$

It may be noticed from equation (2.20) that in present approximation

$$-\frac{dC_t}{dt} \; \alpha \, C_t \qquad (2.21)$$

Which reflects rate of change of charge carrier concentration is proportional to charge carrier concentration raised to power unity. This is the origin of name 1st order kinetics.

Further equation (2.20) may be solved at a constant temperature to get phosphorescence emission intensity as function of time.

Solution of differential equation (2.20) is

$$C_t = \exp(-Rt) \qquad (2.22)$$

Putting the result of equation (2.22) in equation (2.20) and using equation (2.19) we arrive at the phosphorescence decay formula

$$L = L_0 \exp(-Rt) \qquad (2.23)$$

First Order Themoluminescence

Equation (2.20) can be rewritten as

$$-\frac{dC_t}{dt} = C_t \, f \, \exp(-\frac{D}{KT}) \qquad (2.24)$$

Equation (2.24) can be solved with a linear heating profile

$$T = T_0 + \beta t \qquad (2.25)$$

Solution of equation (2.24) is as below

$$C_t = C_{t0} \exp(-\frac{f}{\beta} \int_{T_0}^{T} \exp(-\frac{D}{K\Theta})\, d\Theta) \qquad (2.26)$$

Putting in equation (2.24) and using equation (2.19) we can arrive at

$$L_{TL} = C_{t0}\, f \exp(-\frac{D}{KT}) \exp(-\frac{f}{\beta} \int_{T_0}^{T} \exp(-\frac{D}{K\Theta})\, d\Theta) \qquad (2.27)$$

This is famous Randall and Wilkins equation for first order kinetics.

Equation (2.27) can be written in a transformed form [Kitis et al., 1998]

$$L(T) = L_m \exp\left[1 + \frac{D}{KT}\frac{T-T_m}{T_m} - \frac{T^2}{T_m^2}\exp\left(\frac{D}{KT}\frac{T-T_m}{T_m}\right)(1-\mathrm{V}) - \mathrm{V}_m\right] \qquad (2.27b)$$

Where

$\mathrm{V} = 2KT/D$

$\mathrm{V}_m = 2KT_m/D$

T_m = Peak temperature

L_m= Peak Intensity

2.1.4 Second Order Kinetics

The approximation of second order kinetics

Equation (2.16) was developed further by other authors [Garlick and Gibson, 1948] with a different set of approximations.

Basic approximation is

$$C_r\, B_{tr} \ll (\, C_T - C_t)\, B_t \qquad (2.28)$$

This approximation physically means that there is a high re-trapping probability for electrons escaping from traps by the thermal stimulus as compared to recombination probability at RC.

Additional approximations are

$$C_T \gg C_t \tag{2.29}$$

$$C_t \sim C_r \tag{2.30}$$

$$B_{tr} = B_t \tag{2.31}$$

Using equation (2.29), equation (2.16) becomes

$$L = C_t R[1 - \frac{(C_T) B_t}{(C_T) B_t + C_r B_{tr}}] \tag{2.32}$$

$$\Rightarrow L = C_t R [\frac{C_r B_{tr}}{(C_T) B_t + C_r B_{tr}}] \tag{2.33}$$

Using equation (2.31) we get

$$L = C_t R [\frac{C_r}{C_T + C_r}] \tag{2.34}$$

Using equation (2.30) we get

$$L = C_t R [\frac{C_t}{C_T + C_t}] \tag{2.35}$$

Using equation (2.29) again we get

$$L = C_t^2 \frac{R}{C_T} \tag{2.36}$$

Using equation (2.1) we get

$$L = C_t^2 \frac{f exp(-\frac{D}{KT})}{C_T} \tag{2.37}$$

Putting $f' = f/C_T$ we get

$$L = C_t^2 \, f' exp \, (-\frac{D}{KT}) \tag{2.38}$$

Using equation (2.19) we may arrive at

$$\frac{dC_t}{dt} = -C_t^2 \, f' exp \, (-\frac{D}{KT}) \tag{2.39}$$

$$\frac{dC_t}{dt} \, \alpha \, C_t^2 \tag{2.40}$$

It may be noted that the rate of change of charge carrier's concentration in conduction band is proportional to concentration of charge carrier raised to the power two. This is the origin of name 2nd order kinetics.

Second Order Phosphorescence decay

Using equation (2.39) we may write

$$\frac{dC_t}{dt} = -C_t^2 \, R_0 \tag{2.41}$$

Where

$$R_0 = f' exp \, (-\frac{D}{KT}) \tag{2.42}$$

The solution of differential equation given by equation (2.41) is

$$C_t = \frac{C_{t0}}{1 + \, R_0 \; C_{t0} \, t} \tag{2.43}$$

Putting the value of C_t from equation (2.43) into equation (2.41) we get

$$\frac{dC_t}{dt} = -(\frac{C_{t0}}{1 + \, R_0 \, C_{t0} \, t})^2 \, R_0 \tag{2.44}$$

Using the result of equation (2.19) we may write

$$L = \frac{L_0}{(1 + R_0\, C_{t0}\, t)^2} \tag{2.45}$$

This is the expression for phosphorescence decay for 2nd order of kinetics.

Second Order Themoluminescence

To get the TL emission intensity for 2nd order kinetics of thermoluminescence we have to solve equation (2.39) with a linear heating profile of equation (2.25).

The solution is

$$C_t = \frac{C_{t0}}{1 + \frac{C_{t0}\, f'}{\beta} \int_{T_0}^{T} \exp(-\frac{D}{K\Theta}) d\Theta} \tag{2.46}$$

Putting this solution in equation (2.39) we get

$$\frac{dC_t}{dt} = -C_{t0}^2\, f' exp\, \left(-\frac{D}{KT}\right) [1 + \frac{C_{t0}\, f'}{\beta} \int_{T_0}^{T} \exp\left(-\frac{D}{K\Theta}\right) d\Theta]^{-2} \tag{2.47}$$

Using equation (2.19) we may write

$$L_{TL} = C_{t0}^2\, f' exp\, \left(-\frac{D}{KT}\right) [1 + \frac{C_{t0}\, f'}{\beta} \int_{T_0}^{T} \exp\left(-\frac{D}{K\Theta}\right) d\Theta]^{-2} \tag{2.48}$$

This is the famous Garlick and Gibson equation for 2nd order kinetics of thermoluminescence.

Equation (2.48) can be written in a transformed form

$$L(T) = 4L_m \exp\left[\frac{D}{KT}\,\frac{T-T_m}{T_m}\right] [\frac{T^2}{T_m^2}(1 - V) \exp\left(\frac{D}{KT}\,\frac{T-T_m}{T_m}\right) + 1 + V_m]^{-2} \tag{2.48b}$$

Where

$V = 2KT/D$

$V_m = 2KT_m/D$

T_m = Peak temperature

L_m= Peak Intensity

2.1.5 General Order Kinetics

The expressions of Randall - Wilkins and Garlick – Gibson discussed so far are based on relative magnitude of re trapping and recombination probabilities. With time there was development of empirical expressions for TL kinetics.

Contribution of May and Partridge

Just in analogy with expressions of first and second order kinetics May and Partridge [1964] discovered differential equation for TL kinetics which is known as General Order kinetics equation

$$L = C_t^b \, f' exp\,(-\frac{D}{KT}) \tag{2.49}$$

Where b is a scalar parameter, known as parameter for general order kinetics.

Using equation (2.19) we may arrive at

$$\frac{dC_t}{dt} = -C_t^b \, f' exp\,(-\frac{D}{KT}) \tag{2.50}$$

The solution of above differential equation is

$$C_t = C_{t0}\,[\,1 + (b-1)\frac{f''}{\beta}\int_{T_0}^{T} \exp(-\frac{D}{KT})]^{\frac{1}{1-b}} \tag{2.51}$$

Where $f'' = f' C_{t0}^{b-1}$

Putting this solution back to equation (2.49) we get the expression for TL emission intensity

$$L_{TL} = f'' C_{t0}\, exp\left(-\frac{D}{KT}\right)\left[\,1 + (b-1)\frac{f''}{\beta}\int_{T_0}^{T} \exp\left(-\frac{D}{KT}\right)\right]^{\frac{b}{1-b}} \tag{2.52}$$

Rasheedy's contribution

In above expression there is difficulty. The dimension of the parameter associated with frequency factor (f'') changes with order of kinetics. Rasheedy's contribution was mainly in direction of removing this difficulty.

He wrote the equation in following form [Rasheedy, 1993]

$$L = -\frac{C_t^b}{C_T^{b-1}}\, f exp\left(-\frac{D}{KT}\right) \tag{2.53}$$

$$\Longmapsto L_{TL} = C_{t0}^b\, f\, exp\left(-\frac{D}{KT}\right) C_{T0}^{(1-b)}\left[\,1 + f(b-1)\frac{\left(\frac{C_{t0}}{C_T}\right)^{(b-1)}}{\beta}\int_{T_0}^{T} \exp\left(-\frac{D}{KT}\right)\right]^{\frac{-b}{1-b}} \tag{2.54}$$

Both of the expressions of general order kinetics equation (2.52) and equation (2.54) are not valid for b=1. But both of them boil down to first order kinetics equation as b tends to 1 [Chen, 1969].

The general order kinetics expression can be written in a transformed form as

$$L(T) = L_m b^{\frac{-b}{1-b}} \exp\left[\frac{D}{KT}\,\frac{T-T_m}{T_m}\right]\left[\,(b-1)(1-V)\frac{T^2}{T_m^2}\exp\left[\frac{D}{KT}\,\frac{T-T_m}{T_m}\right] + z_m\right]^{\frac{-b}{1-b}} \tag{2.54b}$$

$V = 2KT/D$

$V_m = 2KT_m/D$

T_m = Peak temperature

L_m= Peak Intensity

$z_m = 1 + (b-1)V_m$

2.1.6 Mixed Order Kinetics

So far the developed equations are based on One trap One recombination centre (OTOR) model. But realistically there will be no material which will have exactly one trapping site. Even if we take temperature range where only one peak is active there will always be traps which are deeper than this trap in the material, though they are "thermally disconnected". This concept has attracted the attention of many authors [Dussel and Bube, 1967; Saunders, 1969; Kelly and Braunlich, 1970].

One can write the rate equations in this case and solve using QE approximation. Following the work of Kelly and Braunich we directly arrive at the equivalent expression for OTOR model (equation 2.15) in this two trap case.

$$L = \frac{C_t\ f \exp(-\frac{D}{KT})\,(C_t + C_h)\ B_{tr}}{(C_T - C_t)\,B_t + (C_t + C_h)\ B_{tr}} \tag{2.55}$$

Where we have substituted the value of C_r in equation (2.15).

C_h = Charge carrier concentration in deeper trap.

Let us obtain the expression for C_r using physical arguments.

We will term the trap type which is under investigation as dosemetric trap and the trap that is deeper than this as the deeper trap.

Charge neutrality dictates

$$C_c + C_t + C_h = C_r \tag{2.56}$$

Using the extension of QE (equation 2.11) we can write

$C_c \sim 0$

Hence equation (2.56) becomes

$$C_t + C_h = C_r \tag{2.57}$$

Using the result of equation (2.57) and following the work of Kelly and Braunich we arrive at equation (2.55) which is equivalent of equation (2.15).

We can further solve equation (2.55).

Assuming $B_t = B_{tr}$ we get

$$L = \frac{C_t \; f \exp(-\frac{D}{KT}) \, (C_t + C_h)}{C_T + C_h} \tag{2.58}$$

$$\Rightarrow L = C_t \; f^* \exp(-\frac{D}{KT}) \; (C_t + C_h) \tag{2.59}$$

$$\Rightarrow L = {C_t}^2 \, f^* \exp(-\frac{D}{KT}) + C_t \; C_h \, f^* \exp(-\frac{D}{KT}) \tag{2.60}$$

For $C_h \ll C_t$ equation (2.60) reduces to second order kinetics equation and for $C_h \gg C_t$, it reduces to first order kinetics equation.

Following Chen [Chen et al, 1981] we may write the solution of equation (2.60)

$$L_{TL} = \frac{f^* \, {C_h}^2 \, \upsilon \exp\{ \left(\frac{C_h \; f^*}{\beta}\right) \int_{T_0}^{T} \exp\left(-\frac{D}{K\theta} \, d\theta\right)\} \exp(-\frac{\mathrm{D}}{\mathrm{KT}})}{[\exp\{ \left(\frac{C_h \; f^*}{\beta}\right) \int_{T_0}^{T} \exp\left(-\frac{D}{K\theta} \, d\theta\right)\} - \upsilon]^2} \tag{2.61}$$

where

$$\upsilon = \mathrm{C_{t0}}/(\mathrm{C_{t0}} + \mathrm{C_h})$$

The transformed form of mixed order kinetics expression may be found in literature [Kitis and Gomez-Ros, 2000].

2.1.7 Some more realistic delocalised models

By the treatment so far it is clear that glow curve is fully described by four parameters f, D, C_{t0} and b (or ʋ). With certain assumptions the complex rate equations can reduce to equations first, second and general (or mixed) order kinetics. Perhaps the most important of these assumptions are

$$\left|\frac{dC_c}{dt}\right| \sim 0 \quad \text{The quasi equilibrium approximation (QE)} \tag{2.62}$$

And $$C_h = C_H \quad \text{Non interactive kinetics approximation (NIK)} \tag{2.63}$$

where C_H is concentration of deeper traps.

Several authors have extended the basic models with these assumptions and many others have examined the applicability of these approximations.

Extension of basic models

There is a plethora of results discussing extension of basic models. We will start with a work that gives physical interpretation to otherwise empirically developed general order kinetics. In this work [Christodoulides, 1990] physical interpretation to parameters f' and b of general order kinetics equations are developed. A Gamma (Γ) distribution in $\ln(f)$ was assumed and was applied to first order kinetics. By doing so general order kinetics equation was derived. Hence, in this interpretation f' and b of general order kinetics equation are characteristic parameters of $\ln(f)$ distribution.

By comparing the results of general order kinetics (equation 2.52 or 2.54) and the expression of mixed order kinetics (equation 2.61) discussed above and by applying certain assumption ($C_h = C_H, C_{t0} = C_T, f' = fC_{t0}^{1-b}$) Opanowicz [Opanowicz, 1989] found temperature dependence of order of kinetics $b(T)$. He found $b(T)$ to be highly temperature dependent in contrast with the discussion so far where order of kinetics b was just assumed to be a constant parameter.

Till present discussion we have assumed localised energy states are single valued well defined energy levels. This is true for ideal defect in ideal crystal. But in actual defective crystal or especially amorphous material, there will be a spread in energy for energy level associated with a defect. This may be because of variation in bond length and bond angles for nearest neighbours. In case of amorphous material one has to compulsory talk about mobility gap where there is a spread of energy levels near Fermi level [Mott and Davies, 1979]. Several kind of distribution have been discussed in literature like linear, exponential and many more [Lampert and Mark, 1970; Meldin, 1961; Grenet et al, 1973; Kao and Hwang, 1981]. Detailed discussion with Gaussian [Hornyak and Franklin, 1988] and uniform [Hronyak and Chen, 1989] distributions are present in literature. It is also possible to fragment the energy range numerically into discrete sets and superimpose the TL of all to get the glow curve. Though, this method has limitation as discussed in next topic (Approaches without QE and NIK).

A distribution in recombination centre may cause distortion in glow curve structure. A distribution in capture cross section leads to a distribution in pre exponential factor. Rudlof et al [Rudlof et al., 1978] has assumed Gaussian distribution in pre exponential factor.

In further discussion we can assume both electron and holes are freed by thermal stimulus.

Hence, $\frac{dn_v}{dt} \neq 0$ and rate equations can be modified accordingly. This case was discussed by Schon [Schon M., 1942] and later by Klasen [Klasen, 1946].

In this case

$$L_{TL} \neq -\frac{dC_t}{dt} \tag{2.64}$$

But $L_{TL} = L_{TLC_t} + L_{TLC_r}$ (2.65)

$\Longmapsto L_{TL} = C_c C_r B_{tr} + C_v C_t B_{rt}$ (2.66)

Where symbols have following meaning

C_c = Charge carrier concentration in conduction band.

C_r = Charge carrier concentration in recombination site for electrons.

C_v= Charge carrier concentration in valence band.

C_t= Charge carrier concentration in recombination site for holes.

B_{tr}= Probability coefficient for an electron in conduction band to recombine at a recombination site for electrons.

B_{rt}= Probability coefficient for a hole in valence band to recombine at a recombination site for holes.

Approaches without QE and NIK

It is possible to write equations for flow of charge carrier for a set of traps relevant to a particular material. Further, the question arises how to solve the obtained set of obtained differential equations to get the TL emission intensity. One approach is of Levy [Levy, 1985; Levy, 1991], as discussed above, who kept the assumption of QE approximation and obtained analytical expression for TL emission intensity. An alternative approach is of other author [Bull et al., 1986]. He solved the set of equations for a set of traps numerically. As the solution was obtained numerically QE was not there. Conclusion of his work is if re trapping is negligible in that case glow curve obtained numerically can be obtained by superposition of set of Randall Wilkins type equations (equation 1.27). But if re trapping is dominant in that case superposition of 2^{nd} or general order kinetics equations may not give the actual glow curve.

Certainly numerical solution of rate equation is one approach which is without these approximations. Few authors have solved the Schon-Klasen rate equations numerically [Mckeever et al., 1985].

Various authors have discussed applicability of QE approximation [Maxia, 1978; Maxia, 1980; Shenker and Chen, 1972; Kelly et.al., 1971].

An entirely different approach is also present in literature where QE and NIK approximations are totally abandoned and analysis is based on two meaning functions P and Q [Lewandowski and Mckeever, 1991; Mckeever et al., 1993; Lewandowski et al. 1994].

It is pertinent to mention that in section 2.7 we have discussed some works which are ahead of basic models but in no way we claim that the list is exhaustive, as there is very vast amount of literature is available in the domain.

2.1.8 Localized transition models

Looking at the mechanism of Figure 2.2, it is possible to have two types of models. One is, in which phenomenon of tunnelling takes place directly between trap and recombination centre. This happens because of spatial closeness of trapping and recombination sites. If the wave function of charge carrier in trapping and recombination sites overlaps appreciably then this

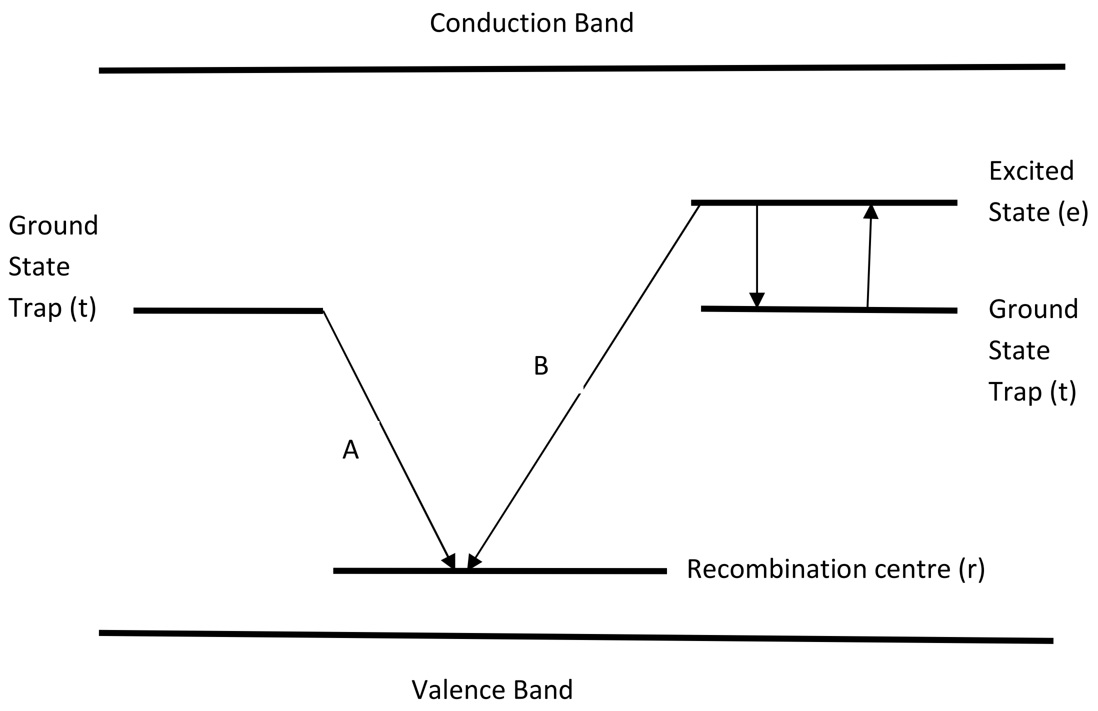

Figure 2.2 Electron transition involving localised energy levels.

(A) is the process of direct recombination from trap to recombination centre. (B) is the process of recombination mediated through excited state.

type of mechanism is dominant. This type of mechanism has been suggested in various phosphor material [Delbecq et al, 1974; Visocekas et al, 1976; Visocekas, 1985; Visocekas, 1988]. This mechanism will be discussed in chapter two under heading “Fading”.

Another possibility is that charge carrier is first excited to a higher localised energy state and further tunnels to the recombination site. The rate equations for this type of mechanism is suggested in the pioneering work of Halperin and Braner [Haperin and Braner, (1960)]

$$L_{TL} = -\frac{dC_r}{dt} = C_e C_r B_{re} \tag{2.67}$$

$$\frac{dC_t}{dt} = fC_e - f\exp(-\frac{D_e}{KT}) \tag{2.68}$$

$$\frac{dC_e}{dt} = f\, C_t\exp(-\frac{D_e}{KT}) - C_e(C_r B_{re} + f) \tag{2.69}$$

It can be shown by principal of detailed balance that the rate of retrapping in this type of transition is given by fC_e [Halperin and Braner, 1960]. Another author [Chen, 1976] replaced the term $C_r B_{re}$ in equation (2.67) and equation (2.69) by a constant probability term, say η. With these replacements the rate equations become

$$L_{TL} = -\frac{dC_r}{dt} = C_e \eta \tag{2.70}$$

$$\frac{dC_t}{dt} = fC_e - f\exp(-\frac{D_e}{KT}) \tag{2.71}$$

$$\frac{dC_e}{dt} = f\, C_t \exp(-\frac{D_e}{KT}) - C_e(\eta + f) \tag{2.72}$$

Charge neutrality dictates

$$C_r = C_t + C_e \tag{2.73}$$

Assuming quasi equilibrium we have

$$\frac{dC_e}{dt} \sim 0 \tag{2.74}$$

Combining with the initial condition

$$C_{e0} = 0 \tag{2.75}$$

We arrive at

$$C_e \sim 0 \tag{2.76}$$

Putting the result of equation (2.76) in equation (2.73) we get

$$C_r \sim C_t \tag{2.77}$$

We can solve equation (2.72) using QE approximation

$$C_e = \frac{f\, C_t \exp(-\frac{D_e}{KT})}{(\eta+f)} \tag{2.78}$$

Putting the result of equation (2.78) in equation (2.70) we arrive at

$$L_{TL} = \frac{\eta f\, C_t \exp(-\frac{D_e}{KT})}{(\eta+f)} \tag{2.79}$$

Case I: $f \gg \eta$

$$L_{TL} = \eta\, C_t \exp(-\frac{D_e}{KT}) \tag{2.80}$$

Case II: $f \ll \eta$

$$L_{TL} = f\, C_t \exp(-\frac{D_e}{KT}) \tag{2.81}$$

In both the conditions we get first order kinetics type of equation. Hence localised transition following this mechanism always follows first order kinetics. The only difference is the magnitude of the term that is place of frequency factor.

2.2 Master equation approach

2.2.1 Analytical Solution of GOT / OTOR model

Equation (2.15) and equation (2.16) are General One Trap (GOT) / One Trap One Recombination centre (OTOR) model equation [Adirovitch, 1956; Halperin and Braner, 1960; Chen and Mckeever, 1997]. For decades it was not solved analytically. After five decades analytical solution was obtained by Kitis and Vlachos [2013] using Lambert W function and later by Lovedy Singh and Gartia [2013] using Wright Omega function. These approaches will be briefed here.

Analytical solution of GOT/OTOR model using Lambert W function

From equation (2.15) we have the

$$L = \frac{C_t\, R C_r\, B_{tr}}{(\,C_T - C_t)\, B_t + \; C_r\, B_{tr}} \tag{2.82}$$

By equation (2.19) we have

$$L \sim \; -\frac{dC_t}{dt} \tag{2.83}$$

By equation (2.82) and equation (2.83) we arrive at

$$-\frac{dC_t}{dt} = \frac{C_t\, R C_r\, B_{tr}}{(\,C_T - C_t)\, B_t + \; C_r\, B_{tr}} \tag{2.84}$$

Using approximation $C_t \sim C_r$ and $\frac{B_t}{B_{tr}} = B$ we get

$$-\frac{dC_t}{dt} = \frac{C_t^2 R}{(\,C_T - C_t)\, B + \; C_t} \tag{2.85}$$

Rearranging equation (2.85) we get

$$C_t\, B \int_{C_{t0}}^{C_t} \frac{dC_t}{C_t^2} + \; (1 - B) \int_{C_{t0}}^{C_t} \frac{dC_t}{C_t} = \; -\int_{t0}^{t} R\, dt \tag{2.86}$$

By doing some algebra we arrive at

$$\frac{C_{t0}}{C_t} + \; c \ln\left(\frac{C_{t0}}{C_t}\right) = 1 + \frac{C_{t0}}{C_T B} \int_{t0}^{t} R\, dt \tag{2.87}$$

Where

$$c = \; \frac{C_{t0}}{C_T} \; \frac{1-B}{B} \tag{2.88}$$

Case I $\quad \boldsymbol{c} > 0$ **or** $\boldsymbol{B} = \frac{\boldsymbol{B_t}}{\boldsymbol{B_{tr}}} < 1$

In above case equation (2.87) becomes

$$\frac{C_{t0}}{C_t\,c} + \ln\left(\frac{C_{t0}}{C_t\,c}\right) = \frac{1}{c} - \ln(c) + \frac{C_{t0}}{c\,C_T B}\int_{t0}^{t} R\,dt \qquad (2.89)$$

Equation (2.89) is transcendental equation of form

$$y + \ln y = z \qquad (2.90)$$

Where

$$y = \frac{C_{t0}}{C_t\,c} \qquad (2.91)$$

$$z = \frac{1}{c} - \ln(c) + \frac{C_{t0}}{c\,C_T B}\int_{t0}^{t} R\,dt \qquad (2.92)$$

Solution of equation (2.90) is Lambert W function [Corless et al., 1996; Corless et al., 1997]

$$y = W\,[e^{z}] \qquad (2.93)$$

By equation (2.91) and (2.88) we arrive at

$$C_t = \frac{C_T\,B}{(1-B)}\,W\,[e^{z}]^{-1} \qquad (2.94)$$

Using equation (2.82) and with some algebra we arrive at

$$L = \frac{C_T\,B}{(1-B)^2}\,\frac{R}{W\,[e^{z}] + W\,[e^{z}]^2} \qquad (2.95)$$

Where

$$z = \frac{1}{c} - \ln(c) + \frac{f}{(1-B)\beta}\int_{T0}^{T}\exp\left(-\frac{D}{KT}\right)dT \qquad (2.96)$$

As it has been practiced in this chapter we would like to present equation (2.96) in a transformed form. Sadek et al. [2015] has done this transformation for first master equation from $L\,(C_{t0}, D, f, B, T)$ to $L\,(L_m, D, T_m, B, T)$ using the general procedure (as explained by Kitis et al. [2019])

The final expression is

$$L = L_m \exp(\frac{D\,(T-T_m)}{K\,T\,T_m})\ [\frac{W\,[e^{z1m}]+W\,[e^{z1m}]^2}{W\,[e^{z1}]+W\,[e^{z1}]^2} \tag{2.97}$$

Where

$$z1 = \frac{1}{c} - \ln(c) + \frac{D\exp(\frac{D}{KT_m})}{K\,T_m^2}\ \frac{F\,(T,D)}{1-1.05\,B^{1.26}}$$

Where

$z1m = z1$ at $T = T_m$ and $F\,(T,D) = \int_{T0}^{T} \exp(-\frac{D}{KT})$

Case II $\boldsymbol{c < 0}$ **or** $\boldsymbol{B = \frac{B_t}{B_{tr}} > 1}$

As $\ln(c)$ will become complex so we define $c = -|c|$ and equation (2.89) will take the form

$$\frac{C_{t0}}{C_t\,|c|} - \ln\left(\frac{C_{t0}}{C_t\,|c|}\right) = \frac{1}{|c|} + \ln\,(|c|) + \frac{C_{t0}}{|c|\,C_{TB}} \int_{t0}^{t} R\,dt \tag{2.98}$$

Equation (2.98) is of the form

$$y - \ln y = z \tag{2.99}$$

Where

$$y = \frac{C_{t0}}{C_t\,|c|} \tag{2.100}$$

$$z = \frac{1}{|c|} + \ln\,(|c|) + \frac{C_{t0}}{|c|\,C_{TB}} \int_{t0}^{t} R\,dt \tag{2.101}$$

For $z > 1$ there are two branches of Lambert W function, but Kitis and Vlachos [2013] showed only one branch has physical significance. Hence, for $c < 0$ the solution of equation (2.99) is

$y = -W\,[-1, -e^{-z}]$

Using equation (2.100) and equation (2.88) we arrive at

$$C_t = -\frac{C_T\,B}{|(1-B)|}\,W\,[-1, -e^{-z}]^{-1} \tag{2.102}$$

Using equation (2.82) we can write

$$L = \frac{C_T\,B}{(1-B)^2}\;\frac{R}{W\,[-1,-e^{-z}] + W\,[-1,-e^{-z}]^2} \tag{2.103}$$

Equation (2.103) is the first master equation (solution of GOT/OTOR model) for $c < 0$ or $B = \frac{B_t}{B_{tr}} > 1$.

It can be presented in a transformed form by using the procedure explained by Kitis et al. [2019]. The final result as developed by Sadek et al. [2015] is

$$L = L_m\,\exp\left(\frac{D\,(T-T_m)}{K\,T\,T_m}\right)\;[\frac{W\,[-1,-e^{-z2m}] + W\,[-1,-e^{-z2m}]^2}{W\,[-1,-e^{-z2}] + W\,[-1,-e^{-z2}]^2} \tag{2.104}$$

Where

$$z2 = \frac{1}{|c|} - \ln(|c|) + \frac{D\exp\left(\frac{D}{KT_m}\right)}{K\,T_m^2}\;\frac{F\,(T,D)}{2.963-3.24\,B^{-0.74}}$$

Where $z2m = z2$ at $T = T_m$ and $F\,(T, D) = \int_{T0}^{T} \exp\left(-\frac{D}{KT}\right)$

Analytical solution of OTOR/GOT model by Wright Omega function

By equation (2.85) we have

$$-\frac{dC_t}{dt} = \frac{C_t^2\,R}{(\,C_T - C_t)\,B + \,C_t} \tag{2.105}$$

Using $\frac{dT}{dt} = \beta$ we may modify above equation as

$$-\frac{dC_t}{dT} = \frac{C_t^2 R}{\beta\,[\,C_T\,B + \,C_t\,(1-B)]} \tag{2.106}$$

Taking $P(T) = R/\beta$ and $C_t = \frac{1}{Y}$ equation (2.106) can be modified to

$$\frac{dY}{dT} = \frac{P(T)}{C_T\,B + \frac{1-B}{Y}} \tag{2.107}$$

$$\frac{dY}{dT} = \frac{Y\,P(T)/(1-B)}{Y\,C_T\frac{B}{1-B} + 1} \tag{2.108}$$

Making following substitutions

$$U = \frac{Y\,C_T\,B}{1-B} \tag{2.109}$$

$$q(T) = \frac{P(T)}{1-B} \tag{2.110}$$

We arrive at

$$\frac{dU}{dT} = \frac{U\,q(T)}{U+1} \tag{2.111}$$

$$U + \log U = \int_{T0}^{T} q(T)dT \quad + C \tag{2.112}$$

The value of integration constant can be found using initial condition at $T = 0\,, C_t = C_{t0}$

Using equation (2.112) and substituting

$$\int_{T0}^{T} q(T)dT \quad + C = \chi_T\,(T) \tag{2.113}$$

We arrive at

$$U + \log U \; = \chi_T\,(T) \tag{2.114}$$

Solution of above equation has contribution of various authors [Wright, 1959; Corless and Jeffrey, 2002; Lawrence et al., 2012] as

$$U = W(\chi_T\ (T)) \tag{2.115}$$

Using equation (2.109), (2.106) and substitution $C_t = \frac{1}{Y}$ we can arrive at expression of TL intensity [Singh and Gartia, 2013]

$$L = \frac{C_T\, B\, f\, \exp(-D/KT)}{\beta\ (1-B)^2\ W\big(\chi_T\ (T)\big)\ (1+W\big(\chi_T\ (T)\big))} \tag{2.116}$$

Where

$$\chi_T\ (T) = \frac{f}{\beta\ (1-B)} \int_{T0}^{T} \exp\left(-\frac{D}{KT}\right)\, dT\ + \frac{C_T\, B}{1-B}\, \frac{1}{C_{t0}} + \log\left(\frac{C_T\, B}{1-B}\, \frac{1}{C_{t0}}\right) \tag{2.117}$$

The details of $W(\chi_T\ (T))$ may be found in literature [Singh and Gartia, 2013].

The above equation is of the form $L\ (D, f, B, C_T, C_{t0})$ it can be transformed to the form $L\ (D, f, B)$ with two known parameters viz. T_m and L_m. As derived by Singh and Gartia [2013] the final expression is written as

$$L\ (T) = L\ (T_m)\, \frac{W(\chi_T\ (T_m))}{W(\chi_T\ (T))} \left[\frac{1+W\big(\chi_T\ (T_m)\big)}{1+W\big(\chi_T\ (T)\big)}\right] \exp\left[\frac{D}{K}\ \left(\frac{1}{T_m} - \frac{1}{T}\right)\right] \tag{2.118}$$

Where

$L\ (T_m)$ and $\chi_T\ (T_m)$ are for saturated case $C_T = C_{t0}$.

Equation (2.118) represents 1st order kinetics for $B < \frac{C_{t0}}{100\, C_T}$ and 2nd order case for $B = 0.999$.

2.2.2 Analytical Solution of mixed order kinetics (MOK) model

From equation (2.55) we get luminescence intensity expression for MOK

$$L = \frac{C_t\ f \exp(-\frac{D}{KT})\, (C_t + C_h)\ B_{tr}}{(\,C_T - C_t)\, B_t + (\,C_t + C_h)\ B_{tr}} \tag{2.119}$$

For $(C_t + C_h) B_{tr} >> (C_T - C_t) B_t$ equation (2.119) reduces to 1st order Kinetics equation.

For $(C_t + C_h) B_{tr} \ll (C_T - C_t) B_t$ and $C_t << C_T$ we can arrive at

$$L = \frac{C_t\ R\ (C_t + C_h)\ B_{tr}}{C_T\ B_t} \tag{2.120}$$

With assuming, $B_t = B_{tr}$ equation (2.119) reformulates to

$$L = \frac{C_t\ R\ (C_t + C_h)}{C_T - C_h} \tag{2.121}$$

Equations (2.120) and equation (2.121) can be written together as

$$L = gR\ C_t\ (C_t + C_h) \tag{2.122}$$

Where

$g = B_{tr}/C_T\ B_t$ or $g = 1/(C_T - C_h)$ in the respective equations.

This is the differential equation for MOK model. Further, its analytical solution will be presented.

By equation (2.19) and (2.122) we may write

$$-\frac{dC_t}{dT} = gRC_t(C_t + C_h) \tag{2.123}$$

Following Kitis et al. [2019] we may write equation (2.123) as

$$\ln\left[\frac{(C_t + C_h)}{C_t} \quad \frac{C_{t0}}{(C_{t0} + C_h)}\right] = g\ C_h \int_0^t R\ dt \tag{2.124}$$

As per Chen et al. [1981] we may define a parameter α

$$\alpha = \frac{C_{t0}}{(C_{t0} + C_h)} \tag{2.125}$$

From equation (2.124) we may write

$$C_t = \frac{\alpha\, C_h}{F(t)-\alpha} \qquad (2.126)$$

Where

$$F(t) = \exp\,(g\, C_h \int_0^t R\, dt)$$

Inserting equation (2.126) in equation (2.123) and using equation (2.19) we may write

$$L = \frac{g\, {C_h}^2\, R\, F(t)\alpha}{(F(t)-\alpha)^2} \qquad (2.127)$$

Where

$$F(t) = \exp\,(g\, C_h \int_0^t R\, dt) = \exp\,(g\, C_h \frac{f}{\beta} \int_{T_0}^{T} \exp\,(-\frac{E}{KT})\, dt \qquad (2.128)$$

This is second master equation which is for MOK. Further, as we have done in all the previous cases, we will write the master equation in transformed form.

Following Kitis and Gomez Ros [1999] and Kitis et al. [2019] we may write

$$L = L_m \exp[\frac{E(T-T_m)}{K\,T\,T_m}]\ \frac{(F(T_m)-\alpha)^2}{F(T_m)}\ \frac{F(t)}{(F(t)-\alpha)^2} \qquad (2.129)$$

Where

$$F(T) = \exp(\frac{1}{f_{MOK}}\ \frac{T^2}{T_m^2}\ \exp\,[\frac{E(T-T_m)}{K\,T\,T_m}])\ (1-\frac{2\,K\,T}{E}) \qquad (2.130)$$

$$f_{MOK} = \frac{2.6-0.9203\ \alpha+.324\ \alpha^{3.338}}{2.6-2.9203\alpha\quad .324\ \alpha^{3.338}} \qquad (2.131)$$

2.2.3 Analytical solution of NMTS model

Multiple traps and competition between them during filling and stimulus give rise to IMTS model. When deep trap is saturated there is no competition during filling. This gives rise to NMTS model.

From equation (2.15) we may write

$$L = \frac{C_t C_r \, R \, B_{tr}}{(C_T - C_t) \, B_t + C_r B_{tr}} \tag{2.132}$$

This can be arranged as

$$L = \frac{C_t C_r \, R}{(C_T - C_t) B + C_r} \tag{2.133}$$

Where

$$B = \frac{B_t}{B_{tr}} \tag{2.134}$$

Let us introduce function $\ddot{\Upsilon} = \frac{C_t\,(T)}{C_r(T)}$

Following the lines of Kitis and Vlachaos [2013] and Sadek et al. [2015] and after doing some algebra we arrive at

$$\int_{C_{r0}}^{C_r} \frac{C_T\, B + C_r\, (1 - \ddot{\Upsilon} B)}{C_r^2} \, dC_r = -\frac{\ddot{\Upsilon} f}{\beta} \int_{T_0}^{T} \exp\left(-\frac{D}{KT}\right) dT \tag{2.135}$$

$$\frac{1}{C_{r0}} - \frac{1}{C_r} + \frac{(1 - \ddot{\Upsilon} B)}{C_T\, B} \ln\left(\frac{C_r}{C_{r0}}\right) = \frac{\ddot{\Upsilon}\, f}{C_T B\, \beta} \int_{T_0}^{T} \exp\left(-\frac{D}{KT}\right) dT \tag{2.136}$$

$$\frac{C_{r0}}{C_r \acute{\varepsilon}} + \ln\left(\frac{C_{r0}}{C_r \acute{\varepsilon}}\right) = \frac{1}{\acute{\varepsilon}} - ln\, \acute{\varepsilon} + \frac{\ddot{\Upsilon} f}{1 - \ddot{\Upsilon} B} \int_{T_0}^{T} \exp\left(-\frac{D}{KT}\right) dT \tag{2.137}$$

Where

$$\acute{\varepsilon} = \frac{C_{r0}(1 - \ddot{\Upsilon} B)}{C_T\, B} \tag{2.138}$$

The solution of equation (2.137) for B<1 is

$$C_r = \frac{C_{r0}}{\acute{\varepsilon}\, W_0[\exp(z1)]} \tag{2.139}$$

Where $W_0[\exp(z1)]$ is the principal branch of Lambert W function for $\exp(z1)$ function and

$$z1 = \frac{1}{\acute{\varepsilon}} - ln\acute{\varepsilon} + \frac{\ddot{Y}f}{1-\ddot{Y}B}\int_{T_0}^{T} \exp\left(-\frac{D}{KT}\right) dT$$

However for B>1 $\acute{\varepsilon} = -|\acute{\varepsilon}|$ solution of equation (2.137) will be

$$C_r = \frac{-C_{r0}}{\acute{\varepsilon}\, W\,[-1,\ \ -\exp(-z2)]} \tag{2.140}$$

Where $W\,[-1,\ \ \exp(z2)]$ is the second branch of Lambert W function for $\exp(z2)$ function and

$$z2 = \frac{1}{|\acute{\varepsilon}|} - \ln\ |\acute{\varepsilon}| + \frac{\ddot{Y}f}{|1-\ddot{Y}B|}\int_{T_0}^{T} \exp\left(-\frac{D}{KT}\right) dT \tag{2.141}$$

Using equation (2.133) we arrive at luminescence intensity equation in the two cases

For B <1

$$L(T) = \frac{C_T\,B\,\ddot{Y}}{\beta(1-\ddot{Y}B)^2}\ \ \frac{f\,\exp(-\frac{D}{KT})}{W_0[\exp(z1)]+W_0[\exp(z1)]^2} \tag{2.142}$$

For B> 1

$$L(T) = \frac{C_T\,B\,\ddot{Y}}{\beta(1-\ddot{Y}B)^2}\ \ \frac{f\,\mathrm{ex}\ \ (-\frac{D}{KT})}{W[-1,\exp(-z1)]+W[-1,-\exp(z2)]^2} \tag{2.143}$$

Equations (2.142) and (2.143) are the third master equations. The transformed form of third master equation is not in literature yet.

2.2.4 Analytical Solution of simple localized transition (SLT) model

Following the procedure given in section 2.1.8 (Localized transition model) i.e. writing the rate equation and using quasi equilibrium condition in the excited state we may arrive at equation (2.144). Following rate equations given by Kitis et al. [2019] and Mckeever [1997] we arrive at

$$C_e = \frac{C_t\,R}{A_D + B_{re}C_r} \tag{2.144}$$

Where

A_D= Rate of de excitation from excited state to ground state.

B_{re}= Probability coefficient for a electron in excited state to recombine with a recombination centre.

Substituting equation (2.144) in equation (2.67) we get

$$\frac{dC_r}{dt} = -C_e B_{re} C_r = -\frac{C_t\,R\,B_{re}C_r}{A_D + B_{re}C_r} \tag{2.145}$$

By charge conservation

$$C_r = C_t + C_e \tag{2.146}$$

And using approximation

$$C_e \ll C_t \tag{2.147}$$

We arrive at

$$C_r \sim C_t \tag{2.148}$$

So equation (2.145) becomes

$$L_{LOC} = -\frac{dC_t}{dt} = \frac{R\,C_t^2}{r + C_t} \tag{2.149}$$

$$r = \frac{A_D}{B_{re}}$$

The analytical solution for equation (2.149) is [Kitis and Pagonis, 2018]

$$L_{LOC} = \frac{Rr}{W[0,\ e^z] + W[0,\ e^z]^2} \tag{2.150}$$

Where

$$z_{LOC} = \frac{r}{C_{t0}} - \ln[\frac{C_{t0}}{r}] + \int_{t0}^{t} R(t)dt \tag{2.151}$$

For the specialized case of TL

$$z_{LOC-TL} = \frac{r}{C_{t0}} - \ln[\frac{C_{t0}}{r}] + s\int_{T0}^{T} \exp\left(-\frac{D}{KT}\right) dT \tag{2.152}$$

Transformed form of fourth master equation is not in literature yet.

2.2.5 Analytical solution of Tunnelling localized transition (TLT) model

The rate equations for TLT model [Kitis et al., 2019] are

$$\frac{dC_g}{dt} = -RC_g + B_{ge}C_e \tag{2.153}$$

$$\frac{dC_e}{dt} = RC_g - B_{ge}C_e - 3C_e\rho''^{1/3} z \, (ln\frac{C_{t0}}{C_t})^{2/3} \tag{2.154}$$

$$-\frac{dC_r}{dt} = \frac{3C_e\rho''^{1/3} z \, (ln\frac{C_{t0}}{C_t})^{2/3}}{\tau_c} \tag{2.155}$$

With

$$\tau_c = f^{-1} \exp[(\frac{1}{\rho''} \, ln\frac{C_{t0}}{C_t})^{\frac{1}{3}}] \tag{2.156}$$

Symbols have following meaning

C_g = Instantaneous concentration of electrons (donors) in ground state

C_e = Instantaneous concentration of electrons (donors) in excited state

C_r = Instantaneous concentration of holes (acceptors)

C_t = Instantaneous concentration of all electrons (donors)

C_h = Concentration of available electrons (donors) in TDDT

D = Thermal activation energy

f = Frequency factor

ρ'' = Dimensionless number density of acceptors

τ_c = Critical tunneling lifetime

z = Dimensionless constant equal to 1.8 introduced in the model

B_{ge} = Relaxation rate from the excited into the ground state

The fifth master equation yields approximate analytical sol of tunnelling localized transition model. Kitis and Pagonis [2013] give this analytical solution from approximate model of Jain et al. [2012]

The approximation used by Kitis and Pagonis [2013] is

$$\frac{1}{C_e}\frac{dC_e}{dt} \ll B_{ge} + \frac{3\rho''^{1/3} z \left(ln\frac{C_{t0}}{C_t}\right)^{2/3}}{\tau_c} \tag{2.157}$$

Using the approximation (2.157) in equation (2.154) we get

$$C_e = \frac{RC_g}{B_{ge} + \frac{3\rho''^{1/3} z \left(ln\frac{C_{t0}}{C_t}\right)^{2/3}}{\tau_c}} \tag{2.158}$$

Putting (2.158) in equation (2.153) and taking some approximation we finally boil down to following

$$\frac{dC_g}{dt} = -RC_g \; \frac{3\rho''^{1/3} z \left(ln\frac{C_{t0}}{C_t}\right)^{2/3}}{\tau_c} \tag{2.159}$$

Since $C_r = C_g + C_e + C_h$ (2.160)

And $C_e \ll C_g$ (2.161)

Hence, $\frac{dC_r}{dt} \sim \frac{dC_g}{dt}$ (2.162)

Using equation (2.162), equation (2.159) becomes

Taking into account $C_t = C_g + C_e \sim C_g$ and after extended algebra we arrive at

$$L(t) = 3\, C_{t0}\, \rho'' z\, R\, F(t)^2 e^{-\rho'' F(t)^3} e^{-F(t)} \qquad (2.163)$$

Where for the case of TL

$$F(t) = \ln\left(1 + \frac{zf}{\beta} \int_{T_0}^{T} e^{-\frac{D}{KT}} dT \right) \qquad (2.164)$$

2.3 Conclusions

This chapter is dedicated to various models proposed for TL phenomenon. The concept and mathematics of basic TL models have been discussed. This chapter is divided into tow subsections. Subsection 2.1 is dedicated to “Traditional Approach” and subsection 2.2 is dedicated “Master equation Approach” for stimulated phenomenon. First subsection starts with rate equation governing the flow of charge carriers in various bands and localised energy levels. From the rate equation and using QE approximation the general expression of luminescence for OTOR model is arrived at.

The conditions of first order kinetics and second order kinetics are explained physically and mathematically. In both the approximations from the general expression the expressions of phosphorescence decay and TL emissions are obtained. Further, expression of general order kinetics is elaborated.

Mixed order kinetics followed by various extensions of discussed models is presented. This concludes our discussion on delocalised transition models. It is followed by the mathematical description of localised transition models.

Second subsection (section 2.2) discusses five master equations one by one. Though full derivation could not be given because of complex algebra, but flow of logic is elaborated to some extent.

As mentioned before, for various TL models the expression for TL intensity as a function of temperature has been obtained in this chapter. This TL intensity as a function of temperature is called as glow curve. But the question arises if the glow curve is recorded experimentally, does it exactly match with the glow curve predicted by the models derived. The answer to this question is: there are various reasons that lead to deviation from model predicted glow curves. In the further Chapter these reasons will be discussed.

CHAPTER III

Deviations in TL intensity from model estimated glow curve: Sources of Uncertainty

In previous chapter we have discussed various models that can be used to simulate the TL glow curve. But there are many reasons due to which experimental glow curves are different from simulated glow curve using these models. There are theoretical factors as well as experimental reasons. There are also reasons that originate from field conditions. This chapter is deals with those factors which cause deviation of experimental glow curve from the simulated one.

3.1 Fading

Fading is the phenomenon of loss of TL signal during irradiation and storage. Fading can be categorized in three categories namely,

- Thermal fading
- Anomalous fading
- Thermally assisted fading

These are discussed as follows.

3.1.1 Thermal Fading

Even if a TLD is stored at room temperature, due to Maxwellian distribution of trap depth for each trap type, there is a finite probability that few charge carriers that are trapped in trap centres will transit to conduction band by gaining sufficient energy and subsequently recombine with RCs through radiative or non radiative processes. In either of the case there is a loss of signal due to this phenomenon and TL obtained on a subsequent readout is lower than what it was expected to be by that amount of incident irradiation. The luminescence that is emitted as function of time due to the phenomenon is called after glow, being a glow after irradiation. It should not be confused with fluorescence as fluorescence is a very short lived effect.

This phenomenon can be modeled in two steps: excitation and isothermal decay.

Isothermal decay may follow first, second or general order kinetics. All three are discussed in detail in chapter two.

Examples of thermal fading in TL material are abundant and well studied. It is summarized by Horowitz and Yossian [Horowitz and Yossian, 1995]. A summary specific to TLD-100 is given by Horowitz [Horowitz, 1990].

3.1.2 Anomalous fading

Anomalous fading is the fading that occurs even if the temperature is not sufficient for excitation of trapped charge carrier. As a matter of fact its mechanism is totally different. It occurs due to spatial closeness of trap and RC. If they are so close that the wave function of opposite charge carriers in trap and in RC overlaps to some extent, phenomenon of anomalous fading may occur. It is characterized by non dependence on temperature unlike thermal or thermally assisted fading.

First report of anomalous fading was given by Bull and Garlick [Bull and Garlick, 1950] for UV stimulated diamond. In the context of meteorites Hasan et al. [Hasan et al., 1986] reported anomalous fading. Tyler and Mckeever [Tyler and Mckeever, 1988] opposed his explanation. Visocekas et al. reported the phenomenon for labradorite [Visocekas et al., 1985]. The amount of literature on the subject is very vast and it is not possible to mention all of them here. Hence, literature survey is stopped here and modeling of anomalous fading is discussed. ***In this discussion focus will be on our contribution to the literature [Sahai et al., 2019; Sahai et al., 2018].***

3.1.2.1 Anomalous fading and power law decay

Due to anomalous fading there is a luminescence signal (afterglow) during the storage of the pre exposed sample. Though, the exact nature of afterglow is not well understood theoretically. But in general it is known to follow power law decay.

$$I \, \alpha \, t^{-k} \tag{3.1}$$

where

I is afterglow intensity and t is time

k is the exponent whose experimental value ranges from 0.5 to 2.0.

If the nature of afterglow is correctly represented by equation (3.1) then the graph between $\log(I)$ and $\log (st)$ is expected to be a straight line with k as the slope. s is just a scaling factor. But in reality the experimental graphs of afterglow many a times show deviation from straight line. In this section the full experimental range of straight line graphs of afterglow is explained and in next section non linearity is discussed.

Before this work power law decay of luminescence was explained only partially [Huntley, 2006]. It was shown that different values of exponent k can be obtained for different recombination centre concentration. But with this approach only range of exponent from 0.95 to 2.0 could be explained. In Huntley's work RPB between trap and RC has been considered. This choice is mainly because of ease of calculations as there is apparently no theoretical reason to justify RPB.

In our approach a NRPB is considered between trap and RC and full range of exponent for different shape parameters of NRPB between trap and RC, has been explained.

Mathematical formalism of the problem

In the present study modelling has been done for charge carrier tunnelling through an isotropic NRPB between trap and RC. It is shown in Figure 3.1 as region I, region II and region III.

Region I: Trap

Region II: Tunnelling region (Region between trap and RC)

Region III: RC

In the present study tunnelling phenomena is approached in three dimensions with isotropic potential. For determining wave function in various regions, SE in spherical polar coordinate is taken, as the tunnelling problem we are dealing with has spherical symmetry

SE in various regions is of the form of equation (3.2)

$$\frac{-\hbar^2}{2m}\,\nabla^2 \;\Lambda\,(r,\theta,\Phi)\; + V(r)\,\Lambda(r,\theta,\Phi) = E\,\Lambda(r,\theta,\Phi) \tag{3.2}$$

It may be noted that the form of V(r) will be region dependent.

$$\mathrm{V(r)} = \begin{cases} V_I & Region\ I \\ C^* + D^*\, r^{b^*} & Region\ II \\ V_{III} & Region\ III \end{cases} \tag{3.3}$$

$C^*\,, D^*\ \ and\ b^*$ are arbitrary constants.

Boundary conditions are $\Lambda\,(r,\theta,\Phi) \to 0$ as $r \to 0, +\infty$.

Wave functions in the regions are given by following [Sahai et. al., 2018]

Region I : $$\Lambda_l\,(k_1\,r) = \frac{C_l}{k_1 r}\;e^{i\left(k_1\,r-\frac{l\Pi}{2}\right)} + \frac{D_l}{k_1 r}e^{-i\left(k_1\,r-\frac{l\Pi}{2}\right)} \tag{3.4a}$$

Region II: $$\Lambda(k_0 r) = \frac{C_0}{r\sqrt{|k_0|}}\quad \exp\left(-\frac{1}{h}\int_{r1}^{r} k_0\,(r')dr'\right) \tag{3.4b}$$

Region III: $$\Lambda_l\,(k_3\,r) = \frac{E_l}{k_3 r}\;e^{i\left(k_3\,r-\frac{l\Pi}{2}\right)} \tag{3.4c}$$

where Λ is radial wave function, k_1, k_3 are wave vectors in region I and region III and $k_0 = \sqrt{2m\,(E - V_{II}(r))}$, where $V_{II}(r)$ is the potential in region II. C_l, D_l, E_l *and* C_0 are arbitrary constants. The suffix l represents the wave functions in various energy levels.

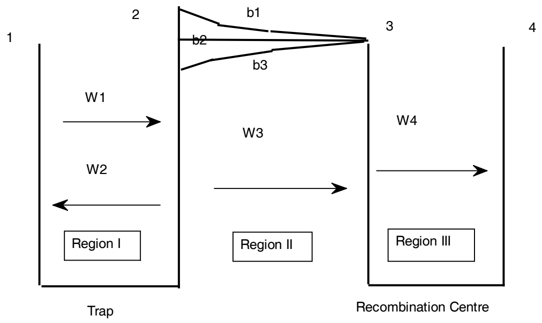

Figure3.1 Illustration of wave functions and boundaries : Figure shows the region I, region II and region III with respective wave functions (W1, W2, W3, W4), their boundaries (1, 2, 3 and 4) and NRPB or RPB between trap and RC, namely b1 (decreasing), b2 (rectangular) and b3 (increasing).. Location of boundary 2 is r_1 and of 3 is r_2.

Further, continuity of wave function and their derivatives at the boundaries dictate following equations

$$\Lambda_I(r_1) = \Lambda_{II}(r_1) \qquad \frac{d\Lambda_I}{dr}\Big|_{r=r1} = \frac{d\Lambda_{II}}{dr}\Big|_{r=r1}$$

$$\Lambda_{II}(r_2) = \Lambda_{III}(r_2) \qquad \frac{d\Lambda_{II}}{dr}\Big|_{r=r2} = \frac{d\Lambda_{III}}{dr}\Big|_{r=r2}$$

Under the conditions of tunneling from ground state of trap to ground state of RC, one can consider $l = l' = 0$. $k_1 = k_3$ is assumed. Under these special conditions, the tunneling probability takes following form [Zittili, 2001; Mathews, 1976].

$$T^* \sim \exp\left(\frac{-2}{\hbar}\int_{r1}^{r2} k_0\,(r)dr\right) \tag{3.5}$$

where $k_0 = \left[\,2m\ |V(r) - E| + \frac{\hbar^2}{r^2}\left(l + \frac{1}{2}\right)^2\,\right]^{\frac{1}{2}}$

T^* is tunneling probability

When a charge carrier (electron/hole) is trapped inside the trap it constantly keeps colliding with its potential barrier and finite probability of barrier tunnelling exists. Tunnelling of charge carrier to RC for a RPB gives a life time

$$\tau = f^{-1}e^{\alpha r} \sim f^{-1}e^{\ddot{Y}} \tag{3.6}$$

α is a constant [Thomas, 1965; Riehl, 1970]. Reasonable value of f and α can be taken as $\sim 10^{15}$ and $\sim 10^{9}$, respectively [Huntley, 2006]. Neglecting $\hbar^2$ term of equation (3.5) $\ddot{Y}$ can be estimated.

$\ddot{Y}$ can be written as follows [Sahai et al., 2018]

$$\ddot{\Upsilon} = (2/\hbar)\ \int_0^r \sqrt{[2m\,\{\,V(r') - E\}]}\ dr' \tag{3.7}$$

where lower limit of integration is the point where tunnelling begins, r_1 in figure 1,and r is arbitrary point between r_1 and r_2.

In the present case, V(r) is not a constant as it is considered to be NRPB. Additionally, there are few more requirements (i) increasing and decreasing NRPB shape should be simulated for different sets of parameter values, (ii) numerical integration required later should be feasible (iii) for applicability of WKB potential should not vary fast as exponentials or power laws. A practical choice may be:

$$V(r) = C^* + D^*\,r^{b^*} \tag{3.8}$$

where, b^*, C^* and D^* are arbitrary constants. Substituting V(r) from equation (3.8) into equation (3.7), equation (3.9) is obtained.

$$\ddot{\Upsilon} = (2/\hbar)\ \int_0^r \sqrt{[2m\,\{\,C^* +\ D^*\,\mathrm{r}'^{b^*}\ - E\}]}\ \ dr' \tag{3.9}$$

$$\ddot{\Upsilon} = (2/\hbar)\ \int_0^r \sqrt{\left[2m\,C^* + 2m\,D^*\,r'^{b^*} -\ E\right]}\ \ dr' \tag{3.10}$$

$$\ddot{\Upsilon} = F\int_0^r \sqrt{1 + Ar'^{b^*}}\ \ dr' \tag{3.11}$$

where $F = \left(\frac{2}{\hbar}\right)\sqrt{[2m\,C^* -\ E]}$ and $A = (2mD^*)/(2mC^* - E)$

A, b^*, C^*, D^* , E and F are constant.

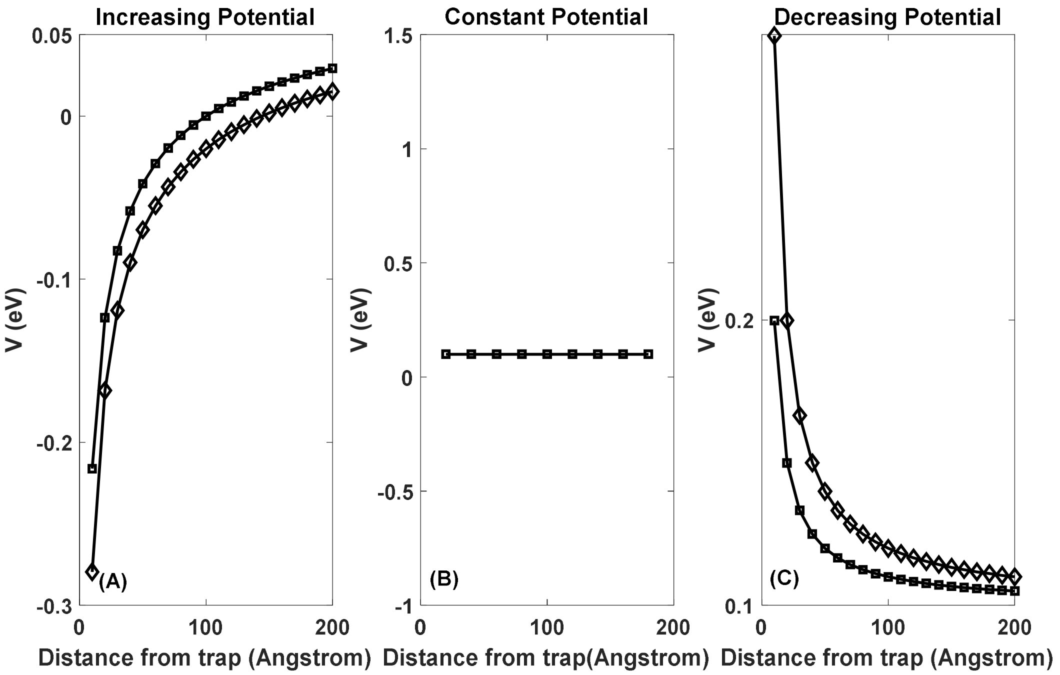

Figure 3.2 Shape of potential barrier in region II. (A) b3 of Figure 3.1, (B) b2 of Figure 3.1 and (C) b1 of Figure 3.1. Plots have been generated for C^*=0.1eV and changing D^* and b^*.

Considering the fact that the contribution of perturbation is small one can write $C^* >> D^*$, this makes A very small

The equation (3.11) can be developed to equation (3.12) with approximations that A is very small and b lies between -1 & +1.

$$\ddot{\Upsilon} = F \int_0^r [\, 1 + \frac{A}{2}\, r'^b \,]\, dr \qquad (3.12)$$

$$\ddot{\Upsilon} = F\, [\, r + \frac{A}{2}\, \frac{r^{b+1}}{b+1}] \qquad (3.13)$$

$$\ddot{\Upsilon} = F\, (r + c1\, r^{c2}) \qquad (3.14)$$

where value of F ~ 10^9 (order of α with rectangular potential barrier [Huntley, 2006] and c1, c2 are related to A and b^* by

$$c1 = \frac{A}{[2(b^*+1)]} \tag{3.15}$$

$$c2 = b^* + 1 \tag{3.16}$$

So far tunnelling of charge carrier from single trap to single RC has been discussed. However, considering that the RCs are distributed around trap within a volume 4/3 πr^3, (r is a variable distance), it requires spatial integration. The probability that the charge carrier will not recombine in the volume 4/3 πr^3 around the trap is given by exp(- 4/3ρ* πr^3) [Huntely, 2006], where ρ* is density of recombination centres.

There is continuous depreciation of charge carrier concentration with time, $C_t(t)$, due to recombination. Following Huntley [2006]

$$\frac{C_t(t)}{C_t(0)} = \int_0^\infty 3\,(\Lambda')^2 \exp\{-(\Lambda')^3\}\, e^{(-\frac{t}{\tau})} d\Lambda' \tag{3.17}$$

Where

Assuming $\Lambda' = (4\pi\rho^*/3)^{1/3}\, r$

By differentiation equation (3.17) with respect to time we obtain

$$\frac{I\,(t)}{C_t(0)} = \int_0^\infty \left(\frac{1}{\tau}\right) 3\,(\Lambda')^2 \exp\{-(\Lambda')^3\}\, e^{(-\frac{t}{\tau})} d\Lambda' \tag{3.18}$$

where I(t) = - $\frac{dC_t(t)}{dt}$ is the intensity of luminescence

$$\frac{I(t)}{C_t(0)} = \int_0^{\infty} Z\,dr \qquad (3.19)$$

Where $Z = \left(\frac{1}{\tau}\right) \rho^* 4\pi\, r^2 \exp\{-\left(\frac{4}{3}\right) \pi r^3\, \rho^*\}\, e^{\left(-\frac{t}{\tau}\right)}$

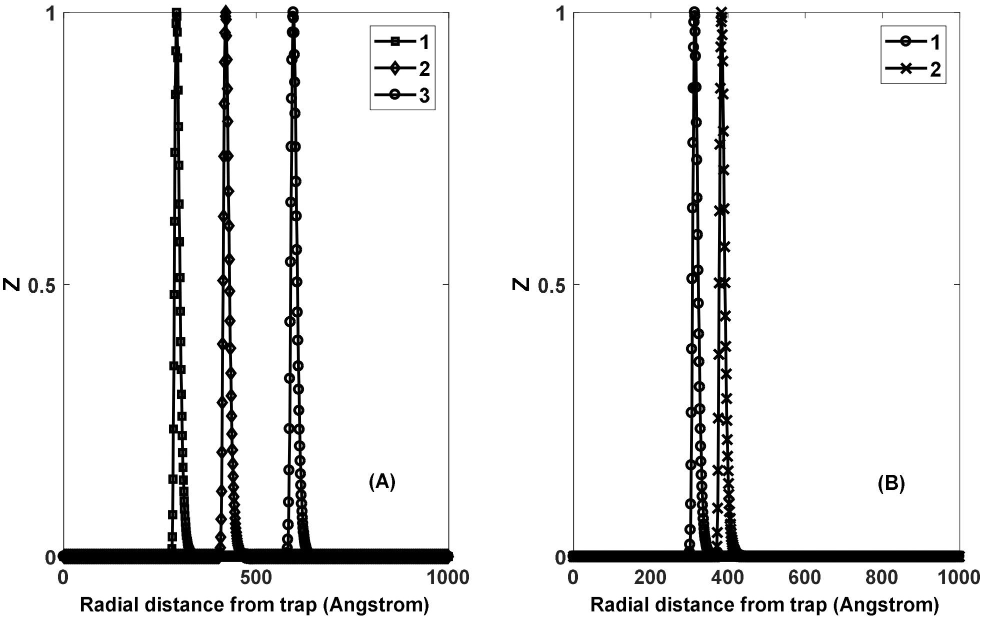

Figure 3.3 Z of equation (3.19) as a function of radial distance (A) for different potential barrier shape and (B) for different time. Plots are normalized with respect to height.

For determination of integration range in equation (3.18), the integrand shape of equation (3.18) with change in r was found. There is a spike in the shape, which shifts towards right with increase in time (with same order of magnitude) as well as with shape of the barrier (many orders of magnitude) as shown in Figure 3.3.

Table 3.1 Location and height of integrand of equation (3.19) with changing shape of NRPB. Normalization is with respect to RPB peak height. Table is for ρ* = 10^{22}m^{-3}, f = 3.0 X 10^{15}second $^{-1}$, C^*=0.10eV, V_I= -1.00eV, V_{III}=-1.250eV, E=-0.70eV

Potential barrier	**Parameter Set**			**Z**	
	D^*	b^*	**t**	**Relative Peak Height**	**Peak location**
Potential 1	0.0	--	10^5 sec	1.0	294 A°
Potential 2	$-5.0\ x\ 10^{-5}$	-0.50	10^5 sec	0.250	422 A°
Potential 3	$-10.0\ x\ 10^{-5}$	-0.50	10^5 sec	0.00150	598 A°

Table 3.2 Location and height of Integrand of equation (3.19) at different times for a fixed shape of NRPB. Normalization of peak height is done as illustrated in table 3.2. Rest of the parameters are same as shown in table 3.1.

Parameter Set			**Z**	
D^*	b^*	**t**	**Relative Peak Height**	**Peak location**
10^{-5}	-0.50	10^5sec	1	313 A°
10^{-5}	-0.50	10^{10} sec	$1.10\ x\ 10^{-5}$	384 A°

Results

Integration of equation (3.19) can be done numerically to obtain I(t) as a function of time. The value of life time τ can be inserted numerically using equation (3.6). For a RPB and changing RC concentration ρ*, the results of Huntley [2006] could be reproduced. The results of Huntley's work was; different values of slope of log(I) vs. log (st) graph can be obtained for different RC concentration. But by changing the concentration of RC he faced a limitation of saturation of slope at a lower limit of 0.95. At higher end, graphs became a poor fit with a straight line. These results are reproduced and illustrated in Figure 3.4.

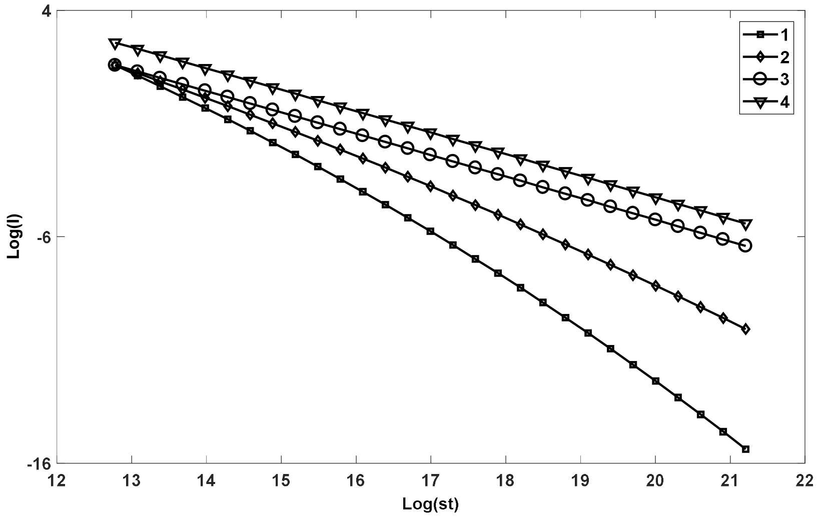

Figure 3.4 Log (I) with Log (st) for different values of recombination center concentration. Data for plots is given in Table 3.3.

Table 3.3 Slopes for different values of RC concentration for curves of Figure 3.4.

Curve No. of Figure 3.4	RC concentration (ρ)	Slope
1	$10^{23.4}$ m^{-3}	2.1
2	10^{23} m^{-3}	1.4
3	10^{20} m^{-3}	0.95
4	10^{18} m^{-3}	0.95

Following different approach in the study i.e. by changing the shape of potential barrier, the full experimental range of slope of log (I) vs. log (st) graphs (0.5 to 2.0) can be obtained. Results are shown in Figure 3.5.

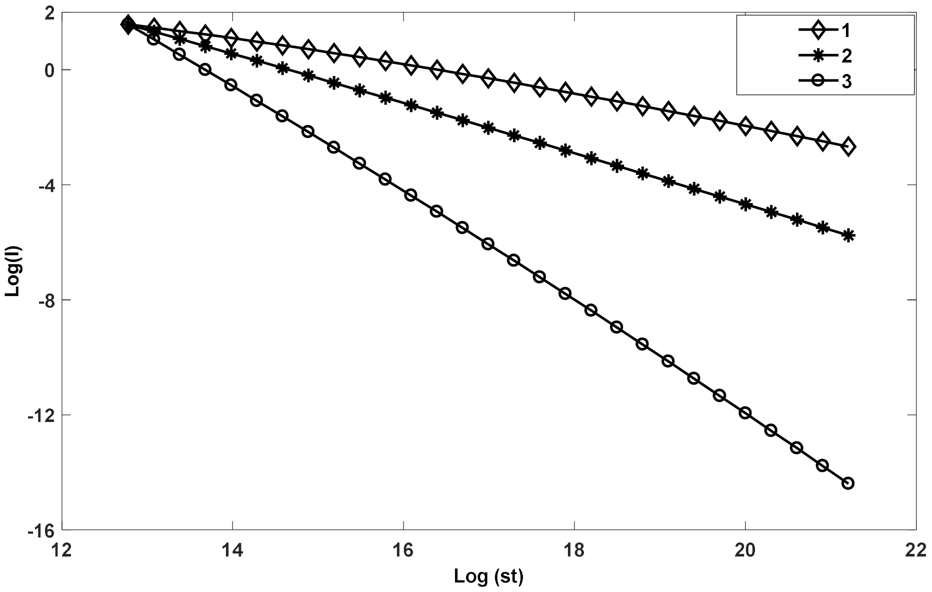

Figure 3.5 Log(I) vs log (st) graph with change in potential barrier shape.

Table 3.4 Slopes for different shape parameters for curves of Figure 3.5.

Curve no. of Figure 3.5	D^*	b^*	Slope
1	4 X 10^{-3} eV m^{-b}	-0.8	0.5
2	0.80 X 10^{-3} eV m^{-b}	-0.5	0.8
3	-7 X 10^{-5} eV m^{-b}	-0.5	2.0

3.1.2.2 Non linearity is general feature of afterglow

Further, the intention is to explore nature of afterglow intensity. Hence, the integrand of equation (3.19) is broken into time dependent and time independent parts with $V_I=V_{III}$ [Sahai et. al., 2019]

$$Z= G_1 \ G_2 \tag{3.20}$$

Where

$$G_1 = \left(\frac{1}{\tau}\right)\rho^{*}4\pi \, r^2 \exp\left\{-\left(\frac{4}{3}\right)\pi r^3 \rho^{*}\right\} \tag{3.21}$$

$$G_2= e^{\left(-\frac{t}{\tau}\right)} \tag{3.22}$$

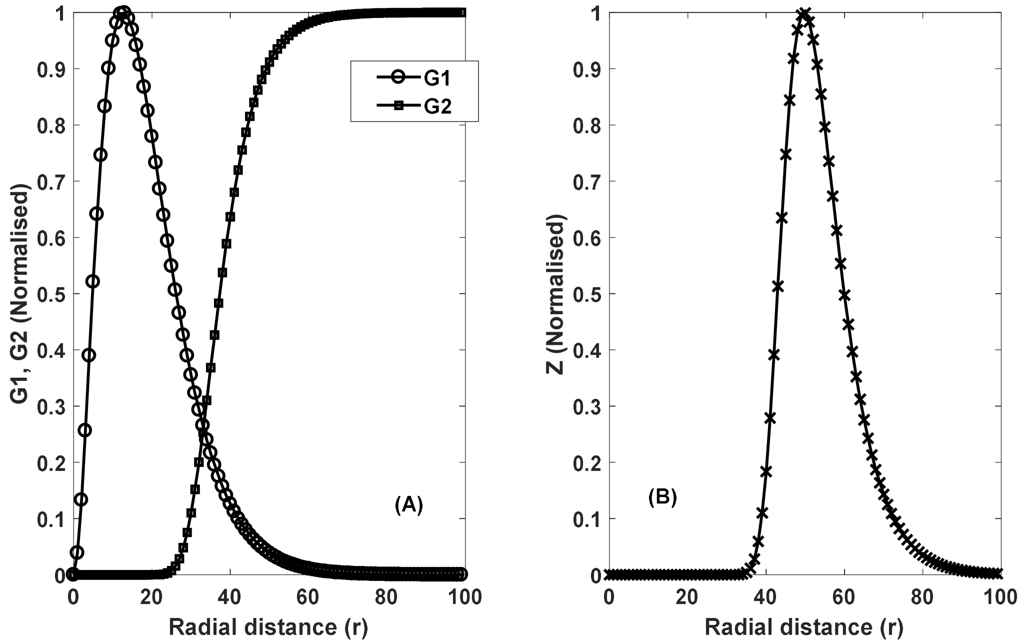

Figure 3.6 (A) Normalized plot of time dependent (G_2) and time independent (G_1) component of Z. (B) Normalized plot of Z for shown value of G_1 and G_2.

Motivation is to understand the experimental graphs given in literature [Jonscher and Polignac, 1984] and to draw a general inference about the nature of log (I) vs log (st) plot. In this pursuit the observed shape of integrand Z is explained in further discussion. Figure 3.6(A) illustrates the components G_1 and G_2. The product of both is Z as per equation (3.20). Initially the G_2 is almost equal to zero and G_1 is non zero. In a much later stage G_1 is almost equal to zero and G_2 is non zero. Hence, the product will be almost zero both in initial and later stage. In between it will have its maximum value. This explains the bell shape nature of Z as shown in Figure 3.6 (B).

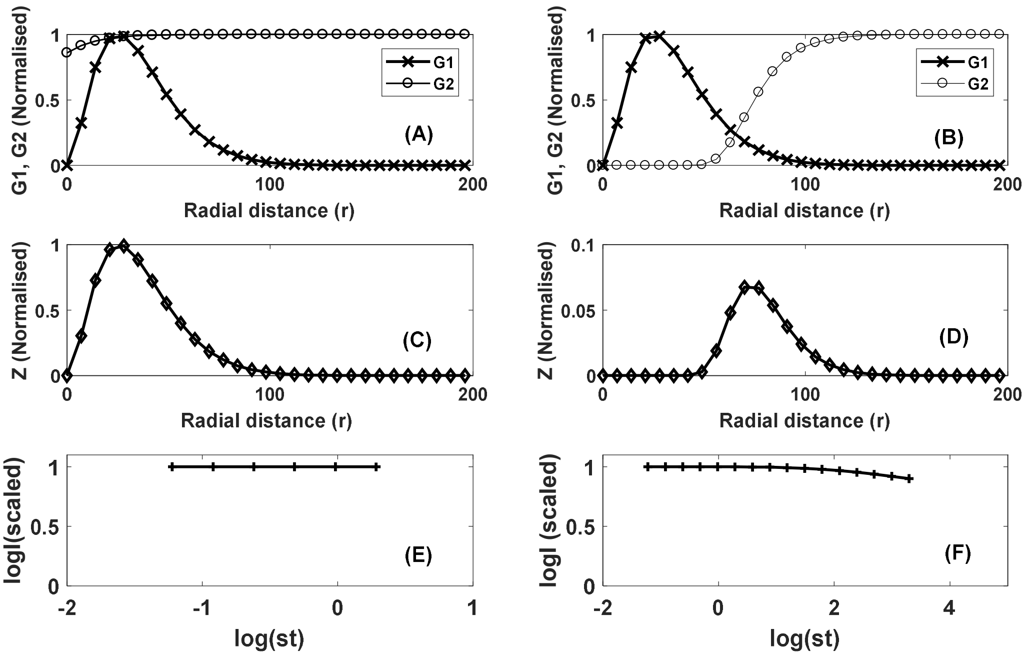

Figure 3.7 Temporal behaviors of the components of integrand Z.

(A) Position of G_1 and G_2 at time = 0.4 femto seconds. (B) Position of G_1 and G_2 at time = 655 femto seconds. (C, D) Location, shape and height of Z at the two points of time. (E, F) Log(I) vs log(st) graphs up to the two points of time. Plots are normalized for better comparison and clarity.

Further, it is intended is to see the progress of G_1 and G_2 with time. Figure 3.7 (A) and Figure 3.7 (B) respectively show G_1 and G_2 at time = 0.4 femto seconds and time = 655 femto seconds. It is obvious from the figure that the time dependent component is preserving its shape and is translating rightwards with time. Hence, the peak of Z will translate rightwards with time. It can also be seen from Figure 3.7 (C) and Figure 3.7 (D) that the height of Z is reduced. Hence, the spatial integration value of Z will be less in case 3.7 (D) as compared to case 3.7 (C). This explains the fall in log(I) vs log (st) graph with time. Figure 3.7 (E) and Figure 3.7 (F) illustrates the log(I) vs log(st) graph up to the two times respectively.

Effect of starting time of observation and period of observation

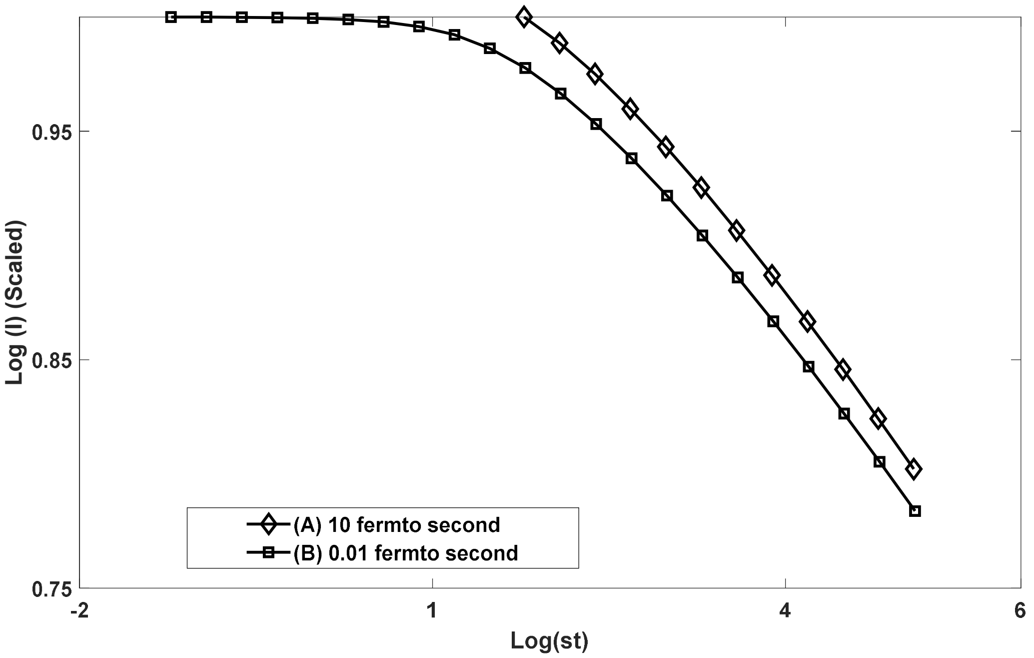

Figure 3.8 Effect of starting time of observation on log (I) vs. log (st) curve for two values of times.

Figure 3.8 illustrates that if we initiate the observation at a much lower value of time there is a larger probability of getting the initial flat region of Figure 3.7 (E). If the observation is initiated at later stage the graph may apparently look straight line as we have missed the horizontal region of Figure 3.7 (E).

Figure 3.9 shows the effect of observation period on log(I) vs. log (st) graph. It may be concluded that for a longer period of time the curvature of log(I) vs. log(st) graph may increase.

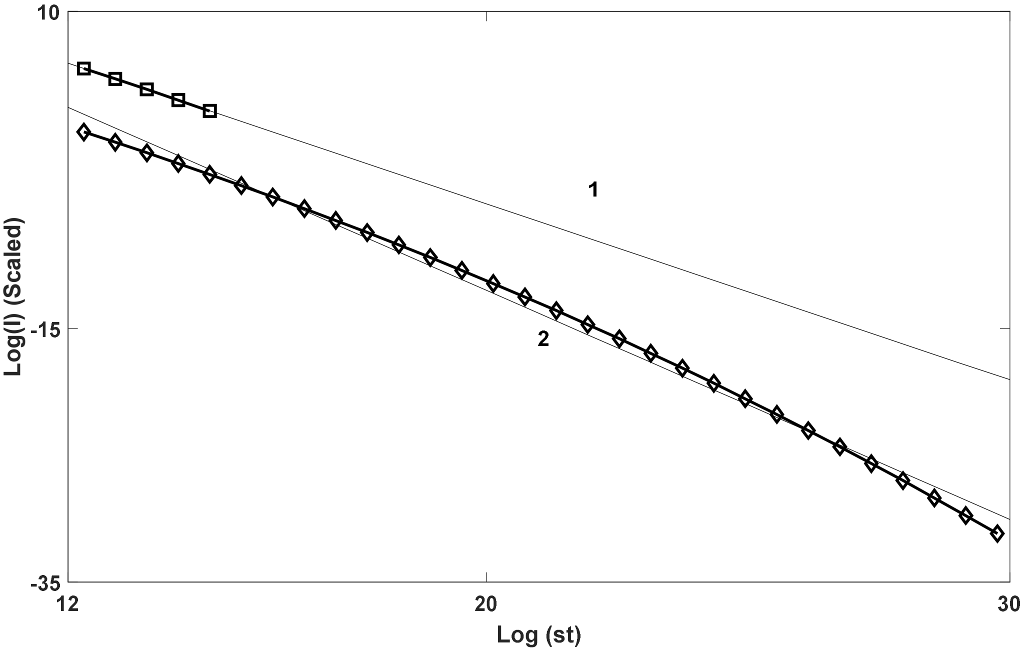

Figure 3.9 Effect of observation period on curvature of log(I) vs log(st) graph. Initial time of observation is 1 milliseconds.

(1) 1 second observation period (2) 3.6 X 10^7 years observation period.

Few other factors which may interfere in advent of non linearity

The other factors that may affect advent of non linearity include recombination center concentration and shape of NRPB between trap and RC. Figure 3.10 and Figure 3.11 illustrate this effect for these parameters respectively.

Curve fitting of log(I) vs. Log(st) plot with various functions

In this heading the motivation is to establish that non linear functions better fit the log (I) vs log(st) graphs as compared to linear functions (straight line). To illustrate this affect the fitting of apprently straight line as well as graphs have obvious curvature in log(I) vs log(st) is done.

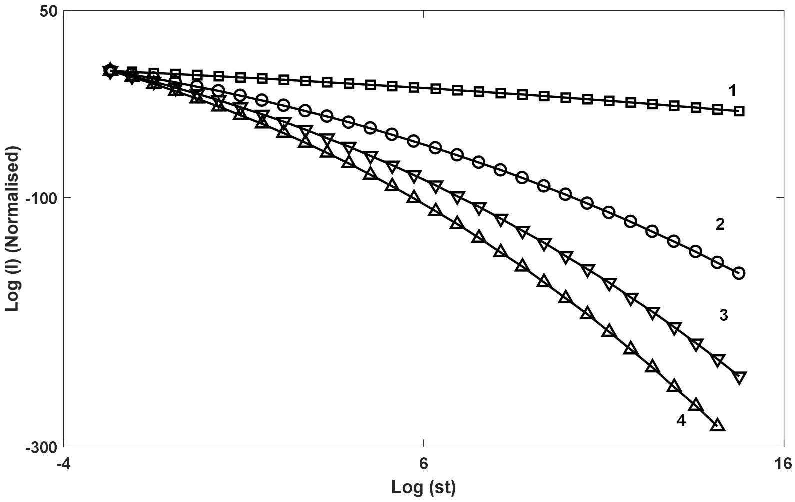

Figure 3.10 Effect of recombination centre concentration on advent of non linearity. The recombination centre concentrations are (1) 1 X 10^{22} m^{-3} (2) 1 X 10^{23} m^{-3} (3) 1 X $10^{23.2}$ m^{-3} (4) 1 X $10^{23.3}$ m^{-3}

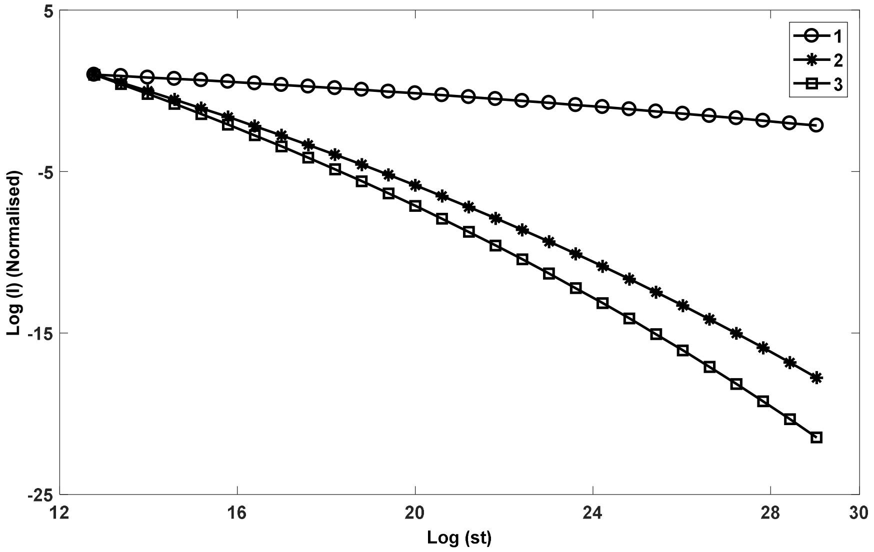

Figure 3.11 Effect of shape of potential barrier on advent of non linearity. The value of shape parameters (eVm^{-b}) are 1.D*=-1.9X10^{-4} 2. D* = 0.0 3. D* =-10^{-5}

Straight line $y = p_1 x + p_2$ (3.23)

Parabola $y = -p_3 x^2 + p_4 x + p_5$ (3.24)

Circle $(x - p_6)^2 + (y - p_7)^2 = p_8{}^2$ (3.25)

The fitting parameters are presented in Table 3.5 and 3.6. Table 3.7 illustrates the comparison of error with least square fitting with these functions

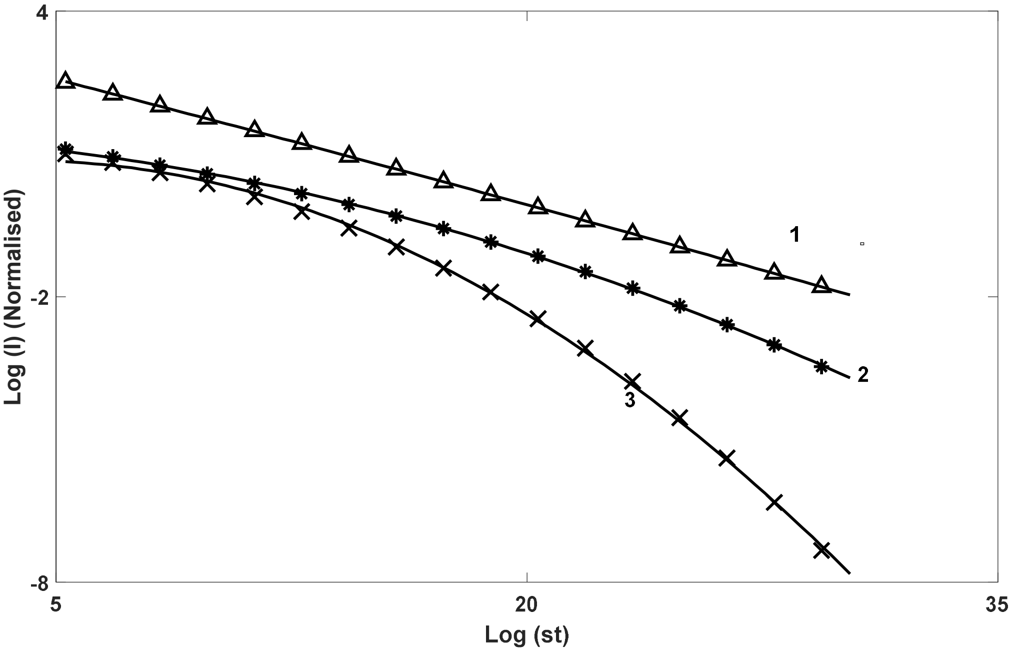

Figure 3.12 Log (I) vs log(st) graph for different RC concentrations. (1)10^{19} m^{-3}, curve (2) for $10^{22.5}m^{-3}$ and curve (3) for 10^{23} m^{-3} . The curve are fitted with $y = -p_3x^2 + p_4x + p_5$. The values of fitting parameters are tabulated in Table 3.5.

Table 3.5 Fitting parameters for the curves of Figure 3.12 with $y = -p_3x^2 + p_4x + p_5$.

Curve	p_3	p_4	p_5
1	0.0004	-0.1688	3.4259
2	0.0043	-0.0354	1.2611
3	0.0121	0.0986	0.6539

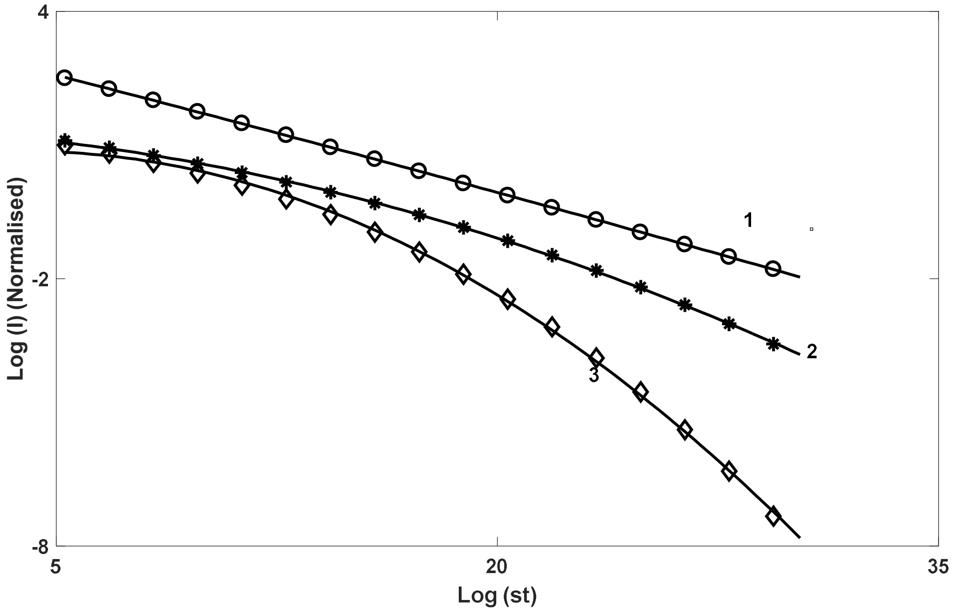

Figure 3.13 Log(I) vs log(st) graph with different RC concentrations (same as figure 3.12) fitted to $(x - p_6)^2 + (y - p_7)^2 = {p_8}^2$. Fitting parameters are shown in Table 3.6.

Table 3.6 Fitting parameters for the curves of Figure 3.13 with $(x - p_6)^2 + (y - p_7)^2 = {p_8}^2$

Curve	p_8	p_6	p_7
1	1.3 X 10^3	-212.5	-1.3 X 10^3
2	123.2	-5.2	-121.8
3	48.4	2.2	-47.8

Table 3.7 Least square fitting error with various functions.

	Curve fitting errors		
Curve	Straight line	Parabola	Circle
1	0.4	0.05	0.02
2	1.9	0.19	0.07
3	5.6	1.1	0.16

3.1.3 Thermally assisted fading

It is possible that the charge carriers get excited to some intermediate level and further tunnel to the recombination center site. This is known as thermally assisted fading.

3.2 Finite life time in conduction band

The assumption that life time of charge carrier in conduction band is negligible is another version (or implication) of QE approximation discussed before. In the previous chapter of this dissertation we have seen that rate equations for OTOR model can be decoupled using the QE approximation. There had been rigorous efforts to test the validity of QE approximation.

The validity of QE approximation can be tested by use of rate equations. Shenker and Chen [Shenker and Chen, 1972] had studied the subject and infer that QE approximation is valid only if $|\frac{dC_c}{dt}| < 10^{-3} |\frac{dC_t}{dt}|$. They further showed by solving the rate equations, that for the parameter set they had, the ratio of $|\frac{dC_c}{dt}|$ and $|\frac{dC_t}{dt}|$ changed from 5X 10^{-5} to 1.0. It is worth noting that towards the end of the peak, the highest ratios were obtained. Kelly et al. [Kelly et al., 1971] also concluded that QE approximation cannot be valid for full range of physically plausible parameters. Recently, Sadek and Kitis [Sadek and Kitis, 2017] has discussed and attempted to overcome some of the objections raised by Kelly et al [Kelly et al, 1971] and Opanowicz [Opanowicz, 1992]

3.3 NIK approximation

While developing the RW, GG and MP equations it was seen that basic assumption was existence of an isolated trap and recombination center. This comes under general conception of OTOR model. But in actual crystal there will be multiple traps and multiple recombination centers. It is obvious that a charge carrier once excited to conduction band will not differentiate between different types of traps for getting re-trapped. In other words, the traps will interact.

Many people studied the interactive kinetics approximation. The general way to approach this problem is to write a set of rate equations for a system of traps and RCs.

For $i = 1\ to\ u$

$$\frac{dC_{ti}}{dt} = -C_{ti}f_i \exp(-D_i/KT) + C_c(C_{ri} - C_{ti})B_{ti} \tag{3.26}$$

For $j = 1\ to\ v$

$$\frac{dC_{rj}}{dt} = -C_c C_{rj} B_{trj} \tag{3.27}$$

For conduction band we may write

$$\frac{dC_c}{dt} = \sum_{i=1}^{u} C_{ti}f_i \exp(-D_i/KT) - C_c\left[\sum_{j=1}^{v} C_{rj}B_{trj} + \sum_{i=1}^{u}(C_{Ti} - C_{ti})B_{ti}\right] \tag{3.28}$$

These equations can be solved in two ways

1. By use of QE approximation these can be decoupled and an equivalent OTOR model can be developed [Levi, 1985; Levi, 1991].
2. With QE the rate equations can be solved numerically. This was done by Bull et al. [1986].

For the case where recombination dominates over re-trapping the two approaches give similar solution. But, as soon as the approximation breaks down, the two approaches start differing.

3.4 Temperature dependence of parameters

As per the conditions under which Arrhenius law can be applied [Gibbs, 1972], frequency factor should not be dependent upon temperature. But as per findings of Eyring, using the absolute reaction theory [Eyring, 1936], frequency factor should be proportional to absolute temperature. Other studies [Keating, 1961] also suggests frequency factor should be slightly temperature dependent.

Law of detailed balance [Bube , 1960] states

$$f = C_c \, u \, \sigma \tag{3.29}$$

Where

u= Speed of charge carrier

σ = Capture cross section of the trap.

It is well known that

$$u \, \alpha \, T^{1/2} \tag{3.30}$$

And σ has dependency on temperature of the form T^{-a} (0< a < 4) [Lax, 1960] and

$$C_c \, \alpha \, T^{3/2} \tag{3.31}$$

Hence,

$f \, \alpha \, T^{-d}$ where $-2 < d < 2$ [Keating, 1961; Chen, 1969; Balarin 1979] (3.32)

But slight temperature dependence of frequency factor is masked by the strong temperature dependence of Arrhenius law.

3.5 Uncertainty in parameters

May the trap parameters be found by any numerical or experimental methodology, there will always be uncertainty associated with it. Hence, it is interesting to see how uncertainty in parameters propagates through the models and appears as final uncertainty in TL output.

Chapter four is dedicated to study of this aspect with a focus on RW, GG and MP models.

3.6 Re absorption

There is a possibility that the TL released may be absorbed by trapped charged carrier and lead to its optical release. The rate equations in this scenario will be as discussed by Chen and Mckeerver [Chen and Mckeerver, 1997]

$$\frac{dC_c}{dt} = C_t\, f \exp\left(-\frac{D}{KT}\right) - C_c C_r B_{tr} \exp(-\beta\, C_t) - C_c B_t\, (C_T - C_t) \tag{3.33}$$

$$\frac{dC_t}{dt} = -C_t\, f \exp\left(-\frac{D}{KT}\right) + C_c B_t\, (C_T - C_t) - (1 - exp\,(-\beta\, C_t))\, C_c\, C_r\, B_r \tag{3.34}$$

$$\frac{dC_r}{dt} = -C_c\, C_r\, B_{tr} \tag{3.35}$$

Where

β = Absorption probability of photons by trapped electrons.

In this case the thermal component of TL will be given by

$$L_{TL} = C_c\, C_r\, B_{tr} \exp(-\beta\, C_t) \tag{3.36}$$

In real material many scenarios may be expected. For example, one possibility is TL emitted may be partially absorbed by the deeper trap. This will not only reduce the TL intensity but also opens a possibility that due to optical excitation charge carriers may be transferred from deeper traps to dosimetric traps.

Over all self absorption will distort the glow curve structure of the material.

3.7 Quenching effects

3.7.1 Thermal Quenching

Whether or not a material is a thermoluminescent material, the luminescence efficiency is given by

$$L_\eta = \frac{P_r}{P_r + P_{nr}} \tag{3.37}$$

L_η is found to be strongly temperature dependent in various material. For example, Johnson and Williams [Johnson and Williams, 1952] and Fillard et al. [Fillard et al., 1978] have discussed few materials in this context. There are various explanations of temperature dependence of luminescence efficiency. Two will be discussed here.

Mott Seitz explanation

The mechanism is given by Seitz [Seitz, 1940] and Mott and Gurney [Mott and Gurney, 1948]. They considered electronic transition within the excited state and ground state of same atom, and made use of configurational co-ordinate diagram and Franck Condon principle. The conclusion of their study is the probability of non radiative transition is related to temperature by Boltzmann factor $\exp\left(-\frac{\Delta E}{KT}\right)$ where ΔE is the minimum energy required by the charge carrier in excited state to lose its energy without emission of radiation. The radiative transition is unaffected by temperature. Hence,

$$L_\eta = \frac{1}{1+c\,\mathrm{ex}\left(-\frac{\Delta E}{KT}\right)} \tag{3.38}$$

Schon – Klasen explanation

The mechanism of this explanation is as follows. Once the charge carriers are excited to conduction band they recombine at RC. But, at high temperature electron recombination center (holes) get detached from their sites and get associated with killer centers. Killer centers are those centers at which recombination do not produce any luminescence. The process is accelerated with temperature. Hence, the probability of non radiative recombination increases with temperature.

There are other explanations also present in the literature. As an example, non radiative capture of an electron in conduction band by the localized energy levels [Rickayzen, 1957] is one suggestion.

3.7.2 Concentration Quenching

With increase in concentration of dopent the luminescence efficiency first increases and after reaching a maximum limit, luminescence efficiency start decreasing. This decrease in luminescence efficiency with increase in concentration of dopent is called as concentration quenching. Schmidt et al. [Schmidt et al., 1974] studied $CaSO_4$: Dy and $CaSO_4$: Tm in context of this effect. Ewles and Lee [Ewles and Lee, 1953] gave mathematical expression for this phenomenon.

$$L_\eta = K'/(1 + \breve{o}\, C_d^{-1} \exp(C_t C_d)) \tag{3.39}$$

where

K', ŏ are constants.

C_d= Dopent concentration

3.7.3 Impurity Quenching

Introduction of certain elemental impurity, especially heavy metals such Cu, Fe, Co, Ni and Cr, reduces the intensity of TL emission drastically. This is called impurity quenching.

Metallic impurities act as killer centers. Killer centers add competitive non radiative recombination path.

3.8 Residual TL

Whatever TL signal is left in the dosimeter after first readout in a previously exposed dosimeter is termed as residual TL. It is obvious that signal will be left in dosimeter because the deeper traps are certainly not emptied completely during the first readout. This happens because the temperature is not sufficient for the excitation of deeper trap.

In a hot gas reader system with $CaSO_4$: Dy Teflon embedded dosimeter the second readout (which is almost equal to the residual TL) is 10% of the first readout. The importance of residual TL in personnel monitoring program is twofold.

- It is used to confirm the first readout dose for the cases where excessive dose is estimated by the first readout.
- In case of loss of first readout data it is used to estimate the dose.

The origin of residual TL is not explicitly explained in the literature. Hence, it is intended to explore the origin of residual TL.

Experimental set up and procedure

The dosimeter used is $CaSO_4$: Dy Teflon embedded disc (13.3mm diameter and 0.8mm thickness). The concentration of Dy is 0.05mole %. The discs are fixed on a nickel plated aluminum plate. The reader model is TLD BR 7B, which is a hot gas based semiautomatic reader with Nitrogen gas jet temperature ~ 285ºC. The flow rate of Nitrogen is 5 liters per minute and dosimeters are exposed for 30 seconds to this jet during the readout process.

For experimental part of the work after annealing (230ºC, 4 hours) the dosimeters were exposed to 3, 5 and 10 mSv using Cs-137 Gamma source. For exposure the dosimeters were sandwitched between 1.6mm PMMA plates for buildup.

Mathematical formulation

The process of heat transfer from hot gas to solid can be modeled using following differential equation [Van Dijk and Julius, 1993]

$$\frac{dT}{dt} = \frac{\varpi \dagger \left(T_G - T(t)\right)}{m^* C_p} \tag{3.40}$$

Where

ϖ = Heat transfer efficiency

$\dagger$ = Area of dosimeter exposed to hot jet

C_p= Heat capacity of material of dosimeter

m^* = Mass of dosimeter

T_G = Temperature of hot gas

$T(t)$ = Time dependent temperature profile of dosimeter

We can solve equation (3.40) with initial condition $T(0) = T_o$

$$T(t) = T_G - (T_G - T_o)\exp(-\text{Ѫ}t) \tag{3.41}$$

Where

$\text{Ѫ} = \varpi\text{Ϯ}/mC_p$

Rate equation for change of trapped charge carrier density is given by [Chen and Mckeever, 1997]

$$-\frac{dC_t}{dt} = C_t\, f \exp(-\frac{D}{KT}) \tag{3.42}$$

Using the profile given by equation (3.41) we may write

$$\frac{dC_t}{dt} = -\,C_t f \exp(-\frac{D}{K(T_G - (T_G - T_o)\exp(-\text{Ѫ}t))}) \tag{3.43}$$

$$\frac{dC_t}{dt} = -C_t f \exp(-\text{Ж}\frac{1}{(T_G - \Pi\exp(-\text{Ѫ}t))}) \tag{3.44}$$

Where

$\text{Ж} = D/K$

$\Pi = (T_G - T_o)$

The solution of equation (3.44) can be obtained numerically

$$\frac{C_{t_{i+1}} - C_{t_i}}{\Delta t} = -C_{t_i} f \exp(-\text{Ж}\frac{1}{(T_G - \Pi\exp(-\text{Ѫ}t))}) \tag{3.45}$$

$$C_{t_{i+1}} = C_{t_i} - \; [C_{t_i} f \; \exp(-\text{Ж}\frac{1}{(T_G - \Pi \; \exp(-\text{Ϫ}t)\,)})] \; \Delta t \qquad (3.46)$$

Using equation (3.46) we may do a book keeping of values of C_t with time and it can be further differentiated to obtain the TL

$$TL = -\frac{dC_t}{dt} \qquad (3.47)$$

For getting the TL from all the traps we may sum up the TL from individual traps

$$TL_{net} = \sum_{j=1}^{N} TL_j \qquad (3.48)$$

TL_j = TL signal obtained from j^{th} type of trap

Numerical simulation

For numerical work the trap structure of $CaSO_4$: Dy given by Oliveri et al [Oliveri, 1978] is used. Initial charge carrier density was calculated to be of the order of $10^{18}m^{-3}$ for an absorbed dose of 3mGy [Sahai et al., 2017]. This can be used as initial condition in equation (3.46) and the value of trapped charge carrier density of each time step (500 steps of 0.06 seconds each) can be obtained. The value of charge carrier density recorded can be further differentiated to obtain the TL as per equation (3.47). TL from each trap can be added to obtain the overall luminescence intensity in accordance with equation (3.48). For a simulation of 30 seconds the data represents the first readout. Taking the left over value of charge carrier densities as the initial concentration we can re-run the simulation code for 30 seconds to obtain the second readout data.

Results

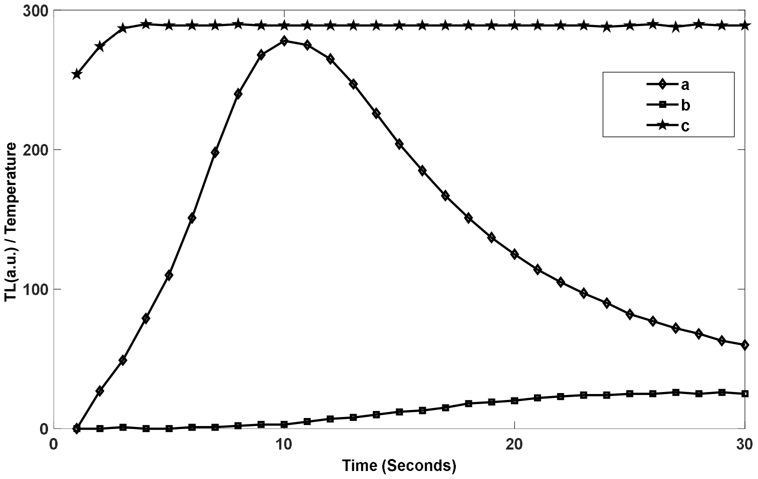

Figure 3.14 Experimental first (a), second (b) read out glow curves and hot gas temperature profile (c).

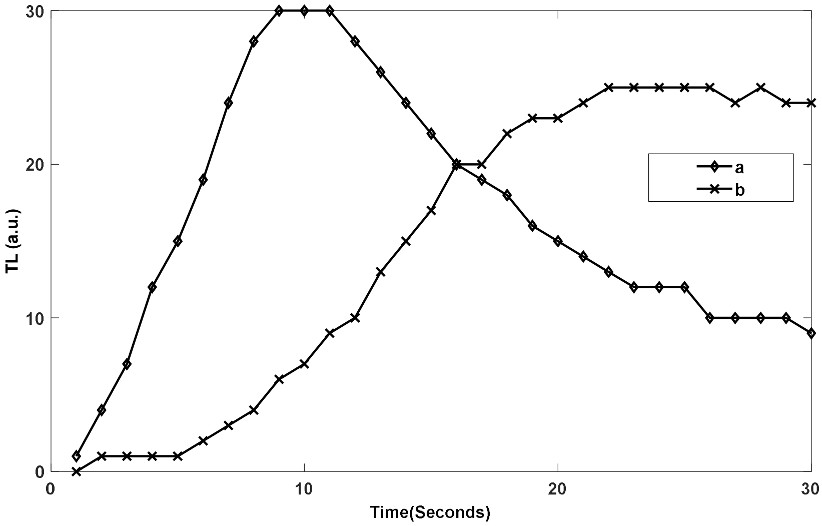

Figure 3.15 Characteristic shape differences in first (a) and second (b) readouts for same dose.

Figure 3.14 is an illustration of experimental first and second readout for 3mSv of dose. Figure also illustrates the profile of temperature of hot gas obtained experimentally. Figure 3.15 is an illustration of characteristic shape difference in first and second readout for same value of dose. Numerically calculated profile of temperature of disc material is compared with profile of temperature of hot gas in Figure 3.16.

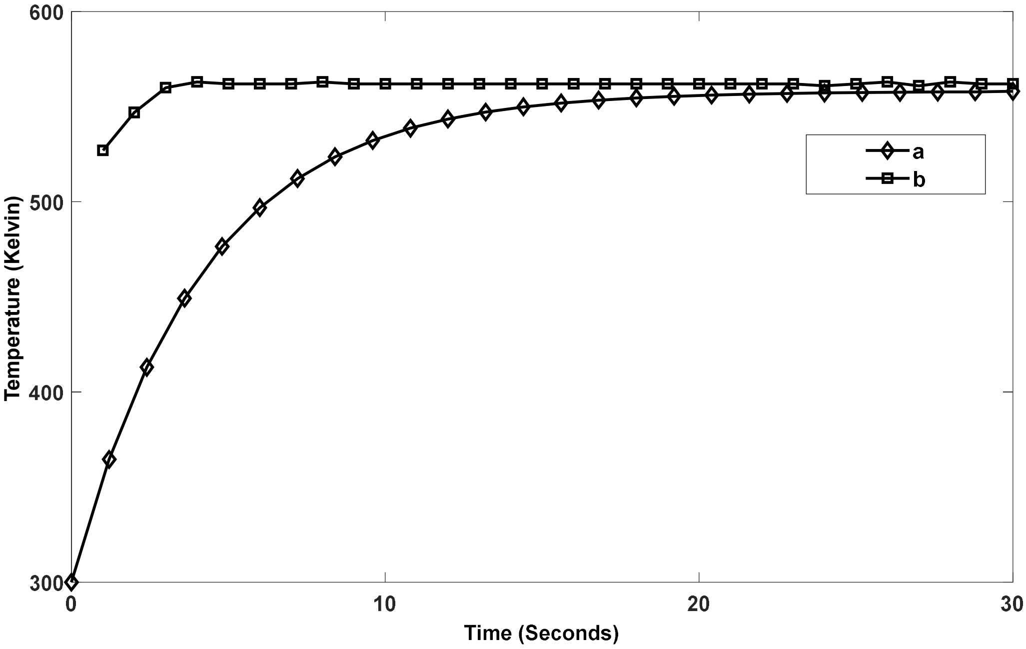

Figure 3.16 Simulated temperature profile of disc (a) and experimental hot gas temperature profile (b).

The first readout from each trap is plotted in Figure 3.17. This illustrates their separation in time scale and characteristic shape difference. It is worth observing that shape of first readout of deeper traps corresponds to residual TL shape closely. Numerically simulated 1st and 2nd readout glow curve data is compared with experimental glow curves for 3mSv of dose in Figure 3.18. It can be seen that there is a reasonable good match. Hence, it can be concluded that residual TL originate from trapped charge carriers in traps deeper than dosemetric trap which do not deplete completely in first readout. The TL left over in dosemetric trap is not a significant contributor to the residual TL.

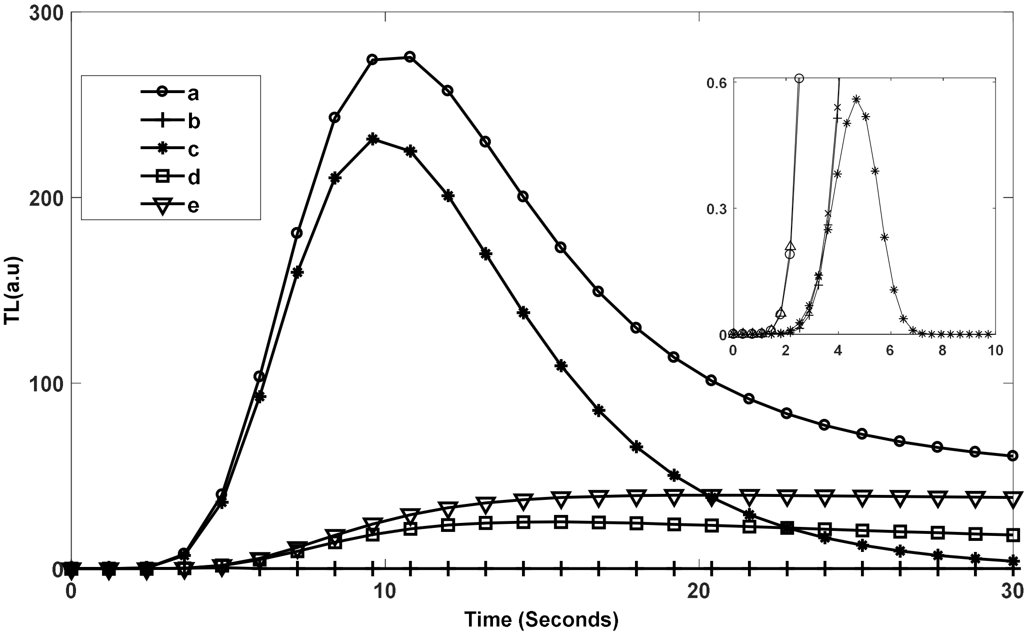

Figure 3.17 First readout glow curve from different types of traps. Overall TL (a) is a summation of TL from shallow (b), dosemetric (c) and deeper (d, e) traps.

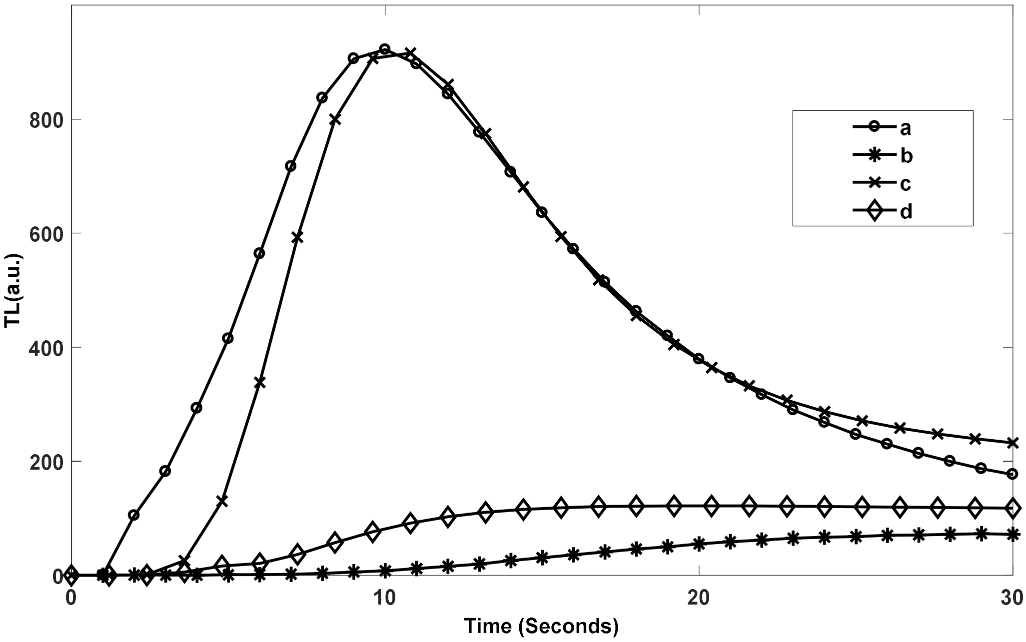

Figure 3.18 Experimental first (a), second (b) readouts and simulated first (c) and second (d) readouts.

3.9 Non linear response of TL dosimeter

As dosimetry is based on calibration of dosimeter at one point on Dose vs TL output graph, if there is a non linearity in TL output vs amount of radiation incident plot, it will obviously result in error in estimated dose. The aim of this section is to study these effects.

Experimentally speaking there are two types of non linearity :

- First we have a linear region in TL output vs imparted dose graph and non linearity comes at a later stage.
- First we have a non linear region in TL output vs imparted dose graph and linear region comes at a later stage.

Two terms have been coined to understand the phenomenon of non linearity.

Supralinearity

Supralinearity index is defined as

$$\chi\,(d) = \frac{(\zeta(d) - \zeta_0)/d}{(\zeta(d_l) - \zeta_0)/d_l} \tag{3.49}$$

$\chi\,(d)$= Response function (or supralinearity index) at dose D.

$\zeta(d)$= TL intensity value at dose D.

$\zeta(d_l)$= TL intensity value at dose D_l.

d= Dose at which investigation is being done.

d= Dose at which linearity exist.

ζ_0= Intercept on TL axis, actually it is the response of dosimeter at zero dose.

The concept of linearity, sublinearity or supralinearity is defined by $\chi\,(D)$.

$\chi\,(d)$= 1	Linear response at dose d
$\chi\,(d) < 1$	Sublinear response at dose d.
$\chi\,(d) > 1$	Supralinear response at dose d.

This has been discussed previously in chapter one but is again given here for the sake of continuity.

Superlinearity

Superlinearity index is defined as

$$\text{ƙ}\,(d) = \frac{D\,\zeta''(d)}{\zeta'(d)} + 1 \qquad (3.50)$$

ƙ (d) > 1 Superlinearity

ƙ (d) = 1 Linearity

ƙ (d) < 1 Sublineariy

It is worth noting that the two terms are similar but not equivalent. We may have cases where ƙ (d) < 1 but still the graph is above the extrapolation range i.e. $\chi\ (d)$ > 1.

Conceptual explanation of non linearity

Conceptually the non linearity is explained on the basis of competition between the traps during filling and during readout.

During filling

Suppose a situation where we have a recombination center and two traps, the dosimetric trap and a competing trap. If the capture cross section of competing trap is larger in that case it will be filled faster (assuming the concentration of the two traps is almost same).

In the starting phase the charge carriers generated will be trapped in both the traps and while reading the signal will be proportional to the charge carriers tapped in the dosimetric trap i.e. a fraction of total amount of charge carriers generated. But as soon as the competing trap goes to saturation, more and more fraction of total amount of charge carriers generated will be trapped in the dosemetric trap and hence, the TL will be proportional to larger fraction of total charge carriers generated. This will lead to super (or supra) linearity in the TL output vs imparted dose graph.

During heating

Again assume a situation of a recombination center and two traps one competing trap and one dosimetric trap. While heating the charge carriers trapped in the dosimetric trap will be excited to the conduction band. A part of it will be recombining with the recombination center to produce luminescence and rest of it will be re-trapped in the competing trap. Hence, the TL will be proportional to a fraction of charge carriers liberated from the dosemetric trap. As the competing trap will tend to saturation more and more fraction of charge carriers liberated from the dosemetric trap will recombine with the recombination center to produce luminescence. Hence, TL will be proportional to larger fraction of charge carriers liberated from the dosemetric trap.

3.10 Other factors

There are various experimental factors which may lead to deviation from true dose in TL based dose estimation. There is extensive literature on it [Chen and Mckeever, 1997]. For the sake of completeness the factors are discussed below.

A) Arising from TL instrumentation

Black body radiation

For TL emission we have to heat the sample. This leads to emission of IR from the planchet as well as from the sample. Though IR filters are used but they do not cut the IR completely. Hence, the luminescence that is emitted from the sample is altered by the IR signal.

Mechanical Misalignment

In TLD reader system, TLD and PMT should be perfectly aligned. Slight shift of TLD from the position at which calibration was done may affect the true dose estimation.

Dark Current of PMT

Due to thermionic emission (at ambient temperature), PMT gives signal even when no dosimeter is there. This is called dark current. It is of the order of nA. It also affects dose estimation.

Non linearity

In TL based dosimetry it is assumed that response of the reader is linear. But many times the output current of PMT is not linearly related to the input luminescence. This mainly happens at high doses.

In addition to above mentioned factors light leakage, fluctuation in temperatue profile during readout, chemiluminescence (luminescence arising due to chemical reactions), triboluminescence (luminescence arising due to mechanical stress) affects the signal.

B) Arising from Dosimeter

Binding material

We use binding material for making disc out of powder. It may also affect the performance of TL dose estimation.

Grain size

Thermoluminescence from TLD material is well known to be affected by the grain size of TLD material.

C) Arising from field conditions

We calibrate the dosimeters in panoramic conditions. Whereas, in field incidence of radiation is possible from all directions. In addition to this, natural background (though it is corrected by use of control cards) also affect the dosimetric performance.

3.11 Conclusions

In this chapter we have discussed various reasons because of which dose estimated by RW, GG and MP models may not be exact. As elaborated in this chapter reasons are theoretical (limitations of models), experimental as well as arising from field conditions. The emphasis in this chapter was on theoretical factors like quasi equilibrium approximation and its validity, non interactive kinetics and its validity, temperature dependence of parameters, re-absorption of TL emission and its after effects, various forms of quenching etc.

Our contribution to literature on fading and residual TL has been emphasized in this chapter at appropriate places. In the domain of residual TL it has been established that the origin of residual TL are the deeper traps and the left over TL in dosemetric trap is not the major contributor to residual TL. In the domain of fading the experimental data on afterglow has been explained theoretically and it has been established that non linearity is general feature of afterglow.

These topics have got sufficient attention in literature, from both theoretical as well as experimental perspective. But there is one domain which is almost unexplored. Parametric uncertainty analysis of these models has not got sufficient attention in the literature. So, in next chapter we will be discussing parametric uncertainty analysis of these models.

CHAPTER IV

Parametric Uncertainty analysis of Basic TL models

In this dissertation various TL models have been discussed. From the models and mathematical expressions derived from them, model predicated temperature vs. TL intensity graphs (known as glow curves) can be obtained. It has also been elaborated that there are various factors that may lead to deviation in TL intensity from model predicated TL intensity values. One of the reasons is uncertainty in trap parameters. This chapter is dedicated to uncertainty propagation through basic TL models (RW and MP). GG models is not given elaborate attention as MP equation holds good for GG model with numerical value of order of kinetics equal to two.

This study is relevant as it can be hypothesized: any theoretical or experimental methodology, used to arrive at the trap parameter values (values of Trap depth (D) and attempt to escape frequency (f)) will always report the values of trap parameters with some uncertainty. This uncertainty will propagate through the TL models and lead to uncertainty in the TL intensity output. What is the trend of temperature vs. Uncertainty in TL intensity due to parametric uncertainty? This is question intended to be probed in this chapter.

This chapter is bifurcated into three sections based on methodology used to carry out the uncertainty analysis. Section 4.1 is based on Monte Carlo (MC) technique, section 4.2 on Fuzzy set theory technique and section 4.3 on Polynomial chaos expansion (PCE) technique. Each section starts with discussing the algorithm for uncertainty propagation using particular method and concluded with results followed by discussion.

4.1 Monte Carlo (MC) approach for uncertainty propagation

There are certain prerequisites to understand this method; hence they are discussed here.

Probability density function (PDF)

If there is a set of data, it is always possible to obtain a histogram of the data by taking a appropriate bin size. This histogram is called as frequency distribution. An area normalised frequency distribution is called as probability density function (PDF).

Cumulative distribution function (CDF)

From a PDF it is possible to arrive at the CDF using following equation.

$$CDF\ (x) = \int_0^x PDF\ (y)dy \tag{4.1}$$

Where x is the parameter value and y is a dummy variable.

Inversion Method

This is a method for generating set of parameter values whose PDF is given. The method is as explained below.

From the given PDF, CDF is to be generated using equation (4.1). In the CDF the X axis has the parameter value and Y axis has range from 0-1. A random number is generated between 0-1 and corresponding point on X axis is to be found using the CDF. This way one value of parameter is obtained. By repeating this process many times a set of values of parameters is obtained whose distribution is as per initially taken PDF.

4.1.1 Algorithm for uncertainty propagation using MC

The general scheme for MC method applied to uncertainty analysis of individual TL peak is illustrated in flow chart on next page

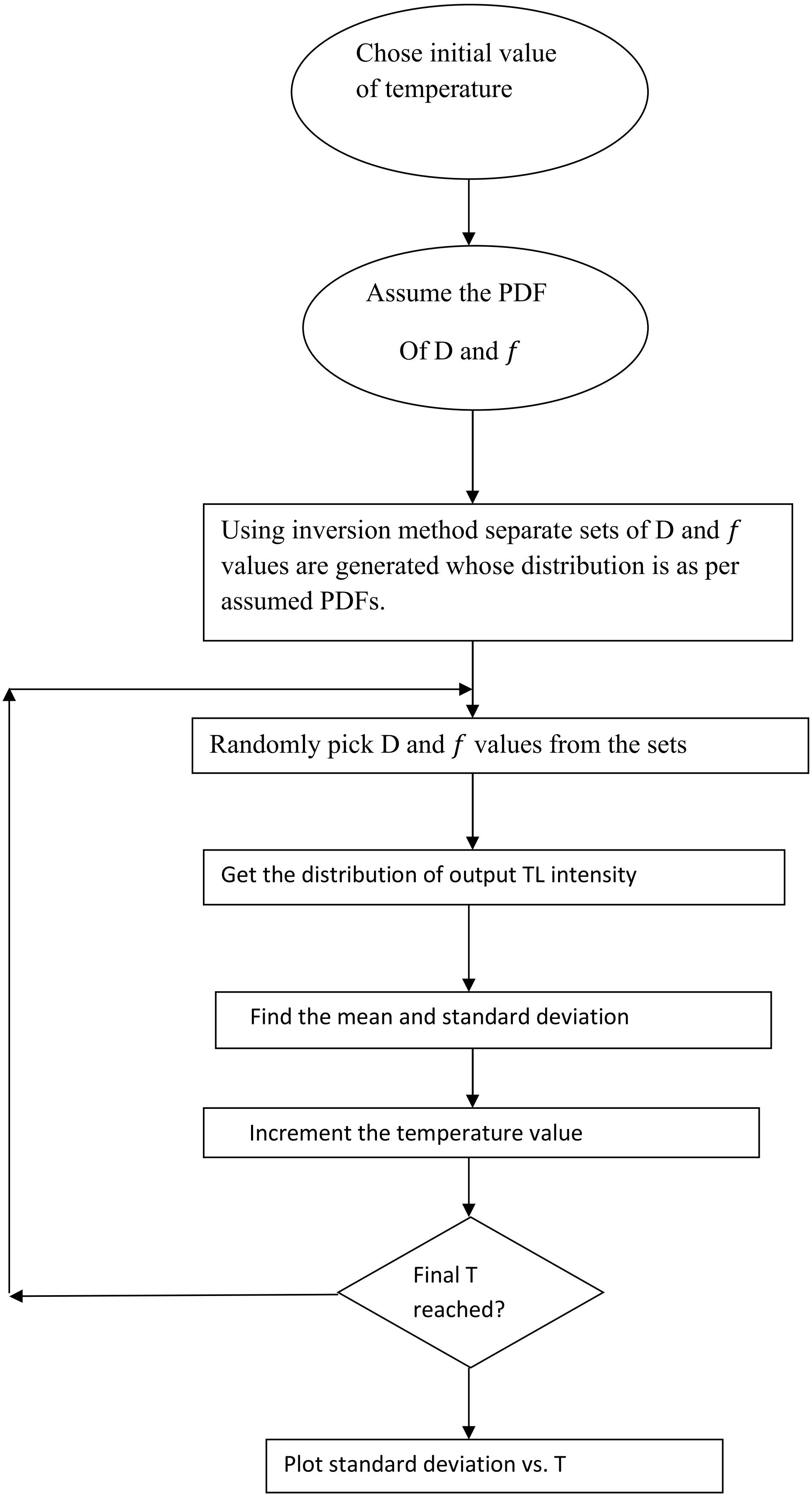

Figure 4.1 Algorithm for uncertainty propagation using MC technique.

4.1.2 Simulation results

In Monte Carlo method the first question that is required to be settled is the sample size. Sample size is the number of data in the parameter set. In present case the sample size is defined as number of data in the set of trap depth (D) and attempt to escape frequency (f) . Hence, it is required to be established that how many data should be in each set of trap parameters. It is pertinent to mention at this point that we have two separate sets, one of trap depth (D) and other of attempt to escape frequency (f) to avoid any confusion.

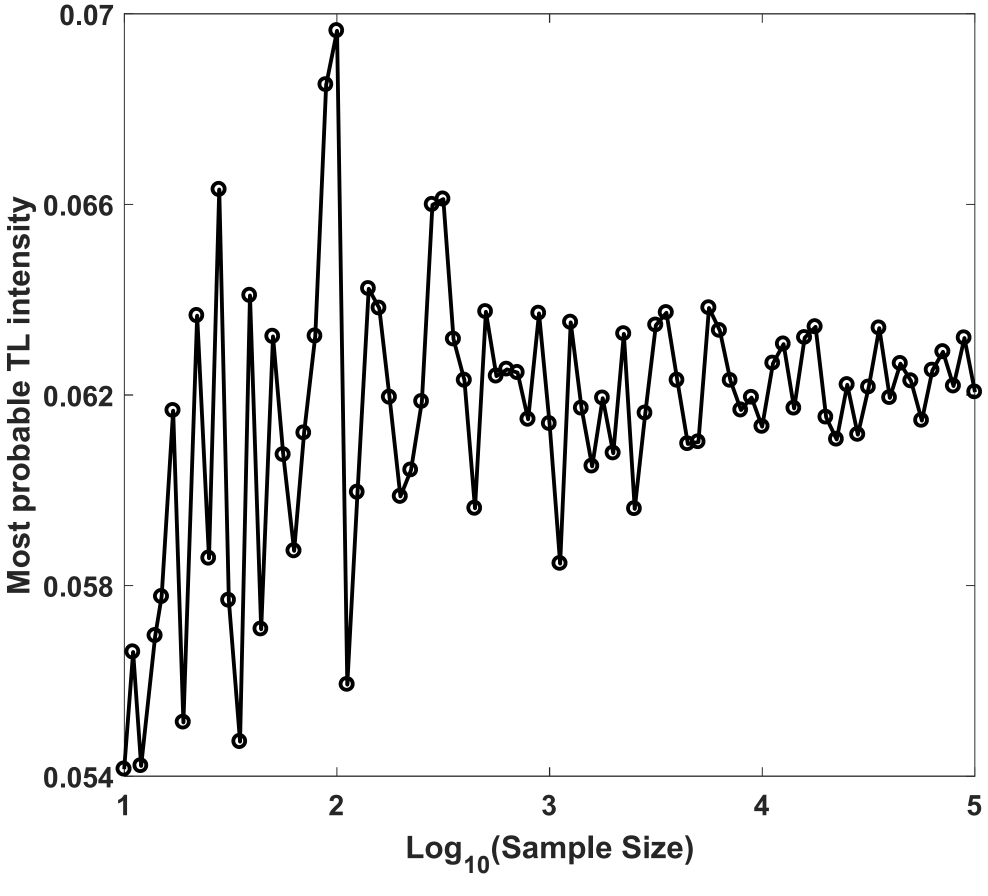

Figure 4.2 Optimisation of sample size. For this plot trap depth (D)=1.3eV, standard deviation in trap depth (σ_D)=.005eV, frequency factor (f)=10^{12}sec^{-1} and standard deviation in attempt to escape frequency (σ_f)=10^{10}sec^{-1}. Heating rate is 5°K/sec.

It is required to optimize the sample size. With increasing sample size the statistical fluctuation will be reduced. At the same time the increasing sample size will also raise the computational burden. Hence, a trade off is required.

In order to do this sample size from 100 to 10^5 is taken. With each sample size D and f values are sampled randomly from respective sets and a set of TL intensity values is obtained. By numerically generating the histogram, the most probable value of TL intensity is found. Further a graph is plotted between sample size and most probable value of TL intensity. This graph is shown in Figure 4.2. It can be seen in the plot that the fluctuation is reduced with increasing sample size. Looking at this graph we optimize the sample size to be 3000.

Further with this sample size parametric uncertainty analysis of individual TL peak is done. This is done for first order and general order kinetic equations of thermoluminescence also known as RW and MP model equations. Analysis of second order kinetic equation (GG model) is not done as general order kinetic equation exactly represents the second order kinetic equation with value of order of kinetics equal to two.

4.1.2.1 First Order Kinetics

After generating a set of Gaussian distributed 3000 values of trap parameters (D and f) having mean and standard deviation as documented in Table 4.1, we randomly sample from respective sets and find the output TL intensity at a given temperature using first order

Table 4.1 Mean value and standard deviation of PDFs of trap parameters

Trap Parameter	Mean value	Standard Deviation
Trap Depth	1.3 eV	0.005 eV
Attempt to escape frequency	10^{12} sec^{-1}	10^{10}sec^{-1}

Kinetic (RW) model equation. By this way a distribution of TL intensity is obtained. 1σ value is calculated from both the sides of the most probable value. This process is repeated for full range of temperature. Figure 4.3 shows the obtained graph.

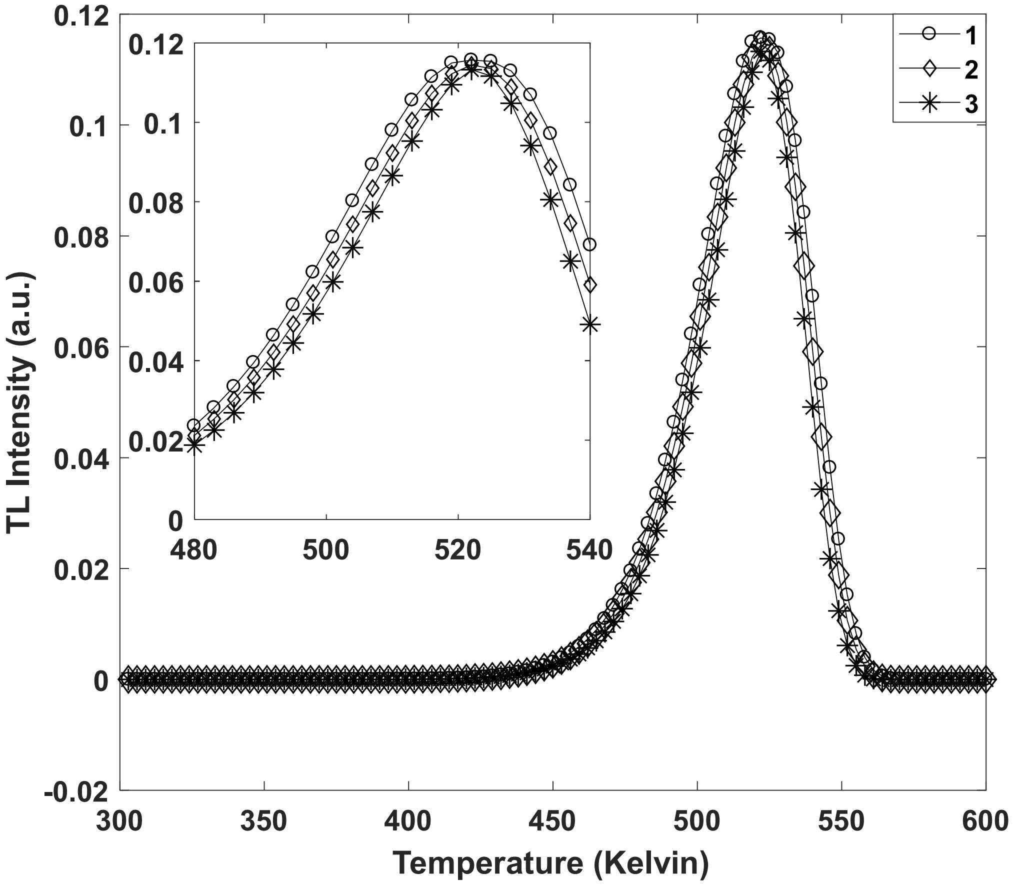

Figure 4.3 Output thermoluminescence intensity (2) with its 1σ values (1, 3) on both side. Values of parameters are same as Figure 4.2.

As not much is obvious from Figure 4.3, hence, the 1σ value is subtracted from the mean on both the sides and is plotted in Figure 4.4. This plot is termed as positive and negative residue plot. From Figure 4.4 the trend of uncertainty along with temperature can be observed which was not evident from Figure 4.3. There are two maximums close to temperature corresponding to half intensity value of TL intensity with a minimum at temperature corresponding to peak of TL intensity in the glow curve. Glow curve has been illustrated in Figure 4.3.

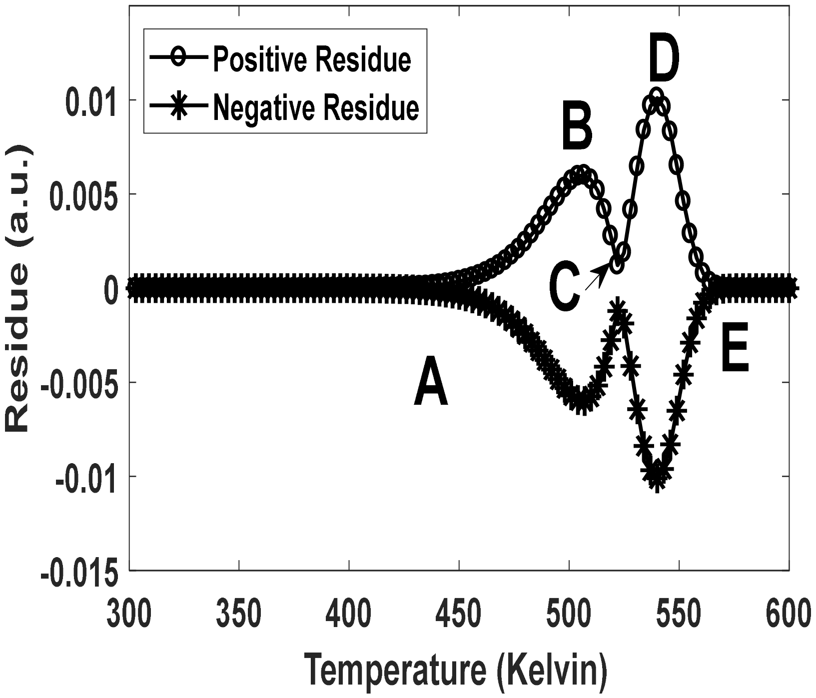

Figure 4.4 Positive and negative residue as a function of temperature for first order kinetics (RW model) of thermoluminescence. The values of parameters are same as Figure 4.2.

There is another way of visualising the same phenomenon. At each point of temperature we have PDF of TL intensity. From these PDFs, the CDFs at each temperature point can be obtained. Figure 4.5 shows the CDFs at five illustrative points. From CDFs at each temperature the 2.5th and 97.5th percentile can be obtained.

These values can be plotted against temperature to get the uncertainty profile. It can be seen from Figure 4.4 that in the region ABC and CDE the trend is same. The graph is raising, reaching a maximum, and then falling. Hence, for visual clarity 2.5th -97.5th percentile plot is done in only one region namely, ABC. This plot is shown in Figure 4.6.

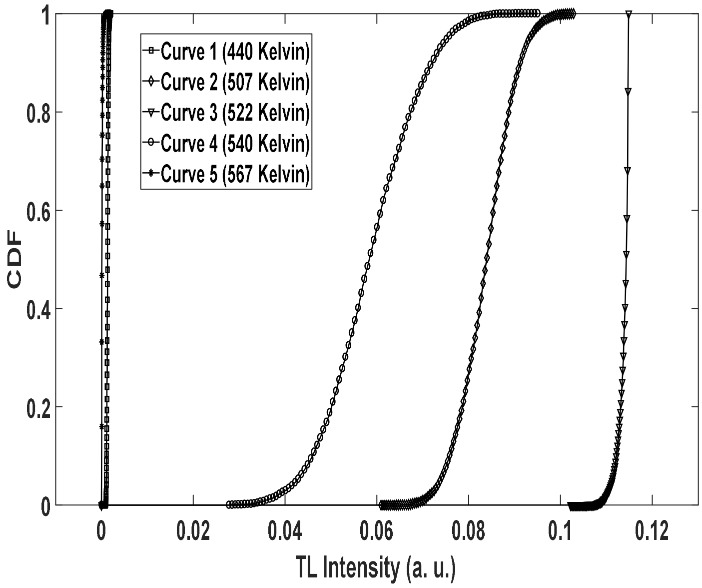

Figure 4.5 CDFs for mentioned values of temperature for first order kinetics of thermoluminescence. Values of parameters are same as Figure 4.2.

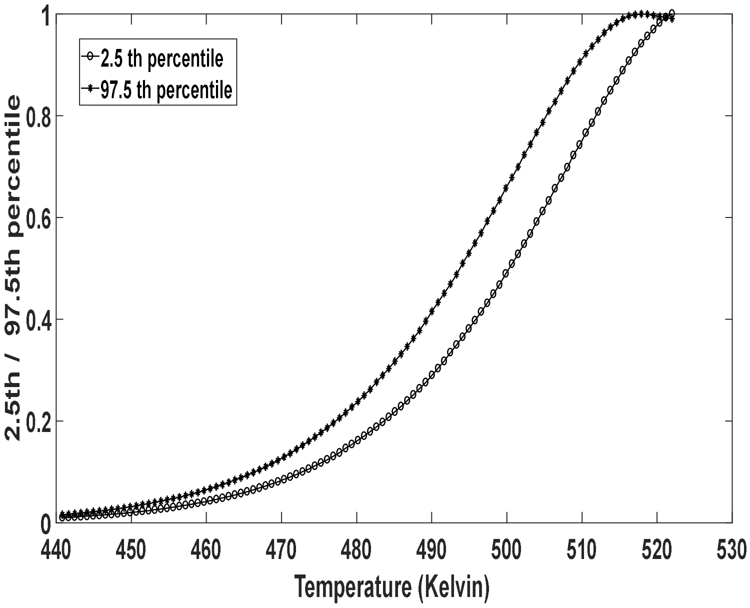

Figure 4.6 2.5th and 97.5th percentile plot for half range of temperature. Graphs are normalised with respect to maximum value. Values of parameters are same as figure 4.2.

Explanation of the trend

In order to understand the phenomenon it is given a thought keeping only one parameter (D) uncertain and fixing the value of another parameter to its mean value (f =10^{12}sec^{-1}). If only one parameter is kept uncertain then actually glow curve is being generated at slightly higher and lower values of that parameter, the magnitude of which is equivalent to uncertainty in that parameter. So, glow curve is plotted at two values of D, 1.3eV and 1.28eV, to get the corresponding glow curves GC1 and GC2. The graphs of which are shown in Figure 4.7. Though the actual uncertainty in our parameter D is much lower (1σ =.005eV) but a larger difference in energies is kept for visual clarity. If we consider a particular temperature say T=500K, then the residue is actually the length AB of Figure 4.7. Where A is a point on GC1 at T=500K and B is a point on GC2 at T=500K.

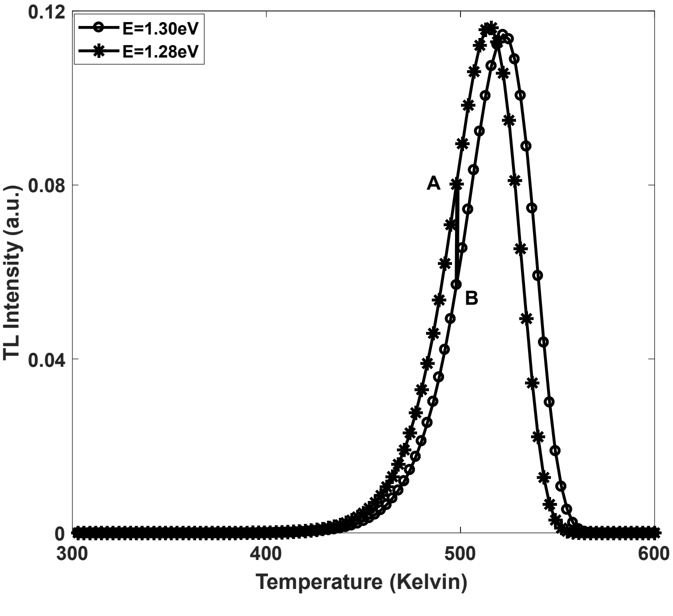

Figure 4.7 Glow curve for two certain (σ_D=0.0) values of trap depth (D). The value of frequency factor is 10^{12} sec^{-1}. Heating rate is 5°K/s.

For further understanding, the modulus of rate of change of TL intensity with change in temperature is plotted, shown in Figure 4.8. It is found that it has similar nature as of the positive residue plot. It is reasonable as due to uncertainty in D we have glow curves shifted along temperature axis. Now, for a given shift along temperature axis larger will be length AB where TL vs. temperature gradient is larger and smaller where TL vs. temperature gradient is smaller. Hence, positive residue plot and $|dTL/dT|$ vs T plot should have similar nature.

Similar analysis can be done by keeping D fixed and f uncertain.

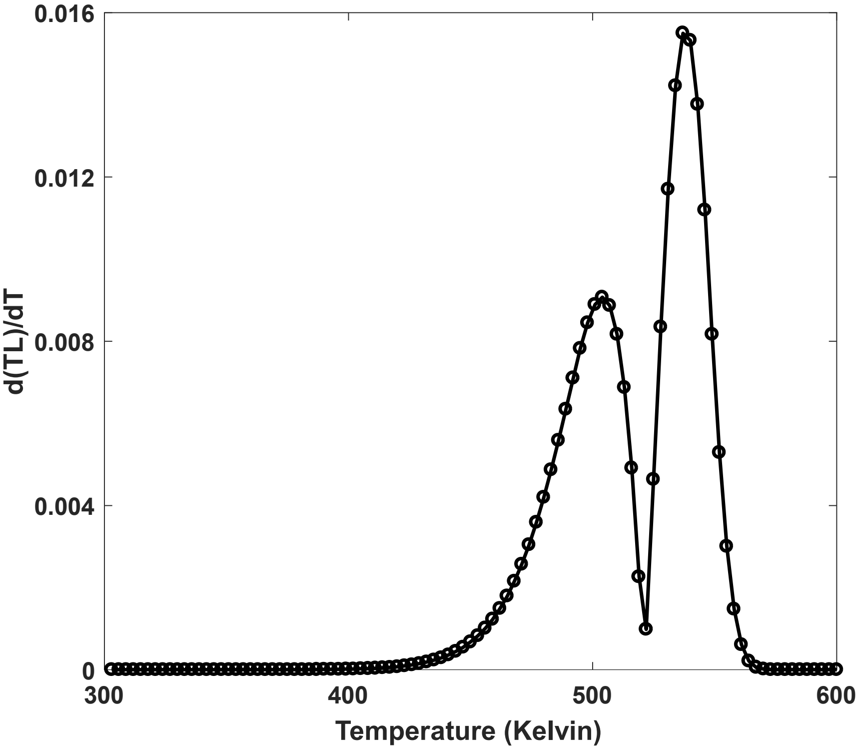

Figure 4.8 Modulus of differentiation of themoluminescence (TL) output as a function of temperature. The value of D=1.3eV. Rest parameters are same as Figure 4.7.

4.1.2.2 General Order Kinetics

For General order kinetics uncertainty analysis is done in similar fashion as explained for the first order kinetics case. Figure 4.9 shows the residue plot for order of kinetics equal to two and Figure 4.10 illustrates the residue plot for order of kinetics equal to 1.8. Figure 4.11 and Figure 4.12 shows the representative CDFs at five values of temperature for two cases of order of kinetics equal to two and order of kinetics equal to 1.8.

It is pertinent to mention at this point that X axis value corresponding to 50th percentile of a CDF plot is mean value of TL intensity. Hence, the CDF close to half intensity values (at which there is maximum of uncertainty, points B and D of residue plot (Fig. 4.4)) are expected to be in between, with CDF corresponding maximum intensity point (at which there is a local minimum of uncertainty, point C of residue plot (Fig. 4.4)) on right hand side and CDF corresponding starting and end points of glow curve (points A and E of residue plot (Fig 4.4)) on the left hand side. This is obvious from Figure 4.11 and Figure 4.12.

It can be seen from the residue plots and the CDFs that they disclose the same information. It can be seen from the residue plot that uncertainty has two local maximums with a minimum in between the two. In the CDF plot larger is the slant of curve larger is uncertainty as larger will be the separation along X axis between 5th and 95th percentile. As is obvious from the CDF plots the CDFs close to half intensity values of TL intensity in glow curve have maximum slant, CDF corresponding to maximum intensity value of TL intensity in glow curve has smaller slant and CDF corresponding to starting and end values of TL intensity in glow curve are almost vertical lines (least slant).

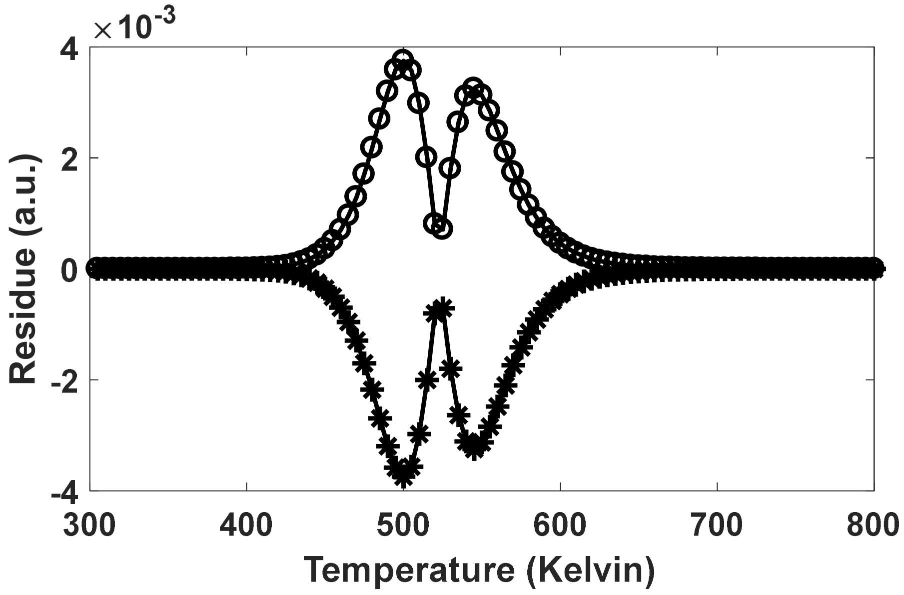

Figure 4.9 Positive and negative residue as a function of temperature for b=2. The values of parameters are D=1.3 eV, f =10^{12}sec^{-1}, C_{t0}=10^{10}m^{-3}, C_T=10^{10}m^{-3}, heating rate=5°C/sec. Uncertainty in D and f are respectively 0.005eV and 10^{10}sec^{-1}.

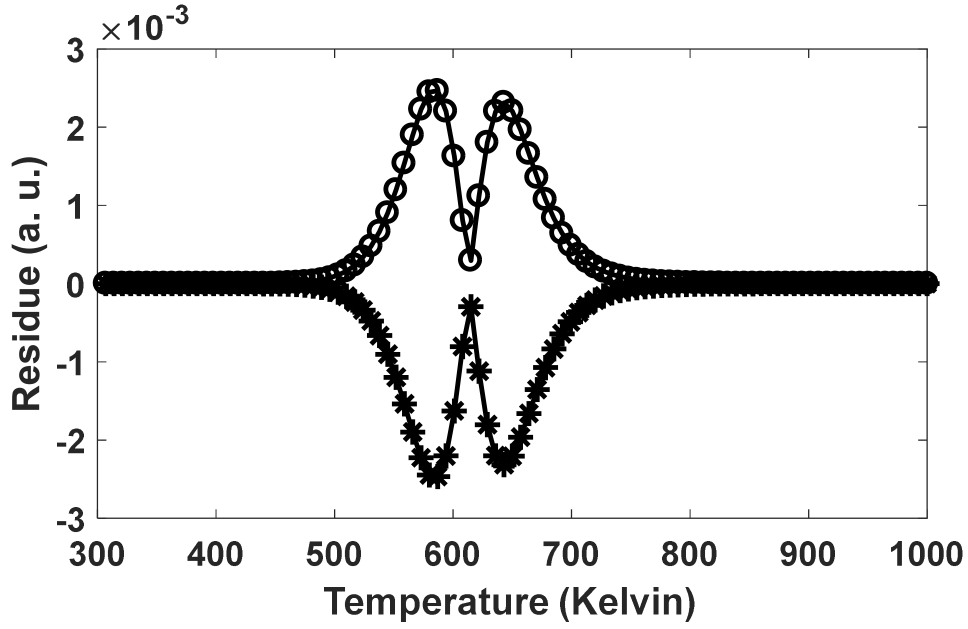

Figure 4.10 Positive and negative residue as a function of temperature for b=1.8.

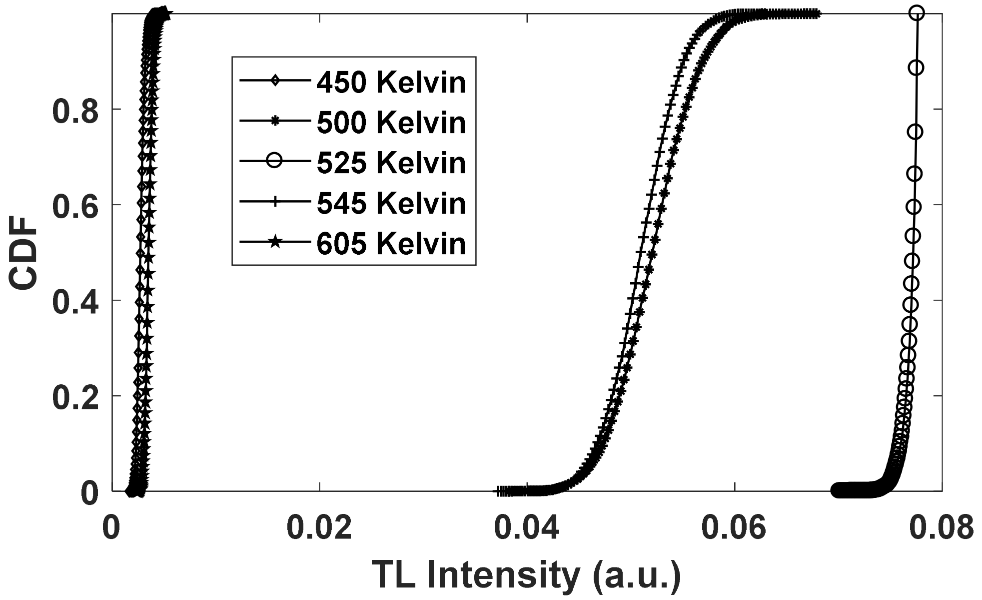

Figure 4.11 The CDFs for mentioned values of temperature for b=2 of general order kinetics.

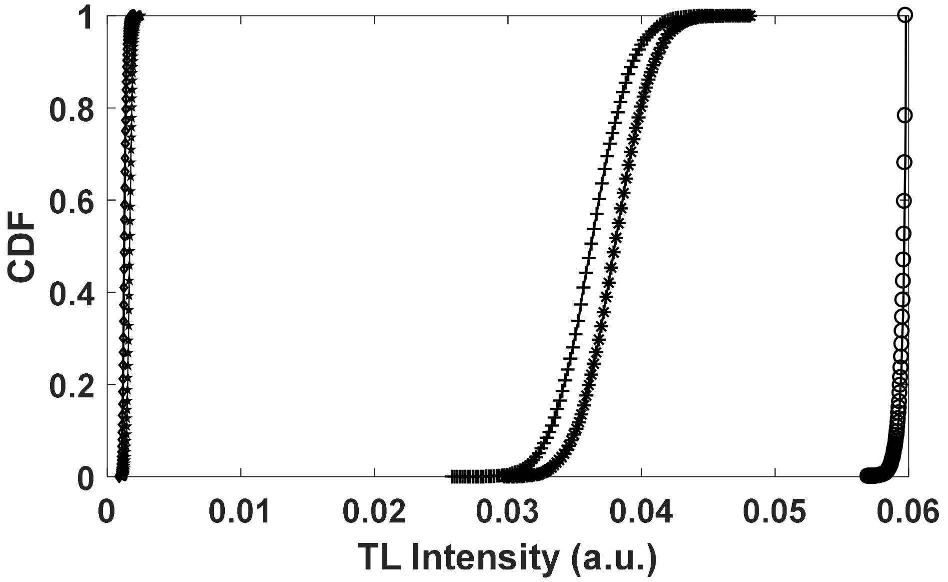

Figure 4.12 The CDFs at five representative temperatures for b=1.8 of general order kinetics.

4.1.3 Discussions

The algorithm aimed at establishing the trend of uncertainty for temperature range of our interest has been discussed in section 4.1.1. In the further section using the algorithm the trend has been obtained. Further, it is required to discuss the benefits of the study. The major benefit of the study is as follows.

In experimental scenario often glow curves are recorded. If under same experimental condition (heating rate, temperature range etc.) glow curve is recorded for same phosphor repeatedly, till sufficiently large number of glow curves are recorded. Each glow curve is deconvoluted to yield individual TL peaks. Further, one of the obtained TL peaks is considered. For the particular glow peak and at a particular temperature, mean and standard deviation of TL intensity can be obtained at that temperature. This process may be repeated for full range of temperature under consideration for that particular TL glow peak. By this way experimental trend of temperature vs. uncertainty plot can be obtained, for the particular TL glow peak. If this trend matches with trend established in this chapter then, it can be inferred that the statistical fluctuation in trap parameters is the major source of uncertainty for that particular TL peak.

In above method the number of simulation runs has to be kept quite large for accurate result. This may be a time consuming affair. Hence, we may use another technique known as α cut method of Fuzzy set theory for reducing computational burden.

4.2 Fuzzy set theory approach for uncertainty propagation

Since its proposition by Zadeh [Zadeh, 1965] Fuzzy set theory has been applied to diverse fields of engineering like fault detection in gearboxes [Joentgen et al., 1999] etc and management like transportation problem [Chanas et al., 1984]. But the estimation of uncertainty in TL signal due to inherent uncertainty in parameter using Fuzzy set theory is relatively unexplored field.

4.2.1 Basics of Fuzzy set theory for uncertainty analysis

Ordinary set

In ordinary (non fuzzy) set theory elements fully belong to set or are fully excluded from it. Membership function $\mu_A(x)$ of x, of a classical set A is defined as

$$\mu_A(x) = \begin{cases} 1 & if\ x\ is\ an\ element\ of\ A \\ 0 & if\ x\ is\ not\ an\ element\ of\ A \end{cases}$$

This means that an element x is either a member of set A ($\mu A(x) = 1$) or not ($\mu A(x) = 0$).

Fuzzy set

A fuzzy set A on universe (domain) X is a set defined by membership function $\mu_A(x)$ which is a mapping from the universe X into unit interval. Membership function represent the degree that specified value belongs to set.

$$\mu_A(x) = \begin{cases} 1 & x\ is\ full\ member\ of\ A \\ \epsilon\ (0,1) & x\ is\ partial\ member\ of\ A \\ 0 & x\ is\ not\ a\ member\ of\ A \end{cases}$$

A triangular membership function is illustrated in Figure 4.13.

α_{cut} method

The α_{cut} method is explained in the subsequent paragraph.

If we take a particular value of membership function (say α_{cut}) and draw a line parallel to horizontal axis, it cuts the membership function at two points. The two points define the range of interval (I_{min} & I_{max}) on the X axis. Figure 4.13 may be seen.

Quantification of uncertainty

For a given α_{cut}value the interval (I_{min}, I_{max}) is a measure of spread (or uncertainty). To quantify the uncertainty we define the degree of uncertainty (DOU).

$$\text{DOU}= I_{max} - I_{min}$$

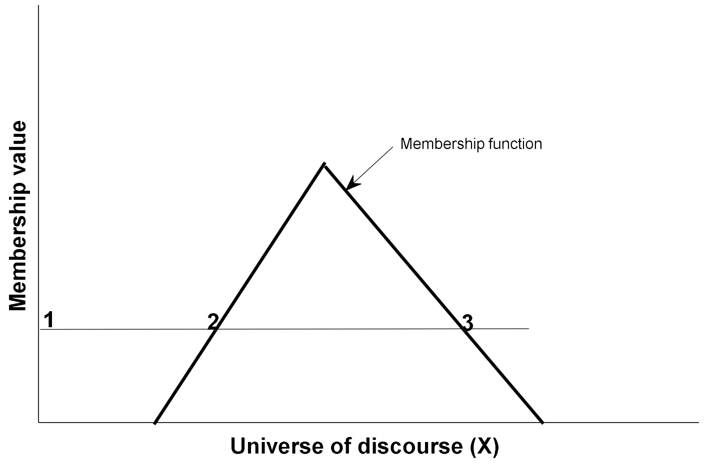

Figure 4.13 Triangular membership function

4.2.2 Algorithm for estimating uncertainty using α cut method

The algorithm for doing uncertainty analysis using α cut method is depicted in flow chart of Figure 4.14.

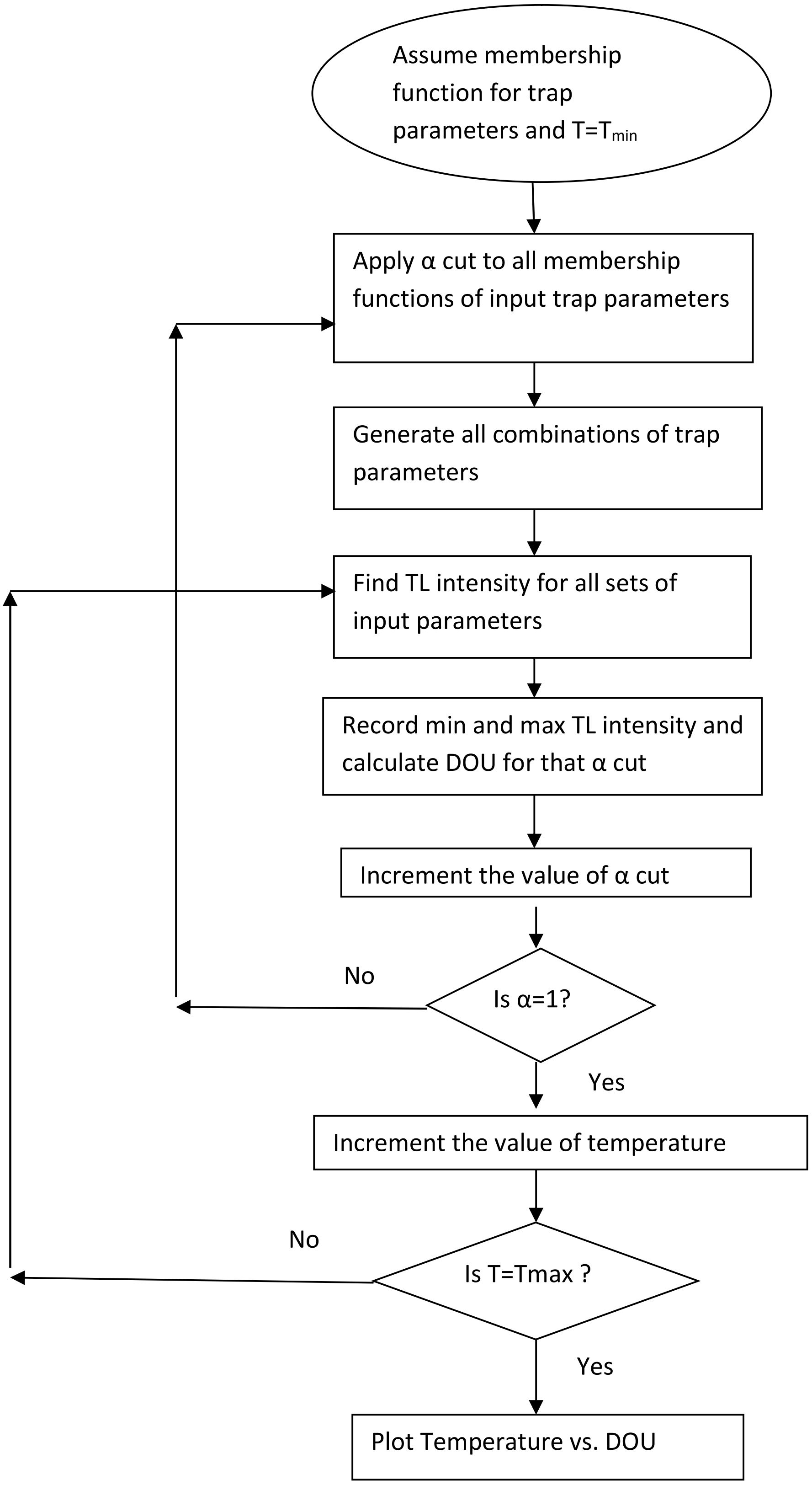

Figure 4.14 Flow chart of α cut method for estimating uncertainty profile of single TL peak.

Justification for adopting triangular membership function for input trap parameters

Gaussian probability density function has been used in section 4.1 for the input trap parameters. Among the generally used membership functions (rectangular, trapezoidal, triangular etc.) triangular membership function is the best approximation of a Gaussian function as shown in Figure 4.15.

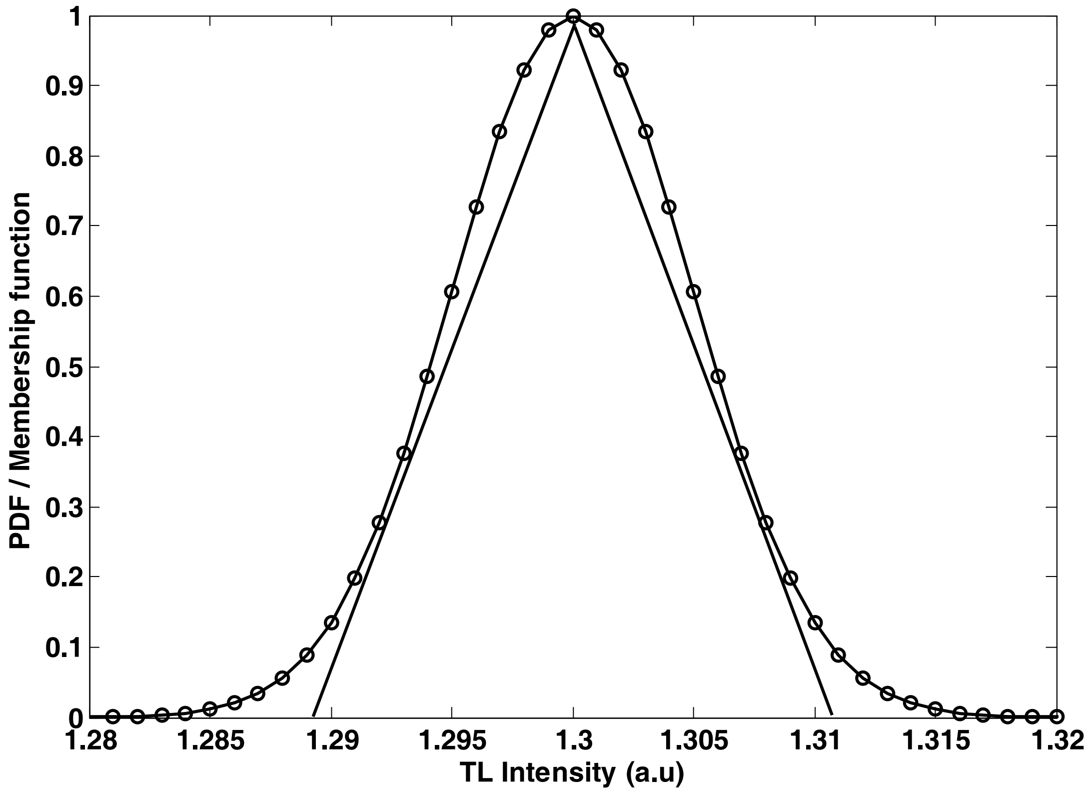

Figure 4.15 Triangular membership function is best approximation of Gaussian PDF.

Another justification that can be furnished for using a triangular membership function is as follows. Any experimental or theoretical methodology will always report the trap parameters with a most probable value and uncertainty (1α or 3α value). Hence, a particular value of trap parameter will be most probable with fall in probability on moving from it on both the sides.

So a triangular membership function with coordinates as shown in Figure 4.16 is most suitable simple membership function for trap parameters.

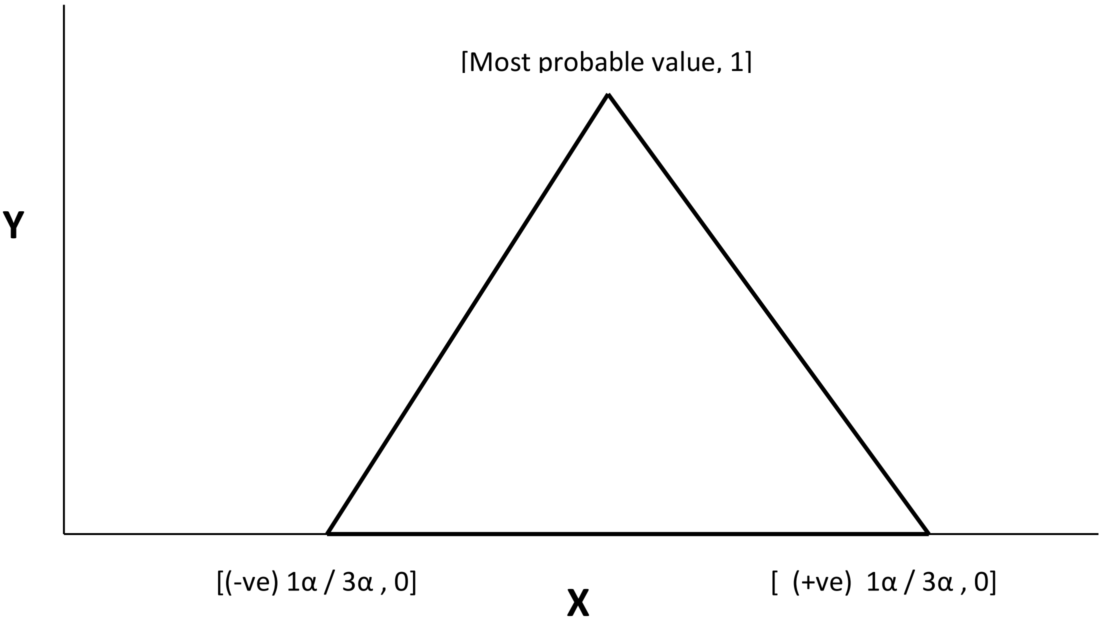

X: Trap parameters (trap depth (D) or attempt to escape frequency (f))

Y: Membership function

Figure 4.16 Triangular membership function is a reasonable approximation for trap parameters.

4.2.3 Simulation Results

The basics of Fuzzy set theory relevant to our case study and the algorithm used to carry out the uncertainty analysis has been discussed in previous sections. Further, in this section it is intended to present the simulation results.

4.2.3.1 First order kinetics

The results are started with the case of first order kinetics.

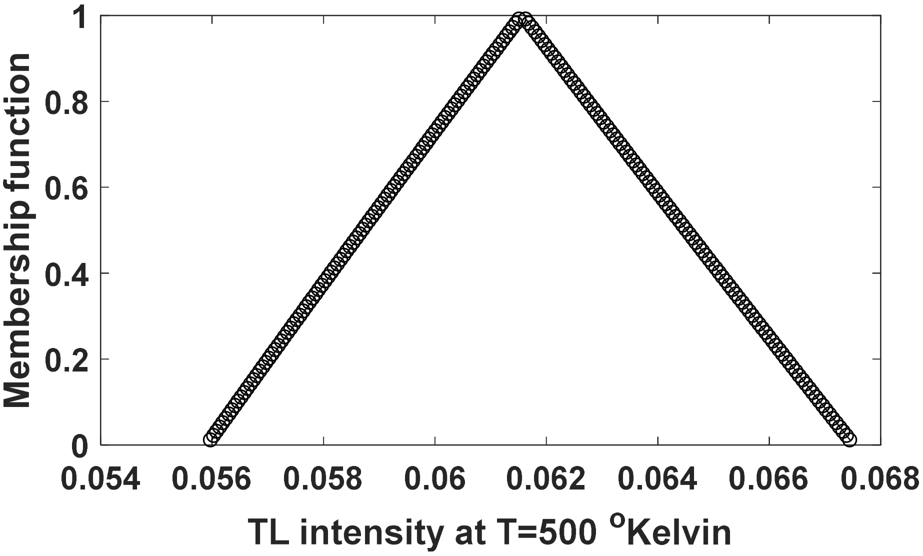

Figure 4.17 Membership function graph of output TL intensity at T=500 ºK for 1st order kinetics.

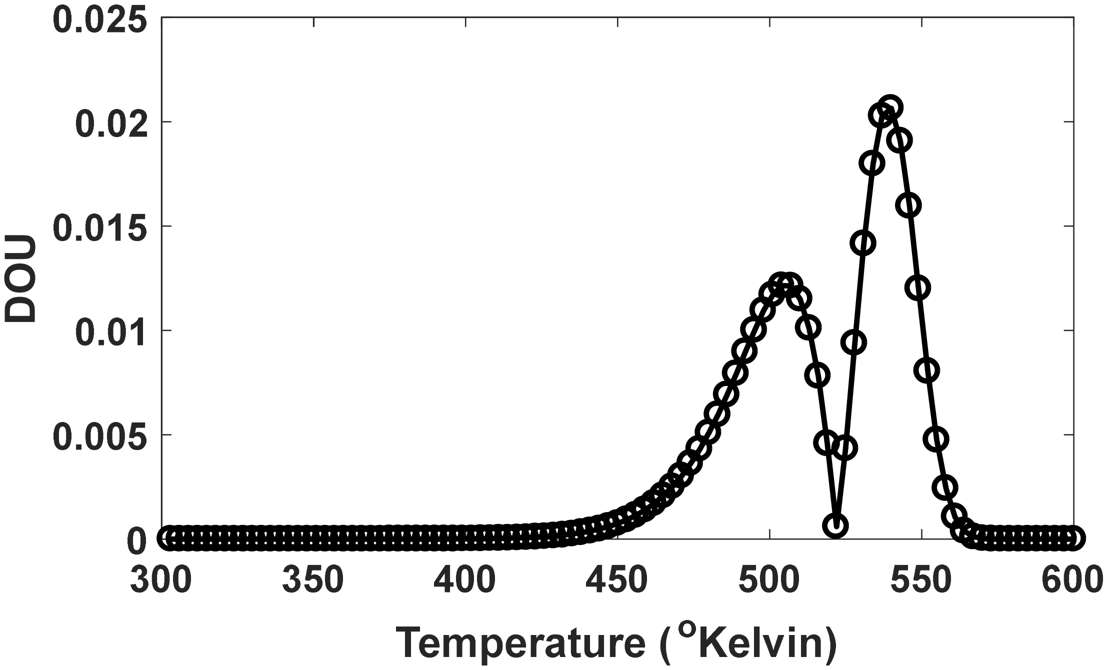

Figure 4.18 DOU with temperature for full range of temperature under consideration for 1st order kinetics.

Figure 4.17 shows the representative membership function for TL intensity for 1st order kinetics of thermoluminescence at a particular temperature (T=500ºK). Similar membership function graphs can be obtained at all temperatures and from each membership function graph DOU $|_{\alpha=0.01}$ can be obtained. Further DOU $|_{\alpha=0.01}$ may be plotted along with temperature to get the uncertainty trend along with temperature. Figure 4.18 shows this result.

4.2.3.2 General order kinetics

Figure 4.19 shows the membership function graph for general order kinetics at a representative temperature (T=500ºK) and Figure 4.20 show the uncertainty plot.

4.2.4 Discussions

In this chapter trend of temperature vs. uncertainty graph is discussed. For minimising the computational time to carry out large number of simulation runs, α cut method of fuzzy set theory was introduced. The major benefit of the study was explained. It was elaborated that by these methods it can be established that whether or not, statistical fluctuation in trap parameters are major source of uncertainty.

Further, it is interesting to look in to the matter in case where, sources of deviation from basic TL model so dominant that basic TL models are no longer valid and to see whether we may do modelling and further the uncertainty analysis in that case with recording a reasonably low number of TL glow curves.

One of the suitable methods for such cases is Polynomial Chaos Expansion (PCE) for modelling the scenario. Hence, PCE will be introduced further.

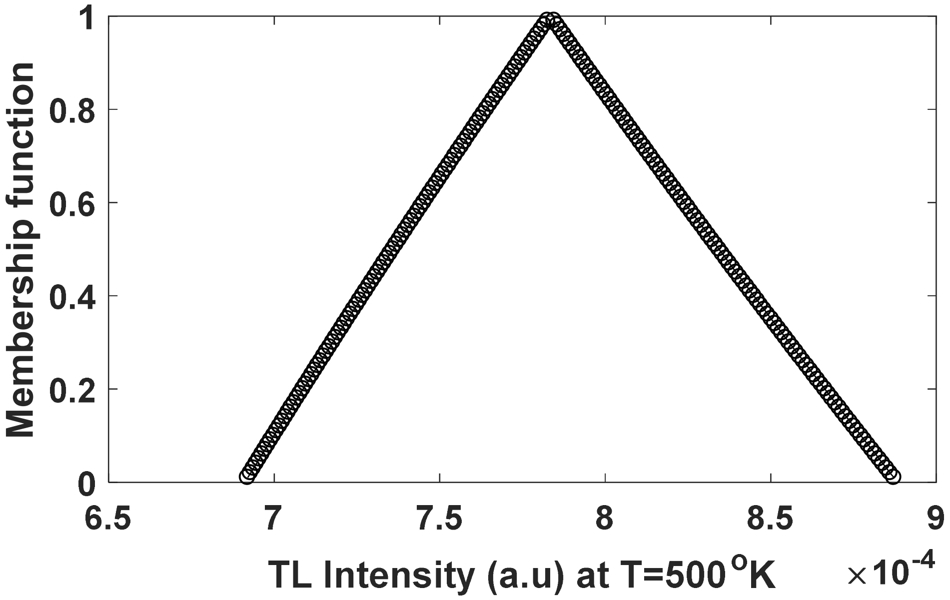

Figure 4.19 Membership function graph of output TL intensity at T=500 ºK for general order kinetics at b=1.8. Rest parameters are same as figure 4.18.

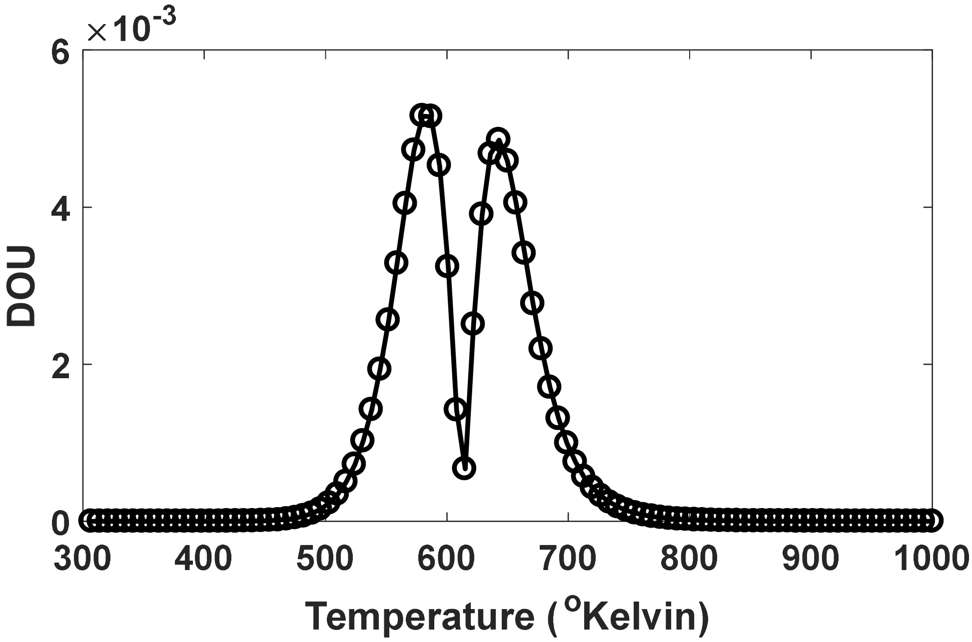

Figure 4.20 DOU with temperature for full range of temperature under consideration for general order kinetics with b=1.8.

4.3 Polynomial Chaos Expansion (PCE) for uncertainty analysis

4.3.1 Basics of PCE

The foundation of PCE theory dates back to 1938 when Wiener represented Gaussian as an infinite series of Hermite polynomials whose argument was a vector of random variables. Further, in 1991 Ghanem and Spanos developed stochastic finite element method based on the theory developed by Wiener. In 2002 Xiu and Karniadakis elaborated further the formalism to non Gaussian cases using different orthogonal polynomials as basis function.

Polynomial chaos expansion (PCE) (Wiener,1938; Ghanem & Spanos, 1991; Isukapalli, 1999; Xiu & Karniadakis, 2002) is an efficient method of simulation. PCE can be used for uncertainty propagation and quantification.

Here it is intended to present algorithm for modelling the TL phenomenon using PCE and further carrying out the uncertainty analysis of the model (response surface) generated.

The motivation here is to illustrate that this technique can be applied to uncertainty analysis of TL intensity in glow peak. Hence, experimental data points may be replaced by model predicated TL values. Obviously in this case repetition of results of section 4.1 and section 4.2 is expected. This will validate the applicability of algorithm to the phenomenon of TL.

4.3.2 Algorithm for uncertainty propagation using PCE

The algorithm is as follows. The number of input variables is two namely, trap depth and attempt to escape frequency (r = 2) and expansion is taken up to second order (n = 2). Hence, the sample size (number of inputs) is given by equation 4.2

$$sample\ size = \frac{(n+r)!}{n!r!} = \frac{(2+2)!}{2!4!} = 6 \tag{4.2}$$

So two sets each containing of 6 normally distributed random numbers with mean and standard deviation (1.3eV, 0.005eV) and (10^{12} sec^{-1}, 10^{10} sec^{-1}) are taken. First set is for trap depth and second set is for pre exponential factor. The corresponding set of output TL intensity is generated using RW model equation at a particular value of temperature. It will contain 6 elements as explained before. Let the elements be $Y_1, Y_2 \ldots . Y_6$. For each output the expansion can be written as follows.

$$Y_1 = a_0 + a_1\xi_{1,1} + a_2\xi_{2,1} + a_3\left(\xi_{1,1}^2 - 1\right) + a_4\left(\xi_{2,1}^2 - 1\right) + a_5\xi_{1,1}\xi_{2,1} \tag{4.3.1}$$

$$Y_2 = a_0 + a_1\xi_{1,2} + a_2\xi_{2,2} + a_3\left(\xi_{1,2}^2 - 1\right) + a_4\left(\xi_{2,2}^2 - 1\right) + a_5\xi_{1,2}\xi_{2,2} \tag{4.3.2}$$

$$Y_3 = a_0 + a_1\xi_{1,3} + a_2\xi_{2,3} + a_3\left(\xi_{1,3}^2 - 1\right) + a_4\left(\xi_{2,3}^2 - 1\right) + a_5\xi_{1,3}\xi_{2,3} \tag{4.3.3}$$

$$Y_4 = a_0 + a_1\xi_{1,4} + a_2\xi_{2,4} + a_3\left(\xi_{1,4}^2 - 1\right) + a_4\left(\xi_{2,4}^2 - 1\right) + a_5\xi_{1,4}\xi_{2,4} \tag{4.3.4}$$

$$Y_5 = a_0 + a_1\xi_{1,5} + a_2\xi_{2,5} + a_3\left(\xi_{1,5}^2 - 1\right) + a_4\left(\xi_{2,5}^2 - 1\right) + a_5\xi_{1,5}\xi_{2,5} \tag{4.3.5}$$

$$Y_6 = a_0 + a_1\xi_{1,6} + a_2\xi_{2,6} + a_3\left(\xi_{1,6}^2 - 1\right) + a_4\left(\xi_{2,6}^2 - 1\right) + a_5\xi_{1,6}\xi_{2,6} \tag{4.3.6}$$

Where $\xi_{1,1}, \xi_{1,2}, \xi_{1,3}, \xi_{1,4}, \xi_{1,5}, \xi_{1,6}$ is one set of normally distributed random numbers whose mean is 0 and standard deviation is 1. Similarly, $\xi_{2,1}, \xi_{2,2}, \xi_{2,3}, \xi_{2,4}, \xi_{2,5}, \xi_{2,6}$ is another set of normally distributed random numbers with mean 0 and standard deviation 1. These two sets correspond to two input variables. Normally distributed random numbers with mean 0 and standard deviation 1 are called standard random variables (srvs)

Equation 4.3.1 to 4.3.6 can be written in matrix form and the values of coefficients $a_1, a_2 \ldots\ a_6$ can be obtained. Once the coefficients are known the response surface is defined.

Further large number of srvs may be input to this response surface to generate the probability density function (PDF) of output (TL intensity at that temperature).

From the obtained PDF the cumulative distribution function (CDF) may be obtained as explained in section 4.1. From this CDF the 2.5th percentile and 97.5th percentile can be obtained to visualise the uncertainty.

Further, the whole process may be repeated at different values of temperature to obtain the variation of uncertainty as a function of temperature.

In order to be more precise it is possible to do a Monte Carlo on coefficients.

4.3.3 Simulation Results

4.3.3.1 First Order Kinetics

As mentioned in the algorithm section (section 4.3.2) by constructing the response surface and further input of large number of srvs, PDF of output TL intensity at that temperature value can be obtained. From the PDF the CDF may be obtained for that temperature. Figure 4.21 shows the CDFs at five representative temperature values for first order kinetics. The values of parameters are as mentioned in algorithm section. Heating rate is 5°Kelvin/sec,

4.3.3.2 Second Order Kinetics

Figure 4.22 illustrates the CDFs at five representative temperature values. For this plot the heating rate is 5°Kelvin/sec.

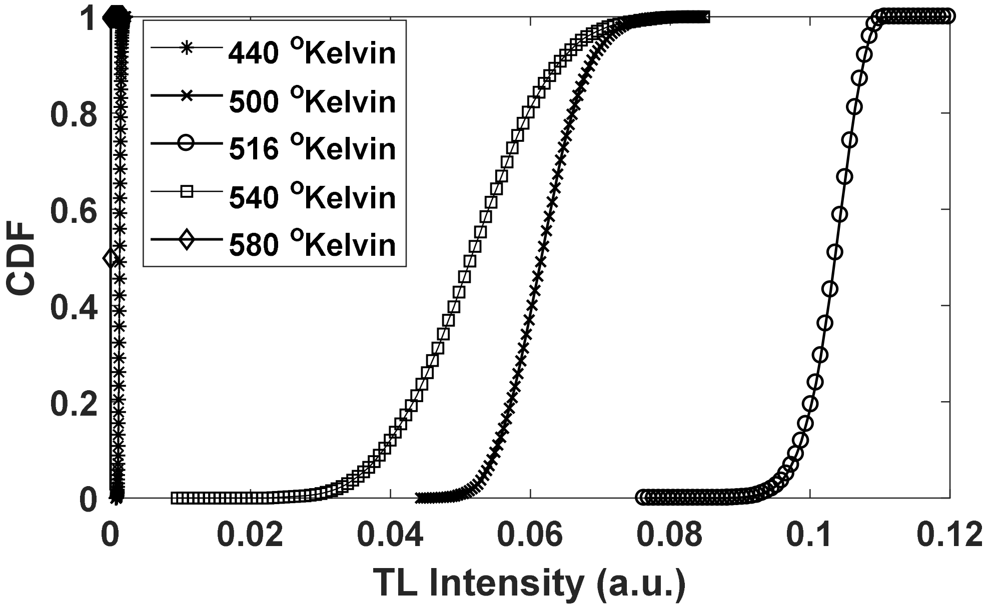

Figure 4.21 CDFs at five representative temperatures generated using PCE for first order kinetics model.

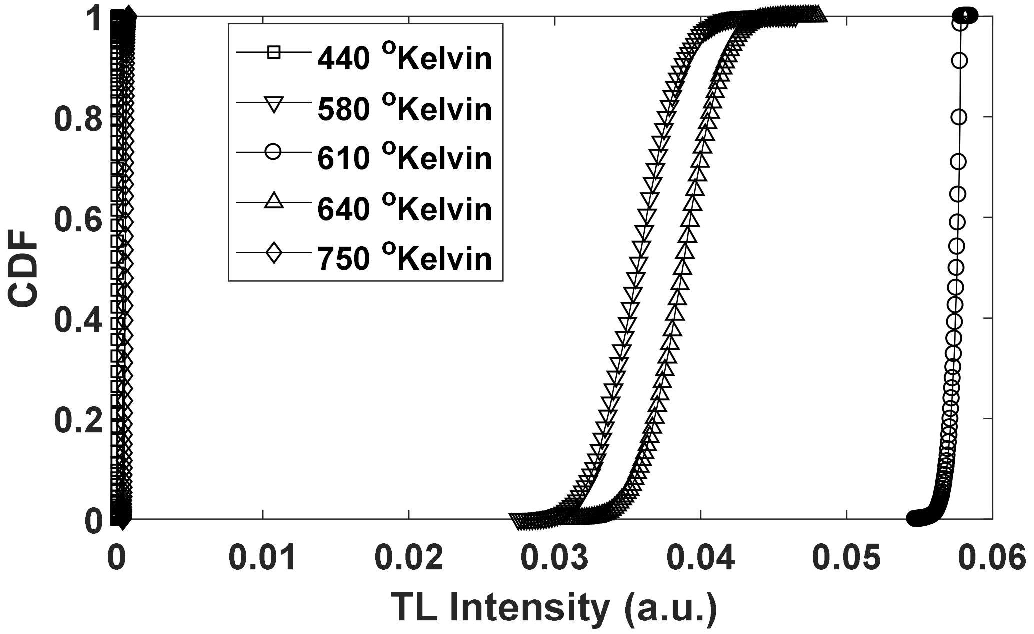

Figure 4.22 CDFs at five representative temperatures generated using PCE for second order kinetics model.

4.4 Conclusions

The trap parameters (trap depth and pre exponential factor) are the model parameters of the RW, GG and MP models. Due to uncertainty in model parameters there will be uncertainty in the TL emission intensity. This uncertainty will also be a function of stimulating temperature. In this chapter the trend of variation of uncertainty in TL emission intensity with variation in temperature has been established.

This chapter started with MC simulations and the objective of uncertainty analysis of various models proposed for TL phenomenon was achieved. It was further established that the results of MC simulation can be obtained using α cut method of Fuzzy Set theory with comparatively much lower computational burden.

In case where mentioned TL models are no longer valid, modelling can be done using PCE by generating response surface. After establishing the response surface, uncertainty analysis can also be done. This method was also introduced and the results obtained from MC simulation and Fuzzy set theory was successfully reproduced using PCE.

CHAPTER V

Deconvolution of TL Glow Curve

Necessity and benefits of CGCD has already been discussed in chapter one of this dissertation. The glow curve is superposition of TL output from various type of trapping centres in the material. Hence, to get any meaningful information regarding one type of trapping centre it is mandatory to deconvolve the glow curve. Due to above reason a novel technique for deconvolution is of interest. In this chapter it is intended to present Mixture Model based Computerised Glow Curve Deconvolution (MM based CGCD). The major benefit of this technique over other CGCD techniques is as follows.

It would be of interest to the CGCD community to find a theoretical platform for determining correct number of glow peaks to which a given glow curve should be deconvolved. Presently, for same phosphor different authors fit the glow curve to different number of glow peaks. Example is the case of $CaSO_4$: Dy [Oliveri, 1978; Souza, 1993; Srivastava and Supe, 1983]. In the context of MM this question has already been addressed by different authors [Fraley and Raftery, 1998; Gassiat and Dacunha-Castelle, 1997]. It is our presumption that on similar line of action it is possible to develop theoretical platform for determining correct number of glow peaks for a given glow curve theoretically. MM based CGCD, that we present here, may be a milestone to the mentioned objective of finding purely theoretical way for correct number of glow peaks for a given glow curve. Author is aware of the fact that there are experimental techniques like fractional glow technique for the purpose. But our interest is in purely theoretical platform for answering the question, which to the best of our knowledge, is missing in TL literature till date.

To develop the formalism of deconvolution using Mixture model (MM), prior knowledge of conditional probability, Bayes' theorem, maximum likelihood and Expectation maximization algorithm is required. Hence, a brief introduction of these topics is given.

5.1 Conditional probability

In basic set theory only information about outcome of a trial of a given experiment, available before trial, is that it corresponds to some point in the sample space. With this assumption, probability of any event A is calculated. If added information that outcome of a trial is contained in a subset of B of sample space with, P(B)≠0, is given, then knowledge of occurrence of event B may change the conditional probability of event A. We define the conditional probability of A given B has occurred. Symbolically it is represented as P (A|B).

5.2 Bayes' theorem

In practice, after the experiment, a situation often arises in which the event A is known to have occurred, but not known directly which of the mutually exclusive and exhaustive events B_1, B_2....B_n has occurred. In situation, we may be interested in finding $P\left(B_j\middle|A\right)$, it is given as

$$P\left(B_j\middle|A\right) = \frac{P\left(A\middle|B_j\right)\ P(B_j)}{\sum_i P\left(A\middle|B_i\right)\ P(B_i)} \tag{5.1}$$

This relation is known as Bayes' theorem. It is also sometimes called as posterior probability.

5.3 Posterior Probability

Posterior probability is the probability of having argument set Φ given the data set X. It is related to likelihood and prior by following relation

$$Posterior\ probability\ \alpha\ Likelihood\ x\ Prior\ probability$$

Mathematically it is written as

$$P(\Phi|\mathrm{X}) = \frac{\mathrm{P(X|\Phi)P(\Phi)}}{\mathrm{P(X)}} \tag{5.2}$$

5.4 Maximum likelihood

Suppose there is a sample of $x_1, x_2 \ldots \ldots . x_n$ n independently and identically distributed observations, coming from an unknown probability distribution. It is how ever known that the distribution belongs to a family of distributions. It is desirable to find the parameter set Φ of the family of distributions specific to the unknown probability distribution. The likelihood is defined as (assuming data to be independent)

$$L\ (\Phi;\ x_1, x_2 \ldots \ldots . x_n = f(x_1, x_2 \ldots \ldots . x_n|\Phi\ ) = \prod_i f(x_i|\Phi) \tag{5.3}$$

The method of maximum likelihood estimates Φ by finding the value of Φ that maximises L(Φ; x). Symbolically it is written as

$$\{\Phi_{mle}\} = \{arg\ max\ L(\Phi; x_1, x_2 \ldots \ldots . x_n)\} \tag{5.4}$$

The concept of maximum likelihood estimate (MLE) of parameters can be explained by an example. It may be assumed that there are three data points and it is known that Gaussian process models the phenomenon under consideration adequately. Joint probability distribution of data set is required, generation of which is complicated. Hence, problem is approached with an assumption that data points are independent.

Hence,

$$P(x_1, x_2, x_3;\ \mu, \sigma) = P(x_1;\ \mu, \sigma)\ P(x_2;\ \mu, \sigma) P(x_3;\ \mu, \sigma) \tag{5.5}$$

$$P(x; \mu, \sigma) = \frac{1}{\sigma\sqrt{2\Pi}} \exp[-\frac{(x-\mu)^2}{2\sigma^2}] \tag{5.6}$$

From equation (5.5) and (5.6) equation (5.7) may be obtained

$$P(x_1, x_2, x_3; \mu, \sigma) = \frac{1}{\sigma\sqrt{2\Pi}} \exp\left[-\frac{(x_1-\mu)^2}{2\sigma^2}\right] \frac{1}{\sigma\sqrt{2\Pi}} \exp[-\frac{(x_2-\mu)^2}{2\sigma^2}] \frac{1}{\sigma\sqrt{2\Pi}} \exp[-\frac{(x_3-\mu)^2}{2\sigma^2}] \tag{5.7}$$

Further, it is known that logarithm is a monotonically increasing function. Hence, maxima of log likelihood will occur at the same point where the maximum of likelihood is.

$$\log (P(x_1, x_2, x_3;\ \mu, \sigma) = 3 \ln \frac{1}{\sigma\sqrt{2\Pi}} - \frac{(x_1-\mu)^2}{2\sigma^2} - \frac{(x_2-\mu)^2}{2\sigma^2} - \frac{(x_3-\mu)^2}{2\sigma^2} \tag{5.8}$$

Taking partial differential of equation (5.8), equation (5.9) may be obtained

$$\frac{\partial P(x_1, x_2, x_3; \mu, \sigma)}{\partial \mu} = \frac{1}{\sigma^2}\ [\, x_1 + x_2 + x_3 - 3\mu\,] \tag{5.9}$$

The condition of maxima is

$$\frac{\partial P(x_1, x_2, x_3; \mu, \sigma)}{\partial \mu} = 0 \tag{5.10}$$

Using equation (5.10), equation (5.11) may be obtained

$$\mu = (x_1 + x_2 + x_3)/3 \tag{5.11}$$

Similarly, $\frac{\partial P(x_1, x_2, x_3; \mu, \sigma)}{\partial \sigma} = 0$ may be used to estimate the σ.

But in real world scenario the MLE always doesn't give the close form of estimate of parameters. Hence there is improved version like Expectation Maximization (EM) algorithm.

5.5 Expectation maximization algorithm (EM)

EM algorithm is a two step iterative algorithm:

(A) Calculate the expectation of log likelihood of complete data set with respect to the latent variable.

(B) Maximize the above (differentiate and equate to zero) with respect to parameter set so as to estimate the parameter set

Proof for convergence of likelihood function to an upper bound in EM algorithm is as follows.

Symbols:

$X: Data\ set$

$x_i: Data$

$Z: Latent\ variable$

$\Phi: Parameter\ set$

$\Phi^t\ : Parameter\ set\ \ in\ t^{th}\ iteration.$

Q: Auxiliary$function$

$L(\Phi)$: Log Liklihood of parameter set Φ

$h\ (x|\Phi)$: Liklihood of incomplete (observed) data

$r(y|\Phi)$: Liklihood of complete data (including latent variable)

$$L\ (\Phi) = \log \mathrm{h}(\mathrm{x}|\ \Phi) \tag{5.12}$$

Following definition can be made for conditional density of complete data set $y = (x, z)$.

$$j\ (y|x, \Phi) = \frac{\mathrm{r}\ (\mathrm{y}|\Phi)}{\mathrm{h}(\mathrm{x}|\Phi)} \tag{5.13}$$

Equation (5.12) can be rewritten as

$$L\ (\Phi) = \log r(y|\Phi) - \log\ j(y|x, \Phi) \tag{5.14}$$

Taking expectation value with respect to latent variable, z, given observation and parameters obtained from previous iteration equation (5.15) can be obtained [McLachlan and Krishnan, 1997; Dempster et al., 1997; Sammaknejad et al., 2019]

$$< L\,(\Phi) > = < \log \mathrm{r}(\mathrm{y}|\,\Phi)\big|\,\mathrm{x}, \Phi^{\mathrm{t}} > - < \log \mathrm{j}(\mathrm{y}|\mathrm{x}, \Phi)\big)|\mathrm{x}, \Phi^{\mathrm{t}} > \tag{5.15}$$

$$= Q(\Phi|\Phi^{\mathrm{t}}) - M(\Phi|\Phi^{\mathrm{t}})$$

Where

$$Q(\Phi|\Phi^{\mathrm{t}}) =< \log \mathrm{r}(\mathrm{y}|\,\Phi)|\mathrm{x}, \Phi^{\mathrm{t}} >$$

$$M(\Phi|\Phi^{\mathrm{t}}) = < \log \mathrm{j}(\mathrm{y}|\mathrm{x}, \Phi)|\mathrm{x}, \Phi^{\mathrm{t}} >$$

$$L\left(\Phi^{t+1}\right) - L\left(\Phi^{t}\right) = Q\left(\Phi^{\mathrm{t+1}}\middle|\Phi^{\mathrm{t}}\right) - Q\left(\Phi^{t}\middle|\Phi^{\mathrm{t}}\right) - \{M\left(\Phi^{\mathrm{t+1}}\middle|\Phi^{\mathrm{t}}\right) - M\left(\Phi^{t}\middle|\Phi^{\mathrm{t}}\right)\} \tag{5.16}$$

In expectation maximization algorithm Q function is maximized. Hence,

$$Q\left(\Phi^{\mathrm{t+1}}\middle|\Phi^{\mathrm{t}}\right) \geq Q\left(\Phi^{t}\middle|\Phi^{\mathrm{t}}\right) \tag{5.17}$$

Therefore $L\left(\Phi^{t+1}\right) \geq L\left(\Phi^{t}\right)$ will be true if $M\left(\Phi^{\mathrm{t+1}}\middle|\Phi^{\mathrm{t}}\right) - M\left(\Phi^{t}\middle|\Phi^{\mathrm{t}}\right) \leq 0$

For an arbitrary Φ [McLachlan and Krishnan, 1997; Dempster et al., 1997; Sammaknejad et al., 2019]

$$M\left(\Phi^{\mathrm{t+1}}\middle|\Phi^{\mathrm{t}}\right) - M\left(\Phi^{t}\middle|\Phi^{\mathrm{t}}\right) = < \log \frac{\mathrm{j}(\mathrm{y}\,|\mathrm{x},\Phi)}{\mathrm{j}(\mathrm{y}|\mathrm{x},\Phi^{\mathrm{t}})}\ |\mathrm{x}, \Phi^{\mathrm{t}} > \tag{5.18}$$

$$\leq\ \log < \frac{\mathrm{j}(\mathrm{y}\,|\mathrm{x},\Phi)}{\mathrm{j}(\mathrm{y}|\mathrm{x},\Phi^{\mathrm{t}})}\ |\,\mathrm{x}, \Phi^{\mathrm{t}} > \tag{5.19}$$

$$=\ \log \int j\,(y|x, \Phi)\ \mathrm{dy} = 0 \tag{5.20}$$

Equation (5.19) is obtained by using Jensen's inequality [McLachlan and Krishnan, 1997]

Hence log likelihood function and thereby, likelihood function $h\,(x|\Phi)$ will increase. If the sequence is bounded it should converge to some upper bound [McLachlan and Krishnan, 1997; Dempster et al., 1997; Sammaknejad et al., 2019]

5.6 Mathematical Background of mixture model (MM) for deconvolution of TL glow curve

The problem of deconvolution of TL glow peaks can be modelled as mixture model (MM). A mixture model is a probability density function represented by weighted sum of several component probability distribution functions. It is assumed that each component density is finite set of data and can be modelled using density functions like Gaussian, Poisson etc. This method is useful when data originates from not one but multiple sources, which are trap types in our case. If each component density is assumed to be a Gaussian, the model is said to be a Gaussian Mixture Model (GMM). The parameters of GMM can be estimated using Expectation – Maximization (EM) algorithm. EM algorithm is an iterative method for finding maximum likelihood estimates of parameters in model, where model depends on unobserved latent variables. If we associate an identifier to each type of trap, then this identifier is our latent variable. The EM iteration alternates between performing an expectation (E) step which generates a function for the expectation of the log likelihood evaluated using the current estimate of the parameters, and a maximization (M) step, which calculates the parameters by maximizing the expected log-likelihood found in the E step. This process goes on iteratively.

Further there is need of mapping the glow curve deconvolution problem to MM formalism. Glow curve is a plot of TL counts as a function of temperature, so, it gives number of counts at each temperature. For application of MM we need a set of distributed data points with a given distribution. So, to map glow curve problem to MM formalism, at each location on temperature axis as many points are put as is the height of glow curve at that temperature. Now the problem can be looked as points distributed in one dimensional temperature space with glow curve as the distribution function. So we have a set of points at various locations in a one dimensional space whose distribution is known. Hence, MM formalism is applicable.

Books [McLachlan and Peel, 2004] discuss Gaussian Mixture Model, Expectation Maximization and likelihood estimation comprehensively but in their own context. So derivation is discussed in following section. In the derivation following symbols are be used.

Symbols:

$X: Data\ set$

$x_i: Data$

$Z: Latent\ variable$

$P(x_i): Probability\ distribution\ of\ data$

$\Phi: Parameter\ set$

$\Phi^t\ : Parameter\ set\ \ in\ t^{th}\ iteration.$

$w_i: Weighting\ factor\ of\ components$

Q: Auxiliary$function$

$t^* = iteration\ step$

$\lambda_A: Lagrangian\ Multiplier$

$\vartheta\ = Arbitrary\ element\ of\ parameter\ set$

The motivation of the section is to estimate the parameters trap depth (D_J), frequency factor (f_j) and the weighting factor (w_j) for each component glow peak, condition that the convoluted graph of glow peaks is known. To do this following route will be followed. In step (I) the convolved graph is written as weighted sum of normalised (with respect to area) glow curves and a latent variable (z_{ij}) is associated with each glow curve. In step (II) likelihood and log likelihood for the combined probability distribution of X and Z at a given Φ, $L\ (X, Z|\Phi)$, will be developed. Further we use EM algorithm for estimation of parameters $(D_J, f_j\ and\ w_j)$ of individual glow peaks . For this, an auxiliary function (Q), which is expectation of log likelihood $\left[\log(\ P\ (X, Z)\right)\big|\ \Phi^{t^*}\big]$ with respect to the latent variable Z, is developed. In step (III) the auxiliary function is introduced. In step (IV), expectation is calculated with respect to Z and in step (V) obtained expression is maximised with respect to parameters. Resulting equation obtained from step (V) has been utilized to have the estimation of the parameters. In final step (step VI) Lagrange multiplier is used to get the estimate of weighting factor w_j.

Step (I):

Let us have a given data set $X = (x_1, x_2, x_3, \ldots\ldots x_N)$ with a probability distribution $P(x_i)$. We assume it is a convolution of $\pounds$ glow peaks, hence it can be written as weighted sum of $\pounds$ normalised glow peaks.

$$P(x_i) = \sum_{j=1}^{\pounds} w_j \; \eta\,(x_i|\Phi) \tag{5.21}$$

Where $\eta\,(x_i|\Phi)$ is a normalised component glow peak.

Indicator variable (latent variable) defined below are introduced as

$$z_{ij} = \begin{cases} 1 & If\ x_i\ is\ emitted\ from\ jth\ glow\ curve \\ 0 & otherwise \end{cases} \tag{5.22}$$

Step (II):

Combined likelihood of X and Z at a given parameter set Φ can be written as

$$L\,(X, Z|\Phi) = P(X, Z|\Phi) \tag{5.23}$$

$$= \prod_{i=1}^{N} \prod_{j=1}^{3} [P\,(x_i, J\,|\Phi]^{z_{ij}} \tag{5.24}$$

$$= \prod_{i=1}^{N} \prod_{j=1}^{3} [\,P(x_i\,|\,J, \Phi]^{z_{ij}}\ [\,P(\,J|\Phi)]^{z_{ij}} \tag{5.25}$$

Taking log of equation (5.25) we get

$$\log L(X, Z|\Phi) = \sum_{i=1}^{N} \sum_{J=1}^{3} [z_{ij} \log\ P(x_i\,|\,J, \Phi)\ +\ z_{ij} \log\ P(\,J|\Phi)] \tag{5.26}$$

Step (III)

Introducing auxiliary function Q

$$Q = < \left[\log(P\,(X,Z)) \middle| \, \Phi^{t^*} \right] >_z \tag{5.27}$$

$$=< [\, \textstyle\sum_{i=1}^{N} \sum_{J=1}^{3} \{ z_{ij} \log\, P(x_i \mid J,\Phi) \;+\; z_{ij} \log\, P(\,J|\Phi)\} \;|\Phi^{t^*}] >_z \tag{5.28}$$

$$= \textstyle\sum_{i=1}^{N} \sum_{J=1}^{3} <\, (z_{ij}|\Phi^{t^*}) >_z \log\, P(x_i \mid J,\Phi) + < (z_{ij}|\Phi^{t^*}) >_z \log\, P(\,J|\Phi) \tag{5.29}$$

Where $< >_Z$ means expectation with respect to z.

Step (IV)

Expectation Step:

$$<\, \left(z_{ij} \middle| \Phi^{t^*}\right) >_z = 1\, \times P\left(z_{ij} = 1 \middle| \Phi^{t^*}\right) + \;0\; \times\; P\left(z_{ij} = 0 \middle| \Phi^{t^*}\right) \tag{5.30}$$

$$= P(\,J\, |x_i, \Phi^{t^*}) \tag{5.31}$$

$$= \frac{P(\,J\, |\Phi^{t^*})\; P\,(x_i|\, J,\Phi^{t^*})}{\sum_{j=1}^{k} P(\,J\, |\Phi^{t^*})\; P\,(x_i|\, J,\Phi^{t^*})} \tag{5.32}$$

Step (V)

Maximization Step:

$$\frac{\partial\, Q}{\partial \Phi} = 0 \tag{5.33}$$

As Φ is a parameter set comprising $E\ f\ and\ w$, auxiliary function Q is to be maximised with respect to each of these parameters

$$\frac{\partial\, Q}{\partial\, \vartheta} = \; \sum_{i=1}^{N} \frac{\partial\, Q}{\partial \log\; P(x_i \mid J,\Phi)} \frac{\partial \log\; P(x_i \mid J,\Phi)}{\partial\, \vartheta} \tag{5.34}$$

$$= \sum_{i=1}^{N} P(J|\, x_i, \Phi^{t^*})\; \frac{\partial\, \mathrm{lo} \quad P(x_i \mid J,\Phi)}{\partial\, \vartheta} \tag{5.35}$$

Step (VI)

To calculate weighting factors we use the constrain $\sum_{J=1}^{3} w_J = 1$ and use Lagrange multiplier

$$A = Q + \left(1 - \sum_{J=1}^{3} w_J\right)\lambda_A \tag{5.36}$$

$$\frac{\partial A}{\partial w_J} = \frac{\partial A}{\partial Q}\frac{\partial Q}{\partial w_J} - \lambda_A \tag{5.37}$$

$$\frac{\partial A}{\partial w_J} = 1 \times \left(\sum_{i=1}^{N} P(J\,|x_i, \Phi^{t^*})\,\frac{1}{w_J}\right) - \lambda_A \tag{5.38}$$

$$w_J = \frac{\sum_{i=1}^{N} P(J\,|x_i, \Phi^{t^*})}{\lambda_A} \tag{5.39}$$

By taking summation on both sides and using $\sum_{J=1}^{3} w_J = 1$ we get $\lambda_A = N$.

$$w_J = \frac{\sum_{i=1}^{N} P(J\,|x_i, \Phi^{t^*})}{N} \tag{5.40}$$

In order to express $P(J\,|x_i, \Phi^{t^*})$ in terms of $P(x_i|\,J, \Phi^{t^*})$ and weighting factor w_J we can use Bayes' theorem (Posterior probability)

$$P(J\,|x_i, \Phi^{t^*}) = \frac{P(x_i|\,J, \Phi^{t^*})\,w_J}{\sum_{J=1}^{K} P(x_i|\,J, \Phi^{t^*}) w_J} \quad \text{(Posterior probability)} \tag{5.41}$$

5.6.1 For Gaussian peaks

As Θ is a parameter set comprising μ, σ *and* w, auxiliary function Q is to be maximised with respect to each of these parameters

$$\frac{\partial Q}{\partial \mu_J} = \sum_{i=1}^{N} \frac{\partial Q}{\partial \log P(x_i\,|\,J, \Theta)} \frac{\partial \log P(x_i\,|\,J, \Theta)}{\partial \mu_J} \tag{5.42}$$

$$= \sum_{i=1}^{N} P(J\,|x_i, \Theta^{t^*})\,\left(\frac{x_i - \mu_J}{\sigma^2}\right) \tag{5.43}$$

$$\mu_j = \frac{\sum_{i=1}^{N} P\left(J\middle|x_i,\ \Theta^{t^*}\right) x_i}{\sum_{i=1}^{N} P\left(J\middle|x_i,\ \Theta^{t^*}\right)} \tag{5.44}$$

$$\frac{\partial Q}{\partial \sigma_J^2} = \sum_{i=1}^{N} \frac{\partial Q}{\partial \log P(x_i\,|\,J, \Theta)} \frac{\partial \log P(x_i\,|\,J, \Theta)}{\partial \sigma_J^2} \tag{5.45}$$

$$= \sum_{i=1}^{N} P(J\ |x_i, \Theta^{t^*})\ (\frac{(x_i-\mu_J)^2}{2\sigma_J^4} - \frac{1}{2\sigma_J^2}) \tag{5.46}$$

$$\sigma_j^2 = \frac{\sum_{i=1}^{N} P\left(J\middle|x_i,\ \Theta^{t^*}\right)(x_i-\mu_J)^2}{\sum_{i=1}^{N} P\left(J\middle|x_i,\ \Theta^{t^*}\right)} \tag{5.47}$$

5.6.2 For First order kinetics peaks

In first order kinetics a similar root of differentiating the auxiliary function Q with respect to parameters D_j and $f_j$can be followed. But in order to reduce the number of variables first f_j is eliminated from 1st order kinetics equation of TL (RW equation) using the maxima condition.

RW 1st order kinetics equation for one trap is

$$L_{TL} = C_{t0,j}\, f_j\ \exp(-\frac{D_j}{KT}) \exp(-\frac{f_j}{\beta}\ \int_{T_0}^{T} \exp(-\frac{D_j}{K\Theta})\ d\Theta) \tag{5.48}$$

Area of glow curve is $C_{t0,j}\beta$, hence glow curve (RW) normalized w. r. t area is

$$\eta_j = \frac{TL_j}{C_{t0,j}\beta} = \frac{f_j}{\beta} \exp\left(-\frac{D_j}{KT}\right) \exp\ (-\frac{f_j}{\beta} \int_{T_0}^{T} \exp\left(-\frac{D_j}{K\alpha}\right) d\alpha\,) \tag{5.49}$$

By maximizing equation (5.48) with respect to temperature (T) we get following condition

$$\frac{f_j}{\beta} = \frac{D_j}{KT_{mj}^2}\ \ \exp\left(\frac{D_j}{KT_{mj}}\right) \tag{5.50}$$

Where,

T_{mj}=Peak temperature for jth peak

Eliminating s_j/β from equation (5.49) using equation (5.50) we get

$$\eta_j = \frac{D_j}{KT_{mj}^2} \exp\left(\frac{D_j}{KT_{mj}}\right) \exp(\left(-\frac{D_j}{KT}\right) \exp[\ \frac{-D_j}{KT_{mj}^2} \exp\left(\frac{D_j}{KT_{mj}}\right)\ \int_{T_0}^{T} \exp\left(-\frac{D_j}{K\alpha}\right) d\alpha\,] \tag{5.51}$$

After this we maximize with respect to the only variable D_j

Using equation (5.33), (5.34), (5.35) & (5.51)

$$\frac{\partial Q}{\partial D_j} = \sum_{i=1}^{N} P(J|\, x_i, \Phi^{t^*})[\frac{K}{D_j} - \frac{1}{T_{mj}} - \frac{1}{x_i} - \frac{1}{T_{mj}^2}\ exp\left(\frac{D_j}{KT_{mj}}\right) \int_{x_{i0}}^{x_i} \exp\left(-\frac{D_j}{K\alpha}\right) d\alpha -$$

$$\frac{D_j}{KT_{mj}^3} exp\left(\frac{D_j}{KT_{mj}}\right) \int_{x_{i0}}^{x_i} \exp\left(-\frac{D_j}{K\alpha}\right) d\alpha + \frac{D_j}{KT_{mj}^2} exp\left(\frac{D_j}{KT_{mj}}\right) \int_{x_{i0}}^{x_i} \exp\left(-\frac{D_j}{K\alpha}\right)\left(\frac{1}{\alpha}\right) d\alpha] \tag{5.52}$$

$$\sum_{i=1}^{N} P(J|\, x_i, \Phi^{t^*})[\frac{K}{E_j} - \frac{1}{T_{mj}} - \frac{1}{x_i} - \frac{1}{T_{mj}^2}\ exp\left(\frac{E_j}{KT_{mj}}\right) \int_{x_{i0}}^{x_i} \exp\left(-\frac{E_j}{K\alpha}\right) d\alpha -$$

$$\frac{E_j}{KT_{mj}^3} exp\left(\frac{E_j}{KT_{mj}}\right) \int_{x_{i0}}^{x_i} \exp\left(-\frac{E_j}{K\alpha}\right) d\alpha + \frac{E_j}{KT_{mj}^2} exp\left(\frac{E_j}{KT_{mj}}\right) \int_{x_{i0}}^{x_i} \exp\left(-\frac{E_j}{K\alpha}\right)\left(\frac{1}{\alpha}\right) d\alpha] =0 \tag{5.53}$$

5.6.3 For General order kinetics peaks

The normalised (with respect to area) general order kinetics equation (GG equation) is

$$\eta_j = \frac{f_j''}{\beta} C_{t0,j} \exp(\ -\frac{D_j}{KT})[\ 1 + \left(b_j - 1\right) \frac{f_j''}{\beta} \int_{T_0}^{T} \exp\left(-\frac{D_j}{K\alpha}\right) d\alpha\ ]^{\frac{-b_j}{(b_j-1)}} \tag{5.54}$$

The parameters set is Φ ={ D_j, f_j'' and b_j}

Using equation (5.33), (5.34), (5.35) and (5.54) we following procedure

The partial derivatives with respect to the parameters give us following equations

$$\frac{\partial Q}{\partial D_j} = \sum_{i=1}^{N} P(J|\, x_i, \Phi^{t^*})[\frac{-1}{K\,T} + \frac{b_j\, f_j''}{\beta K}\ \frac{\int_{x_{i0}}^{x_i} \exp\left(-\frac{D_j}{K\alpha}\right) d\alpha}{1+ \left(b_j-1\right)\frac{f_j''}{\beta} \int_{x_{i0}}^{x_i} \exp\left(-\frac{D_j}{K\alpha}\right) d\alpha}] \tag{5.55}$$

$$\frac{\partial Q}{\partial f_j''} = \sum_{i=1}^{N} P(J|\, x_i, \Phi^{t^*})[\frac{1}{f_j''} - \frac{b_j}{\beta}\ \frac{\int_{x_{i0}}^{x_i} \exp\left(-\frac{D_j}{K\alpha}\right) d\alpha}{1+ \left(b_j-1\right)\frac{f_j''}{\beta} \int_{x_{i0}}^{x_i} \exp\left(-\frac{D_j}{K\alpha}\right) d\alpha}] \tag{5.56}$$

$$\frac{\partial Q}{\partial b_j} = \sum_{i=1}^{N} P(J|\, x_i, \Phi^{t^*})[\frac{b_j}{(b_j-1)} \left\{ \frac{\frac{f_j''}{\beta} \int_{x_{i0}}^{x_i} \exp\left(-\frac{D_j}{K\alpha}\right) d\alpha}{1+ \left(b_j-1\right)\frac{f_j''}{\beta} \int_{x_{i0}}^{x_i} \exp\left(-\frac{D_j}{K\alpha}\right) d\alpha} \right\} +$$

$$\log\left\{1 + \ \left(b_j - 1\right) \frac{f_j''}{\beta}\ \int_{x_{i0}}^{x_i} \exp\left(-\frac{D_j}{K\alpha}\right) d\alpha\right\} \frac{1}{(1-b_j)^2}] \tag{5.57}$$

By equating derivatives to zero we get following equations

$$\sum_{i=1}^{N} P(J|\, x_i, \Phi^{t^*}) \left[\frac{-1}{K\,T} + \frac{b_j\, f_j''}{\beta K} \, \frac{\int_{x_{i0}}^{x_i} \exp\left(-\frac{D_j}{K\alpha}\right) d\alpha}{1 + (b_j - 1)\frac{f_j''}{\beta} \int_{x_{i0}}^{x_i} \exp\left(-\frac{D_j}{K\alpha}\right) d\alpha} \right] = 0 \tag{5.58}$$

$$\sum_{i=1}^{N} P(J|\, x_i, \Phi^{t^*}) \left[\frac{1}{f_j''} - \frac{b_j}{\beta} \, \frac{\int_{x_{i0}}^{x_i} \exp\left(-\frac{D_j}{K\alpha}\right) d\alpha}{1 + (b_j - 1)\frac{f_j''}{\beta} \int_{x_{i0}}^{x_i} \exp\left(-\frac{D_j}{K\alpha}\right) d\alpha} \right] = 0 \tag{5.59}$$

$$\sum_{i=1}^{N} P(J|\, x_i, \Phi^{t^*}) [\frac{b_j}{(b_j - 1)} \left\{ \frac{\frac{f_j''}{\beta} \int_{x_{i0}}^{x_i} \exp\left(-\frac{D_j}{K\alpha}\right) d\alpha}{1 + (b_j - 1)\frac{f_j''}{\beta} \int_{x_{i0}}^{x_i} \exp\left(-\frac{D_j}{K\alpha}\right) d\alpha} \right\} + \log\left\{ 1 + \left(b_j - 1\right) \frac{f_j''}{\beta} \int_{x_{i0}}^{x_i} \exp\left(-\frac{D_j}{K\alpha}\right) d\alpha \right\} \frac{1}{\left(1 - b_j\right)^2}] = 0 \tag{5.60}$$

5.7 Algorithm for MM based CGCD

$$p(i,j) = P(x_i|\, J, \Phi^{t^*}) = \eta_j \tag{5.61}$$

$$\tau\,(i,j) = P(J\,|x_i, \Phi^{t^*}) \tag{5.62}$$

Algorithm to calculate the parameter set (E_J, s_J, w_J) is given below.

(I) Randomly choose value of parameters.

(II) Calculate $p(i,j)$ using equation (5.61).

(III) Calculate $\tau\,(i,j)$ using equation (5.62) and (5.41).

(IV) Calculate updated value of parameters using the non linear equations obtained in section 5.6.1 / 5.6.2 / 5.6.3.

(V) Generate the single peak glow curves with D_J and f_j using equation (5.49) or (5.54).

(VI) Superimpose them with weighting factors $w_J$to obtain simulated GC.

(VII) Normalise height of simulated GC with the experimental GC.

(VIII) Calculate Figure of Merit.

Reiterate with step (II) till good figure of merit (FOM) is achieved.

5.8 Validation with simulated glow curve

In this section we will validate the algorithm developed in this chapter. For this purpose we will use simulated glow curve.

Simulation of glow curve

The thermoluminescence intensity (TL) is given as

$$TL = -\sum_{j=1}^{k} \frac{dC_{t,j}}{dt} \tag{5.63}$$

The rate of change of trapped charge carrier density for a particular trap type (jth) is given by

$$TL_j = -\frac{dC_{t,j}}{dt} = C_{t,j}^{b} f_j^{'} \exp(-\frac{D_j}{KT}) \tag{5.64}$$

$$T = T_0 + \beta\, t$$

$$f'_j = f_j / C_{T,j}$$

where,

$C_{t,j}$ is trapped charge carrier density for jth trap type at time t

b is order of kinetics

D is trap depth

K is Boltzmann Constant

T is temperature °K

T_0 is initial temperature

β is heating rate

t is time of heating

f'_j is modified pre exponential factor for jth trap type

f_j is pre exponential factor or frequency factor for jth trap type

$C_{T,j}$ is trap concentration for jth trap type

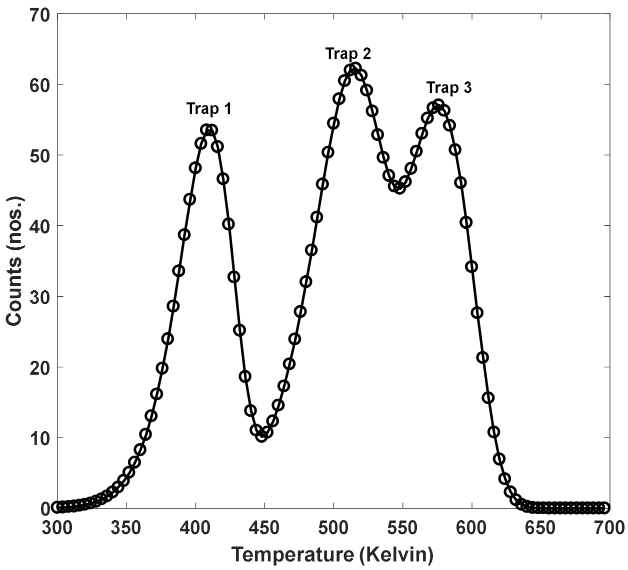

Figure 5.1 Convolved glow curve which is to be deconvoluted using MM formalism. The actual values of trap parameters for the component glow curve are mentioned in text.

Equation (5.64) cannot be solved analytically hence to get the thermoluminescence intensity TL_j we need to solve equation (5.64) numerically to obtain the charge carrier density $C_{t,j}(t)$. Thermoluminescence intensity from j^{th} trap(TL_j) is further obtained by taking derivative of $C_{t,j}(t)$ with respect of time. Overall thermoluminescence intensity (TL) may be obtained by summation over ‘j’ for all the trap types.

For illustration purpose, glow curve of our interest with three peaks, each of 1st order kinetics, is taken. Heating rate (β) is considered 5.0 ^{O}K/s. The parameters for each glow peak considered are given below:

1st peak: Trap depth (E)=0.7 eV, Initial trapped charge carrier concentration $=10^{23}m^{-3}$, Pre exponential factor (s)=10^8 sec^{-1}

2nd peak: Trap depth (E)=0.88 eV, Initial trapped charge carrier concentration =1.2 X 10^{23} m^{-3}, Pre exponential factor (s)=10^8 sec^{-1}

3rd peak: Trap depth (E)=1.0 eV, Initial trapped charge carrier concentration =1.5 X 10^{23} m^{-3} , Pre exponential factor (s)=10^8 sec^{-1}

All the three single peaks were superimposed to obtain the convolved glow curve. The convolved glow curve was divided by its area to get the normalised convolved glow curve. Further the obtained convolved glow curve was multiplied with suitable factor. This factor is 10000 in our case. This factor only effects computational time and to some extent accuracy of the deconvolution process. Larger this factor longer will be the computational time and better will be the accuracy. The effect on accuracy is not expected to be drastic. The obtained glow curve will be referred to as test gc.

Results

Figure 5.1 shows the glow curve which is to be deconvolved, the test gc. Figure 5.2 shows equation (5.53) in the probable range where solution may exist for three types of traps, namely, trap one (Figure 5.2 (a)), trap two (Figure 5.2 (b)) and trap three (Figure 5.2 (c)). In equation (5.53), j has three values ($j = 1, 2, 3$). In order to obtain Figure 5.2 (a) we have put $j = 1$ in equation (5.53) and obtain its value for $D_{j=1} = 0.1$ eV to $D_{j=1} = 1.5$ eV. Similarly Figure 5.2 (b) and Figure 5.2 (c) are obtained by putting $j = 2$ and $j = 3$ in equation (5.53) and obtaining its value in specified range of trap depth (0.1 eV to 1.5 eV). It is necessary to plot these graphs for two reasons. Firstly it checks that the solution of equation (5.53) lies in the range we have considered. Secondly if there are more than one solutions or local minima, then due care is to be taken accordingly.

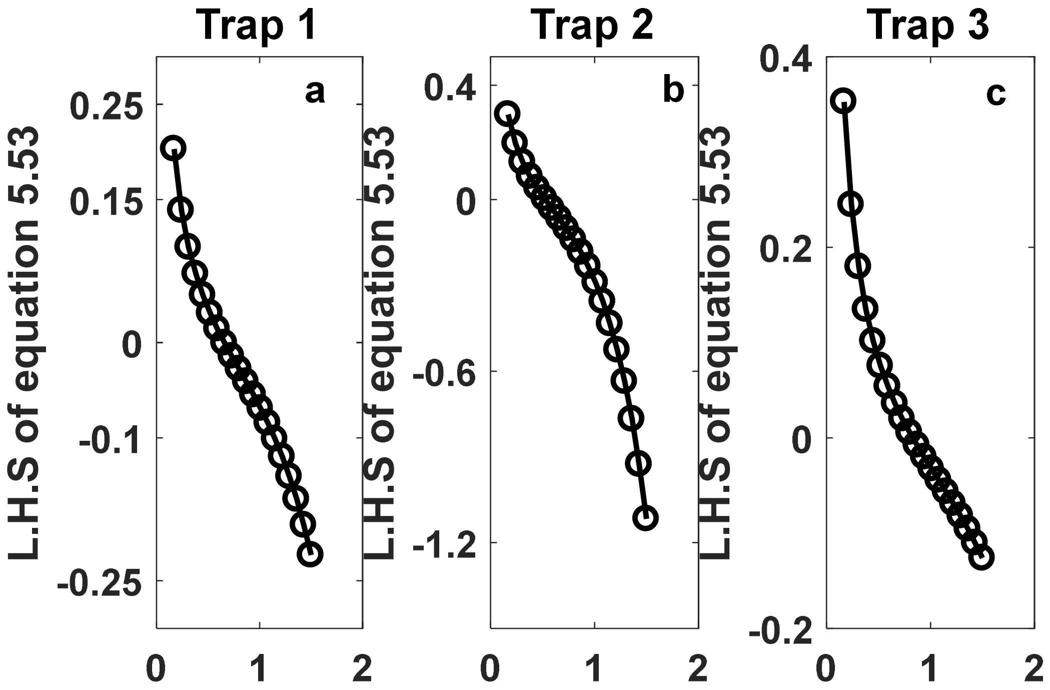

Figure 5.2 Plot of equation (5.53) with its independent variable i.e. trap depth for the three types of traps considered.

In equation (5.53), peak temperatures ($T_{mj},\ j = 1, 2, 3$) is a parameter. Hence it has to be evaluated before. It can be evaluated using 2nd derivative of the convolved glow curve data. It has been shown in Figure 5.3. It has been discussed in literature that 2nd derivative of composite glow curve data can be utilised to estimate the peak temperature and number of peaks [Reddy et al, 2018, Karmakar, 2017]. 2nd derivative is a reflection of curvature of graph; hence, at peak temperatures maximum curvatures will be obtained. By plotting 2nd derivative graph peak positions can be obtained from the locations of minima [Reddy et al, 2018, Karmakar, 2017]. By counting the number of peak locations we can estimate number of glow peaks. We are aware of the fact that this method has some limitations and it will not work for the cases where peaks do not show their existence at all in the overall convolved glow curve (test gc).

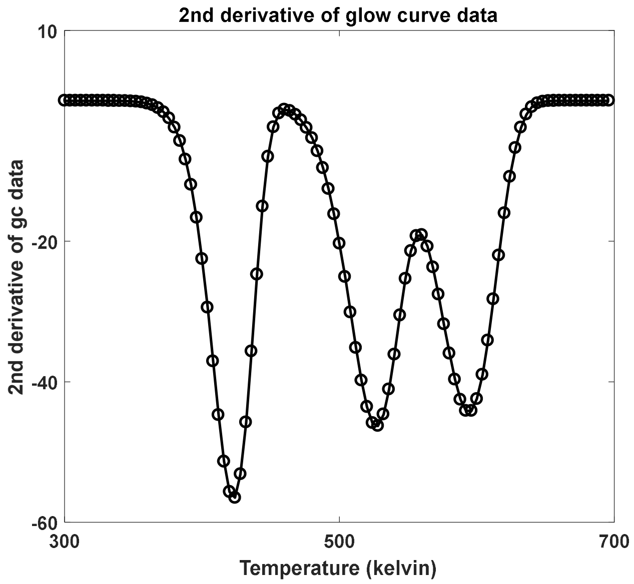

Figure 5.3 Figure show variation of 2^{nd} derivative of convolved glow curve data with variation in temperature.

Further we solve equation (5.53) to obtain the values of different trap depths (D_J) and equation (5.40 & 5.41) for weighting factors (w_J). For each set of parameters (D_J & w_J) values of pre exponential factor (f_j) can be calculated using equation (5.50). By obtained values of parameter set (D_J, f_j and w_J) graph of glow curves can be obtained and superimposed. The peak value of computed superimposed graph and the graph which was to be deconvolved is to be matched by applying suitable factor obtained from ratio of maximum values of the two.

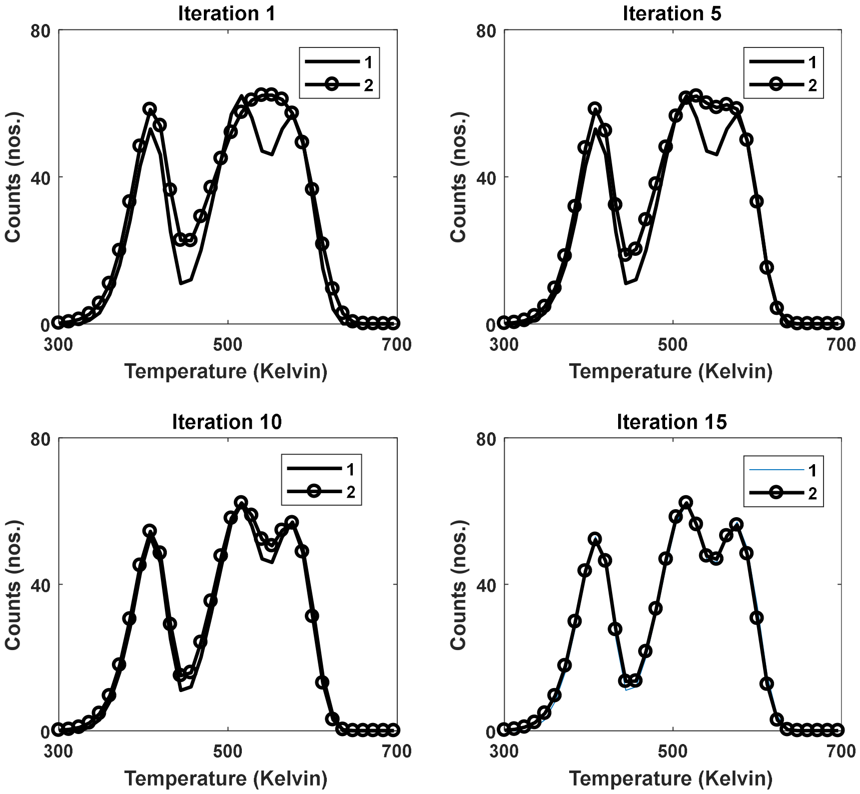

Figure 5.4 Deconvolution process at different iteration steps.

Figure 5.4 shows the evolution of iterative process at 1st, 5th, 10th and 15th iteration and figure 5.5 shows the final deconvolved graph. Values of parameters at concluding iteration step are tabulated in table 5.1. For comparing accuracy of results with current literature, data of all the three peaks were superimposed. This produces the simulated data set comprising TL counts and temperature. Figure of merit (FOM) was calculated using the following relation.

$$\text{FOM (\%)} = \frac{\left|\sum_{i=1}^{m}\left(y_{test\,gc} - y_{simulated}\right)\right|}{A} \text{ X } 100 \qquad (5.65)$$

Where m is the number of data points in unconvolved glow curve.

$y_{test\,gc}$ is the counts at a given temperature in glow curve initially generated for deconvolution.

$y_{simulated}$ is the counts obtained by superposition of deconvolved individual glow curve at that temperature.

A is area under the glow curve.

Figure 5.6 shows the variation in FOM with iteration steps.

FOM < 1% was calculated and computational time was few seconds, which is comparable to data in recent literature [Harvey et al, 2011].

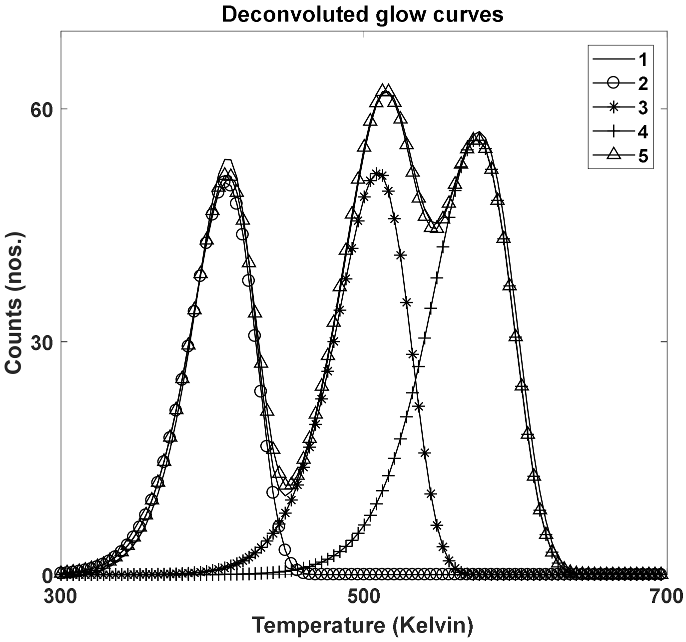

Figure5.5 Original convolved graph (1), deconvolved glow peaks (2,3,4) and superposition of the deconvolved glow peaks (5) at concluding iteration step.

Table 5.1 Actual value of parameters trap depth (D), frequency factor (f), initial concentration (C_0) and values obtained from simulation for three trap types (indicated by subscript indices).

	D_1(eV)	D_2(eV)	D_3(eV)	$f_1(sec^{-1})$	$f_2(sec^{-1})$	$f_3(sec^{-1})$	$C_{01}(m^{-3})$	$C_{02}(m^{-3})$	$C_{03}(m^{-3})$
Actual value	0.7000	0.8800	1.0000	1 X 10^8	1 X 10^8	1 X 10^8	1 X 10^{23}	1.2 X 10^{23}	1.5 X 10^{23}
Calculated value	0.6589	0.9110	1.0295	0.2583 X 10^8	1.9528 X 10^8	1.8311 X10^8	2.7794 X10^{23}	3.2238 X10^{23}	3.9248 X10^{23}

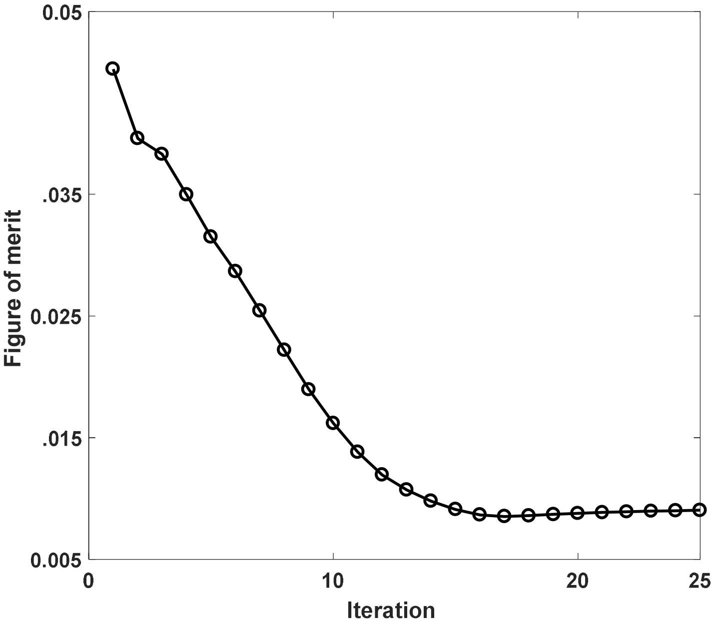

Figure 5.6 Figure of merit (FOM) during the iteration process. FOM is computed between original unconvolved glow curve and the superposition of deconvolved glow peaks as per formula given in text

5.9 Deconvolution of experimental glow curve

Figure 5.7 shows the experimental glow curve of $CaSO_4$: Dy which we intent to deconvolve and figure 5.8 show the deconvolved glow curve which is our result. Table 5.1 shows the trap parameters obtained from the deconvolution process. The weighting factors are also reported. Individual glow peaks were be generated, superimposed with applying weighting factors and further the total height of the obtained simulated glow curve was normalised with respect to the height of the experimental glow curve. By this way the deconvolution process was validated.

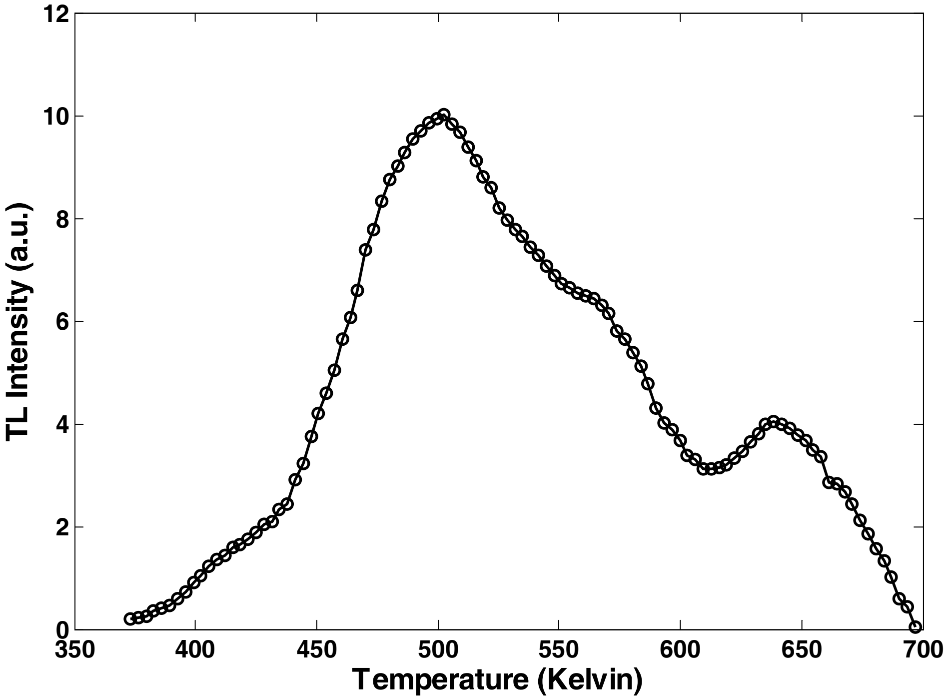

Figure 5.7 Experimental glow curve of CaSO4: Dy for a dose of 3.00 gray and heating rate of 1 °K/sec [Souza et. al., 1993].

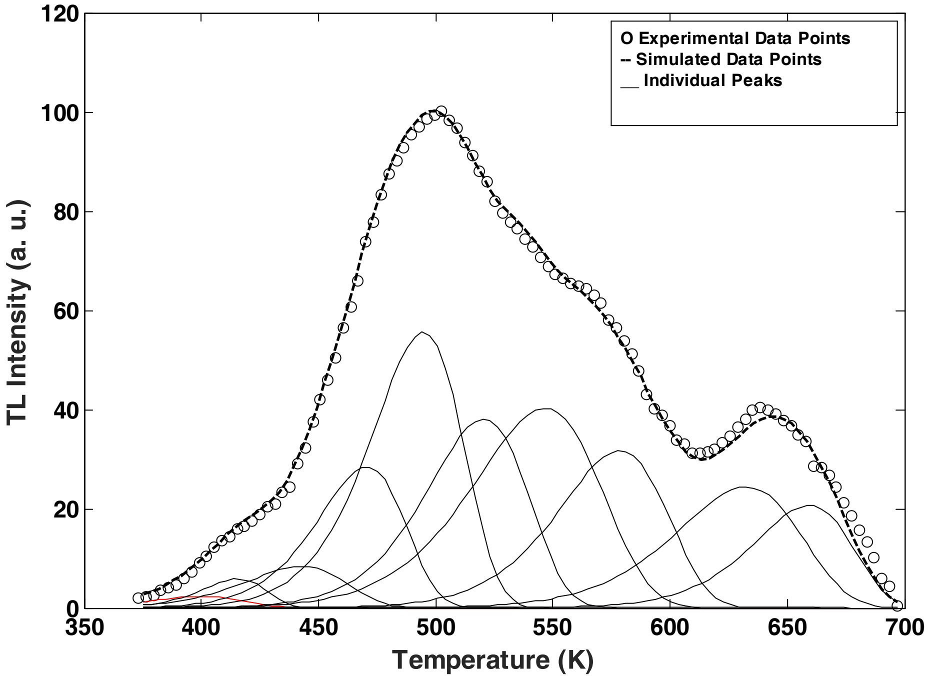

Figure 5.8 The deconvolved graph of Figure 5.7 glow curve.

Table 5.2 Trap parameters obtained by MM algorithm for $CaSO_4$: Dy.

Peak No.	**Weighting factor (w_j)**	**D_j (eV)**	**f_j (sec^{-1})**
1	0.0082	0.83	1.8×10^{9}
2	0.0139	0.99	7.5×10^{10}
3	0.0365	0.92	1.6×10^{9}
4	0.1016	1.10	3.8×10^{10}
5	0.1648	1.20	1.2×10^{11}
6	0.1638	1.10	3.0×10^{9}
7	0.1595	0.98	4.0×10^{7}
8	0.1445	1.09	1.3×10^{8}
9	0.1137	1.15	4.0×10^{7}
10	0.0774	1.73	7.9×10^{11}

5.10 Comparison with Synthetic glow curve of GLOCANIN Project

GLOw Curve ANalysis INtercomparision (GLOCANIN) was an international project carried out for comparison of computer programs for deconvolution of glow curves into individual glow peaks. Total number of computer programs that were intercomparied was thirteen. Reference glow curves were provided with specifications. REFGLOW.002 was having four peaks as per glow curve of TLD-100. The comparison of figure of merits (FOM) are given in table 5.3 with results of Sature et al [2017] and GLOCANIN projects. The superposition of individual peaks obtained by deconvolution (shown by symbol ‘o’) along with provided glow curve (shown by ‘-‘) are plotted in Figure 5.9. The FOM is plotted in Figure 5.10.

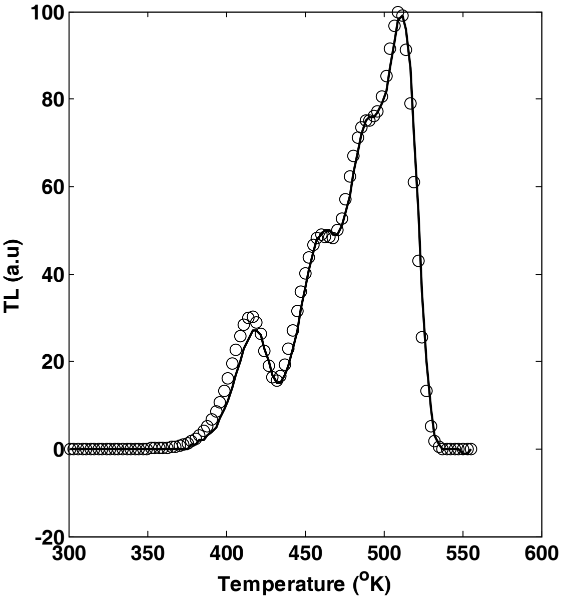

Figure 5.9 Deconvolution of Ref glow curve-002 of GLOCANIN project.

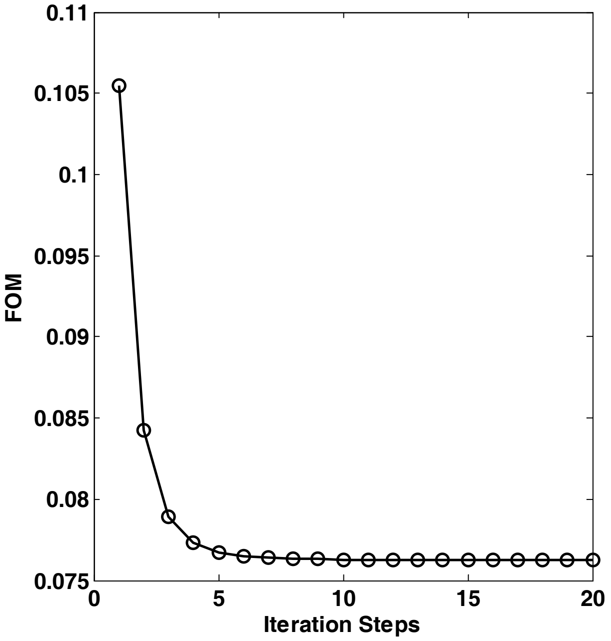

Figure 5.10 Plot of figure of merit (FOM) with iteration steps for Ref glow curve-002 of GLOCANIN project.

Table 5.3 Comparison of Figure of Merits (FOM) of our algorithm with results of Sature et al. [2017] and those of program in GLOCANIN projects.

	Result of our algorithm	**Results of Sature et al [2017]**	**Prog. B of GLOCANIN project**	**Prog. F of GLOCANIN project**
FOM (%)	**0 .07**	**0 .27**	**0.01**	**0.2950**

5.11 Advantage and disadvantage of MM based CGCD over other CGCD techniques

As already mentioned in the introduction of this chapter MM based is not only a novel technique for CGCD but has an added advantage over other CGCD techniques. It may be pivotal in development of theoretical platform for uniqueness of trap parameters.

On the disadvantage side it is possible to say that it is mathematically more involved.

5.12 Conclusion

In this chapter prerequisite for EM algorithm like conditional probability, Bayes' theorem etc. are discussed, following that MLE and EM is explained. Further, it has been elaborated that how the deconvolution problem of TL glow curve can be mapped to general formalism of MM. Its mathematics is also discussed.

Our algorithm for deconvolution of TL glow curve based on MM using EM algorithm is elaborated. Mathematical calculations have been done for three cases: (a) assuming the glow peaks to be Gaussian (b) assuming the glow peaks to be of first order kinetics and (c) assuming the glow peaks to be of general order kinetics. It is validated with a simulated glow curve. For validation a synthetic glow curve has been generated comprising of three TL peaks. Further this is deconvoluted using our algorithm and the obtained value of trap parameters are compared with the original values of trap parameters which were used to generate the synthetic glow curve.

And in the last deconvolution of experimental glow curve of $CaSO_4$: Dy is done. Its deconvoluted graph and the calculated value of trap parameters are presented.

Lastly, comparision with simulated glow curve of GLOCANIN project is done by data given by Sature et al [Sature et al, 2017].

Our method is quite robust as for any value of trap parameters it is equally efficient and has no bias for small or large value of activation energy. Once the code is written (which can be provided with reader as an executable file) there is not much left for the uses to do. User just need to input number glow peaks and give input glow curve file a particular name (which is recognized by the program). The result has been compared with experimental glow curve of $CaSO_4$: Dy (which is phosphor important for dosimetric applications in India) in section 5.9, self simulated glow curve in section 5.8 and simulated glow curve of GLOCANIN project in section 5.10.

As far as fitting experimental glow curve of $CaSO_4$: Dy with 10 peaks is concerned, it is well known that this phosphor has a continuous distribution of traps (Srivastava J K and Supe S J, Trap distribution analysis for thermoluminescence of $CaSO_4$: Dy, Journal of Phyiscs D: Applied physics 16 (1983) 1813-1818. But it also exists in literature that it gives good figure of merit if fitted with 10 glow peaks for the range of temperature important to us (Souza et al, Radiation protection dosimetry 47 (1993) 103-106. Hence, a comparison with 10 glow peaks is done.

CHAPTER VI

Summary and Future Plans

CHAPTER III: Deviation in TL intensity from model predicted glow curve: Sources of Uncertainty

Coming back to the basic models of 1st ,2nd and general order kinetics and analysing things from the perspective of these models following observations can be made. RW, GG and MP predict TL intensity at a particular stimulating temperature, given the model parameters. But, there are various sources which lead to deviation from these predicted values. This topic is discussed from a theoretical perspective and experimental reasons are not elaborated much, though they have been briefed.

One of the most important reasons that lead to deviation from predicted values from these models is fading. Fading is loss of signal with storage time. Types of fading are thermal fading, anomalous fading and thermally assisted fading. Thermal fading is loss of TL signal due to excitation of trapped charge carrier as a result of ambient temperature. Anomalous fading is due to tunnelling of charge carrier from ground state of trap to recombination centre. It is obvious that the fading will lead to luminescence from the sample during the period of storage. This is known as afterglow. ***As we have contributed to the literature in the domain of anomalous fading, it is pertinent to elaborate on it at this point.***

Extensive experimental work exists on afterglow in literature for period of time ranging from fraction of second to decades. But the exact expression for afterglow is not existing in literature, though for a very long time it is said to follow a power law $I \,\alpha\, t^{-k}$. This means a graph between log (I) and log(st) should be a straight line. Where, s is just a scaling factor. Before our work it was prevalent in literature that different slopes of log (I) - log(st) graph can be obtained with different recombination centre concentration. But with this approach full experimental range of exponent k, could not be obtained theoretically. Our work considered the trap and the recombination centre as two potential wells separated by potential barrier of different shapes (increasing, decreasing and constant). Further, the tunnelling probability of charge carrier from trap to recombination centre using WKB theory was calculated. Finally an expression of afterglow intensity was obtained. This approach could obtain full experimental range of exponent k, for different potential barrier shape between trap and recombination centre.

But experimental literature not only reports straight line graph between log (I) and log(st) but also non linear graphs. In a further work it has been established by us that non linearity is general nature of afterglow and the linear graph that are obtain in experiment or simulation is an artefact of limited period of observation. In this work, various factors that may affect the advent of non linearity in afterglow like initial time at which observation is started, recombination centre concentration etc. are also discussed.

Among other reasons of deviation, finite life time of charge carrier in conduction band already referred to as quasi equilibrium approximation is an important factor. It has been shown by simulation that this approximation is always not valid.

Non interactive kinetics approximation of OTOR model also discussed in this chapter is certainly a reason of deviation from values predicated by OTOR model based expressions i.e RW, GG and MP.

The trap parameters, trap depth (D) and attempt to escape frequency (f) are assumed to be a constant parameter for full stimulating range of temperature. But, as matter of fact they are temperature dependent. This point is also elaborated.

It is possible that the TL emission from the sample may be partially absorbed by the sample, which may lead to different repercussions like optical excitation of charge carriers from deeper traps.

Quenching is reduction of TL intensity with temperature (thermal quenching), concentration of dopant (concentration quenching) and with added impurity (impurity quenching). This is another factor which is not accounted for in the basic RW, GG and MP expressions for TL emission.

TL left in dosimeter after 1st readout which comes out in subsequent readouts is termed as residual TL. The origin of residual TL was a dilemma in literature before our contribution. ***It has been established by our work that the deeper traps that are excited to a very little extent by thermal stimulus are the source of residual TL.*** Due to contribution of deeper traps during the readout process the predication from RW, GG and MP models will be erroneous if only dosimetric trap is considered.

But all these sources of deviation are explored to a good extent in literature. Only one reason i.e. uncertainty in trap parameters, trap depth (D) and pre exponential factor (f), leading to deviation from values predicated by RW, GG and MP models is a domain which is almost unexplored. Hence, we explore this in full detail.

Chapter IV: Parametric uncertainty analysis of basic TL models

In this section it has been studied how uncertainty in trap parameters, trap depth (D) and pre exponential factor (f), propagate through RW, GG and MP models for full range of stimulating temperature. Uncertainty analysis has been done using Monte Carlo, Fuzzy set theory and Polynomial Chaos.

Monte Carlo

Gaussian PDF has been assumed for the trap parameters (D & f) with typical values of mean and standard deviation. From these PDFs random samplings of the values of trap parameters, as per standard Monte Carlo procedure has been done. From the sampled values the set of output TL has been generated. By histograming, the PDF of output TL has been obtained. From PDF, the CDF could be generated and further the uncertainty, using 5th and 95th percentile. By repeating the whole process for full range of temperature, temperature vs uncertainty graph could be obtained. It has typical shape with two maxima with a minimum in between. The minimum is located at the temperature value at which we have a peak in the glow curve. Qualitative explanation of the nature of graph is also provided in the text.

The major benefit of above study is; it could be used to establish that effects like temperature quenching are dominant in a particular glow peak or not.

As MC simulation involves large number of simulation runs. Hence, α cut method of Fuzzy set theory is introduced for uncertainty analysis of TL models.

Fuzzy set theory

α-cut method of fuzzy set theory is used to do the uncertainty analysis of RW, GG and MP models. Triangular membership function for D & f has been assumed. A membership function is a graph between parameter value (x axis) and membership value α (y axis).

Further, a particular value of α-cut was taken and book keeping of the minimum and maximum value of the parameters corresponding to this value α-cut had been done. After this all combinations of obtained parameter sets were generated and the TL values corresponding to them were obtained. The minimum and maximum values of TL output from these TL values were obtained. This is the minimum and maximum value of TL corresponding to considered value of α-cut.

By scanning whole range of α (0-1) and repeating the above procedure the membership function graph for the output TL could be obtained. From the membership function graph uncertainty for a particular value of temperature could be obtained, at which the above procedure is done. Repeating the whole process for full range of stimulating temperature the temperature vs uncertainty graph could be obtained.

It is found that it has similar qualitative nature as the temperature vs uncertainty graph obtained from the Monte Carlo analysis.

Polynomial Chaos

This is yet another way of propagation of uncertainty from uncertain input parameters (trap depth and pre exponential factor in our case) of model to output of the model (TL intensity in our case). The major advantage of this method over conventional methods is requires very small number of simulation runs unlike conventional methods like Monte Carlo.

Using this technique the output TL intensity was expanded in terms of Hermite Polynomials with standard random variables (srvs) as arguments of Hermite Polynomials. The srvs were randomly selected from sets of independently identically distributed (iid) normally distributed sets of random numbers. Using this expansion the response surface was simulated. The sample size required for this simulation, for number of input variables equal to two and expansion up to second order Hermite Polynomials, was just equal to six. With this small sample size the response surface could be simulated and used to generate the probability distribution function (PDF) of output TL intensity. From this PDF the cumulative distribution function (CDF), and thereby uncertainty, was quantified.

CHAPTER V: Deconvolution of TL glow curve

In this chapter a novel method of deconvolution of TL glow curve was established using Mixture Model (MM) techniques. The results were verified using simulated glow curve.

The chapter was started with discussing the prerequisites of the technique like conditional probability, Bayes' theorem, Posterior probability, Maximum likelihood estimation (MLE) and Expectation Maximization (EM) algorithm. Further, using MLE and EM an algebraic expression for trap parameters was established, which requires and iterative solution. This was done for both first order kinetics (RW model) and general order kinetics (MP model).

In the end the method was verified using simulated glow curve (including simulated glow curve from GLOCANIN project). Further, experimental glow curve of $CaSO_4$: Dy was deconvolved.

CHAPTER VI: Summary and Future Plans

In this chapter the whole work was summarized and the chapter concludes with probable future directions.

Probable future directions

1. Algorithm for Deconvolution based dosimetry of radiation workers

The three element dosimeter based on $CaSO_4$: Dy phosphor mixed with Teflon is prevalent in Indian Personnel Monitoring programme. It involves phosphorescence decay with non linear clamped heating profile with saturation temperature 285°C for all the three discs. Further an algorithm evaluates the dose. This method still involves all the traps present in the phosphor. I intent to develop this process for single peak i.e. the main dosemetric peak. During the work of this thesis I have gone through various advantages of single peak dosimetry like increase in precision and reduction of MMD. Hence, further work can be initiated in this direction to increase precision and MMD for PMS of my country.

2. Estimating time elapsed from single shot exposure for $CaSO_4$: Dy based three element dosimeter used in PMS of India.

Though I understand the idea of estimating the time elapsed from single shot exposure is not a new idea for international community but this technique is not yet fully developed and used in PMS provided by Indian laboratories. Hence, developing this technique for the TLD used in Indian scenario is another target which can be explored. It will certainly require deconvolution of peaks. Hence, the work done on deconvolution in this thesis will be a milestone for proposed work.

3. Establishment of mathematical formulation for correct number of individual peaks for a given glow curve (a purely theoretical approach).

During the period of thesis I have gone through lot of literature on deconvolution. There is lack of concrete theoretical research paper on what should be the correct number of glow peaks for a given glow curve.

4. Effect of temperature quenching to be introduced inside deconvolution code.

If a phosphor is having thermal quenching in that case application of LMM for deconvolution will certainly result in wrong trap parameters. It would be interested to develop a code for deconvolution in this case.

5. Re establishment of experimental work citied by Sahai et al, 2018.

As suggested by Dr. Georgios S. Polymeris (Reviewer 1) it would be of interest to re establish the theoretical results of Sahai et al [Sahai et al, 2018] experimentally, using Durango apatite or some other persistent phosphor.

6. In the context of power law decay discussed in Chapter three, non linear estimation of fractal and multifractal techniques will be discussed.

A fractal is a self similar subset of Euclidean space whose fractal dimension strictly exceeds topological dimension.

For example, if we look at earth from moon it will be more or less a sphere. But as we come closer, new features like hill, valleys start coming up into picture. If there is a self similarity as we zoom in the object is called a fractal.

Another example is measuring length of a sea coast. If we measure it using a meter scale it has a different value, as compared to, if we measure it with a scale of millimeter length. Hence the length of a sea coast is also a function of the length of the scale with which it is measured. This property makes it distinct from geometric figures like line, side of triangle etc. where choice of length of scale does not make any difference. Again self similarity is important as we zoom in for being categorized as fractal.

An important way of discriminating fractal from geometric figures is the way scale. For example if we double the radius of a sphere, its volume becomes eight times. However if fractal's one dimensional lengths are doubled the spatial content of fractal scales by a power which is not necessarily a integer. This power is called fractal dimension.

If we generalize the concept of fractal system in which single fractal dimension is not enough, rather a continuous spectrum of exponents (so called singularity spectrum) is required. The system is called multifractal.

The behavior of a multifractal system s* around any point x is described by a local power law.

$$s^*\ (\bar{x}+\bar{a}) - s^*(\bar{x}) = a^{h^*\overline{(x)}}$$

Where, $h^*\overline{(x)}$ is singularity exponent as it describes singularity or regularity around a point x.

Singularity manifold of exponent h^* is the ensemble formed by all points that share same singularity exponent and is a fractal set of fractal dimension $D'(h^*)$. Curve of $D'(h^*)$ vs. h^* is called singularity spectrum.

As in our case we are talking about power law decay of luminescence hence, non linear estimation and application of fractal and multifractal techniques will be really very interesting. We thankfully add it to our list of future directions of work.

ABSTRACT

Thermoluminescence (TL) is the phenomenon of emission of energy in form of light when thermal stimulus is given to a pre exposed thermoluminescent material (known as phosphor). When ionizing radiation falls on a phosphor, it generates charge carriers, which subsequently get trapped at defect centers of the material. When stimulus is given, the trapped charge carriers get excited to delocalized energy levels and when they eventually get in the vicinity of defect centers which have opposite charge carrier trapped at its site (known as recombination center), they recombine to produce luminescence. This is mechanism of TL phenomenon. Various models collectively known as delocalized transition models of thermoluminescence have been developed for simulation of the phenomenon.

If the traps and recombination centers are spatially close. Charge leakage is possible due to tunneling (thermally assisted/anomalous). The luminescence arising due to charge leakage is called after glow. The loss signal due to the phenomenon is called fading. Localized transition models exist for its modeling.

Analyzing from perspective of basic models there are various sources that lead to deviation from TL predicted from these models like residual TL, uncertainty in model parameters, etc. As uncertainty in model parameters is a possible reason of deviation from model predicted values, it is interesting to do a parametric uncertainty analysis of basic models.

As real life materials will have more than one type of trap the TL emission will be a superposition of TL from all the trap types. Hence deconvolution of TL glow curve is another aspect covered in dissertation.

We have five major achievements during the period of thesis.

1. A novel methodology of deconvolution of TL signal based on Expectation Maximization (EM) algorithm and Maximum Likelihood estimation (MLE) is developed. It has been validated with simulated glow curve (GC). Further deconvolution experimental GC of $CaSO_4$: Dy is achieved.
2. The origin of Residual TL has been investigated. Results of theoretical model and experiments are matching to a good extent.
3. After glow from thermoluminescent material was mostly investigated experimentally. Theoretical explanation of experimental findings has been one of the achievements of this dissertation.
4. It has been established that non linearity is general feature of afterglow.
5. Monte Carlo, fuzzy set theory and Polynomial chaos expansion based study for parametric uncertainty analysis of RW, GG and MP models has been conducted.

References

Adamiec G, Bluszcz A, Bailey R, Garcia-Talavera M, Finding model parameters: Genetic algorithms and the numerical modelling of quartz luminescence, Radiation Measurements 41 (2006) 897-902

Adirovitch E I, La formule de Becquerel et la loi elementaire du declin de la luminescence des phosphores crystallins, Journal of Phys. Radium 17 (1956) 705-707

Afouxenidis D, Polymeris G S, Tsirliganis N C and Kitis G, Computerised Curve Deconvolution of TL/OSL Curves using a Popular Spreadsheet Program, Radiation Protection Dosimetry 149 (2012) 363-370

Aitken M. J., Thermoluminescence dating, Academic Press (1985), London

Altekar W, Tatake U G and Sane P V, Proceedings of national symposium of thermoluminescence and its applications, Kalpakkam (1975) 309

Aramu F, Maxia V, Serra M and Spano G, Thermoluminescence of hydroxy and aminobenzoic acids, Journal of Luminescence 5 (1972) 439-448

Askorft N W and Mermin N D, Solid State Physics, Holt: Rinehart and Winston (1976), New York

Atone M S, Dhoble S J, Moharil S V, Dhopte S M, Muthal P L and Kondawar V K, Sensitization of Luminescence of $CaSO_4$: Dy, physica status solidi (a) 135 (1993) 299-305

Ayyangar K, Chandra B and Lakshmanan A R, Mixed Field Dosimetry with $CaSO_4$: Dy, Physics in Medicine &. Biology 19 (1974) 656-664

Bacci C, Bernabei R, Dangelo S and Furetta C, Analysis of TLD-900 glow-curves: Results on single peak properties, Radiation Effects 69 (1983) 127-133

Barthe J, Hickman C, Heindl R and Portal G, Thermoluminescence Dosimetry at High Temperature and High Doses, Radiation Protection Dosimetry 47 (1993) 567-569

Ben Shachar B and Horowitz Y S, Dosimetric Characterisation of the High Temperature Peaks of LiF: Mg, Ti and CaF_2: Tm using Computerised Glow Curve Deconvolution, Radiation Protection Dosimetry 22 (1988) 87-96

Benavente J F, Gomez-Ros J M and Romero A M, Themoluminescence glow curve deconvolution for discrete and continuous trap distribution, Applied Radiation and Isotopes 153 (2019) 108843

Bhatt B C, Lakshmanan A R, Shinde S S and Bhatt R C, Radiation Damage in LiF: Mg, Ti and $CaSO_4$: Dy TLD phosphors, Radiation Protection Dosimetry 25 (1988) 37-41

Bhatt B C, Shinde S S, Srivastava J K and Gundu Rao T. K, Effect of Charge Compensator/ Co dopent on the TL Charactristics of $CaSO_4$: Dy and $CaSO_4$: Tm phosphors, Radiation Protection Dosimetry 65 (1996) 287-290

Bos A J J, Piters T M, Gomez-Ros J M and Delgado A, An Intercomparison of Glow Curve Analysis Computers Programs: I. Synthetic Glow Curves, Radiation Protection Dosimetry 47 (1993) 473-477

Bos A J J, Piters T M, Gomez-Ros J M and Delgado A, An Intercomparison of Glow Curve Analysis Computers Programs: II. Measured Glow Curves, Radiation Protection Dosimetry 51 (1994) 257-264

Brinck W, Gross K, Gels G and Partridge J, Special External Radiation Field Study at the Vermont Yankee Nuclear Power Station, Health Physics 32 (1977) 221-230

Bube R H, Photoconductivity of Solids, Wiley and Sons (1960), New York

Budd T, Marshall M, Peaple L H J and Douglas J A, The Low-and High-temperature Response of Lithium Fluoride Dosemeters to X-rays, Physics in Medicine and Biology 24 (1979) 71-80

Bull C and Garlick G F J, Proceedings of the Physical Society of London 63 (1950) 1283.

Bull R K, Mckeever S W S, Chen R, Mathur V K, Rhodes J F and Brown M D, Thermoluminescence kinetics for multipeak glow curves produced by the release of electrons and holes, Journal of Physics D: Applied Physics 19 (1986) 1321-1334

Bull R K, Kinetics of localized transition model for thermoluminescence, Journal of physics D: Applied Physics 22 (1989) 1375-1379

Cameron J R and Kenney G N, Abstracts of Papers for the Eleventh Annual Meeting of Radiation Research Society, Milwaukee, Wisconsin, May 27-29, Radiation Research 19 (1963) 199

Cameron J R, Suntharalingam N and Kenney G N, Thermoluminescence Dosimetry, University of Wisconsin Press (1968), Medison

Chanas S, Kolodziejczyk W and Machaj A, A fuzzy approach to the transportation problem, Fuzzy sets and system 13 (1984) 211-221

Chandra B and Bhatt R C, Effect of Dysprosium Concentration on the TL Characteristics of $CaSO_4$: Dy Phosphor, Nuclear Instruments and Methods 164 (1979) 571-577

Chandra B, Shinde S S, Lakshmanan A R and Bhatt R C, Effect of Doping with Monovalent Cation Impurites on Thermoluminescence Response of CaSO4: Dy Phosphor, physica Status solidi. (a) 103 (1987) 599-605

Chandrasekharan P C, Proceedings of national symposium on themoluminescence and its applications, Kalpakkam (1975) 638-647

Charles M W, An extended role for thermoluminescent phosphors in personnel environmental and accident dosimetry using sensitisation, re-estimation and fast fading, Nuclear Instruments and Methods in Physics Research 206 (1983) 239-242

Chase W J, Bezaire M D, Vanderzwet F P and Taylor C E, A glow curve analyser (GCA) for routine analysis of personnel thermoluminescent dosemeter results, Radiation Measurements 43 (2008) 621-625

Chen R, Glow Curves with General Order Kinetics, Journal of Electrochemical Society 116 (1969) 1254-1257

Chen R, Methods for kinetic analysis of thermally stimulated processes, Journal of Material Science 11 (1976) 1521-1541

Chen R, Kristianpoller N, Davidson Z and Visocekas R, Mixed First and Second Order Kinetics in Thermally Stimulated Processes, Journal of Luminescence 23 (1981) 293-303

Chen R and Mckeever S W S, Characterization of nonlinearities in dose dependence of thermoluminescence, Radiation Measurements 23 (1994) 667-673

Chen R and Mckeever S W S, Theory of thermoluminescence and related phenomenon, World Scientific (1997), London

Chen R and Pagonis V, Thermally and optically simulated luminescence A simulation approach, John Wiley and Sons Ltd. (2011) UK

Christodoulides C, General-order kinetics in thermoluminescence resulting from a distribution of the frequency factor, physica status solidi (a) 118 (1990) 333-342

Chung K S, Choe H S, Lee J I, Kim J L and Chang S Y, A computer program for deconvolution of themoluminescence glow curves, Radiation Protection Dosimetry 115 (2005) 345-349

Chung K S, Choe H S, Lee J I and Kim J L, A new method for the numerical analysis of thermoluminescence glow curve, Radiation measurements 42 (2007) 731-734

Chung K S, Lee J I and Kim J L, A computer program for the deconvolution of the thermoluminescence glow curves by employing the interactive trap model, Radiation Measurements, 47 (2012) 766-769

Corless R M, Gonnet G H, Hare D G E, Jeffrey D J and Knuth D E, On Lambert-W function, Adv. Comput. Math. 5 (1996) 329-359

Corless R M, Jeffrey D J and Knuth D E, A sequence series for Lambert W function, Proceedings of the international symposium on Symbolic and Algebraic Computation ISSAC 133-140

Corless R M and Jeffrey D J, The Wright ω function, Lecture Notes Computer Science, 2385 (2002) 76-89

Danby R J, Boas J F, Calvert R L and Pilbrow J R, ESR of thermoluminescent centres in CaSO4 single crystal, Journal of Physics C: Solid State Physics 15 (1982) 2483-2493

Daniels F, Boyd C A and Saunders D F, Thermoluminescence as a Research Tool, Science 117 (1953) 343-349

Delbecq C J, Toyozawa Y and Yuster P H, Tunneling recombination of trapped electrons and holes in KCl: AgCl and KCI:TlCl, Physical Review B 9 (1974) 4497-4505

Delgado A, Gomez Ros J M, A simple method for glow curve analysis improving TLD 100 performance in dose region below 100 gray, Radiation Protection Dosimetry 34 (1990) 357-360

Delgado A, Gomez Ros J M, Muniz J L and Portillo J C, Application of Glow Curve Analysis Methods to Improve TLD-100 Dose Reassessment Performance, Health Physics 62 (1992) 228-234

Delgado A and Gomez Ros J M, Computerized Glow Curve Analysis: A Tool For Routine Thermoluminescence Dosimetry, Radiation Protection Dosimetry 96 (2001) 127-132

Dempster A P, Laird N M and Rubin D B, Maximum likelihood from incomplete data via EM algorithm, Journal of the Royal Statistical Society. Series B (Methodological) 39 (1997) 1-38

Draai W T and Blasse G, Energy transfer from vanadate to rare-earth ions in calcium sulphate, physica status solidi (a) 21 (1974) 569-579

Duran-Munoz H, Hernandez-Ortiz M, Sifuentes-Gallardo C, Galvan-Tejeda J I, Sanchez-Zeferino R and Castano-Meneses V M, Comparative study of kinetic parameters induced by different excitation sources using a novel and user friendly glow curve deconvolution spreadsheet, Journal of Material Science: Material in Electronics 29 (2018) 15732-15740

Dussel G A and Bube R H, Theory of Thermally Stimulated Conductivity in a Previously Photoexcited Crystal, Physical Review 155 (1967) 764-779

El-Hafez A I, Yasin M M and Sadek A M, GCAFIT- A new tool for glow curve analysis in thermoluminescence nanodosimetry, Nuclear Instruments and methods in Physics Research 637 (2011) 158-163

El-Kinawy M, El-Nashar H F and El-Faramawy N, New designed software to deconvolute the thermoluminescence glow curves, SN applied Science 1 (2019) 843

Ewles J and Lee N, Studies on the Concept of Large Activator Centers in Crystal Phosphors I. Dependence of Luminescent Efficiency on concentration of Activator. Size of Luminescent Centers, Journal of Electrochemical Society 100 (1953) 392-398

Eyring H, Viscosity, Plasticity and Diffusion as Examples of Absolute Reaction Rates, Journal of Chemical Physics 4 (1936) 283-291

Fillard J P, Gasiot J and Manifacier J C, New approach to thermally stimulated transients: Experimental evidence for ZnSe: Al crystals, Physical Review B 18 (1978) 4497-4508

Fraley C and Raftery A, How many clusters? Which Clustering Method? Answers Via Model-Based Cluster Analysis, The computer Journal (1998) 41 578-587

Fiorella O, Mangia M, Oliveri E, Thermoluminescence Isothermal Decay in γ Irradiated $CaSO_4$: Dy Phosphors- Kinetics and Distribution of Trap Depths, International Journal for Radiation Physics and Chemistry 8 (1976) 441-447

Furetta C, Tuyn J W N, Louis F, Azorin-Nieto J, Gutierrez A and Driscoll C M H, A method for determining simultaneously the dose and the elapsed time since irradiation using TLDs, International Journal of Radiation Applications Instrumentation. Part A. Applied Radiation and Isotopes 39 (1988) 59-69

Furetta C, Kitis G and Kuo C H, Kinetics parameters of CVD diamond by computerised glow- curve deconvolution (CGCD), Nuclear instruments and methods in physics research B 160 (2000) 65-72

Furetta C, Handbook of thermoluminescence, World Scientific (2003), Singapore

Garlick G F J and Gibson A F, Proceedings of Physical Society 60 (1948) 574-590

Ghanem, Roger G and Spanos P, Stochastic Finite elements: A spectral Approach, Springer (1991)

Gassiat E and Dacunha-Castelle D, Estimation of the number of components in a mixture, Bernoulli 3 (1997) 279-299

Gibbs J H, Sufficient Conditions for the Arrhenius Rate Law, The Journal of Chemical Physics 57 (1972) 4473-4478

Glover F, Tabu search for nonlinear and parametric optimization (with links to genetic algorithm), Discrete Applied Mathematics 49 (1994) 231-255

Gomez-Ros J M, Muniz J L, Delgado A, Botter-Jensen L and Jorgensen F, A Glow Curve Analysis Method for Non-Linear Heating Hot Gas Readers, Radiation Protection Dosimetry 47 (1993) 483-487

Gomez-Ros J M, Saez Vergara J C, Romero A M and Budzanowski M, Fast automatic glow curve deconvolution of LiF: Mg, Cu, P curves and its application in routine dosimetry, Radiation Protection Dosimetry 85 (1999) 249-252

Gomez-Ros and Kitis G, Computerized glow curve deconvolution using mixed and general order kinetics, Radiation Protection Dosimetry 101 (2002) 47-52

Gorkums A A van, A new method for analyzing 1st and 2nd order desorption spectra and glow curves, Journal of Applied physics 51 (1980) 2594-2602

Grenet J, Vautier C, Carles D and Chabrier J J, Space charge conduction in presence of a Gaussian distribution of localized state, The Philosophical Magazine 28 (1973) 1265-1277

Gundu Rao T K, Bhatt B C, Srivastava J K and Nambi K S V, On the sulphoxy radicals in $CaSO_4$: Dy, Na thermoluminescent phosphor: electron paramagnetic resonance studies, Journal of Physics: Condensed Matter 5 (1993) 1791-1800

Halperin A and Braner A A, Evaluation of Thermal Activation Energies from Glow Curve, Physical Review 117 (1960) 408-415

Harvey J A, Rodrigues M L and Kearfott K J, A computerized glow curve (GCA) method for WinREMS thermoluminescent dosimeter data using MATLAB, Applied Radiation and Isotope 69 (2011) 1282-1286

Hasan F A, Keck B D, Hartmetz C and Sears D W G, Anomalous fading of thermoluminescence in meteorites, Journal of Luminescence 34 (1986) 327-335

Holm N W and Berry J (Eds) Manual of Radiation Dosimetry (1970), New York

Hornyak W F and Franklin A D, Single level isothermal TL-decay (with energy level distribution and retrapping), International journal of Radiation Applications and Instrumentation. Part D. Nuclear Tracks and Radiation Measurements 14 (1988) 81-89

Hornyak W F and Chen R, Thermoluminescence and Phosphorescence with a continuous distribution of Activation Energy, Journal of Luminescence 44 (1989) 73-81

Horowitz Y S and Moscovitch M, Computerized Glow Curve Deconvolution Applied to High Dose (10^2-10^5 Gy) TL Dosimetry, Nuclear instruments and methods in physics research A 243 (1986) 207-214

Horowitz Y S and Mosowitch M, LiF-TLD in microgray dose range via computerized glow curve deconvolution and background smoothing, Radiation Protection dosimetry 17 (1986) 337-342

Horowitz Y S, Moscovitch M and Wilt M, Computerized Glow Curve Deconvolution Applied to Ultralow Dose LiF Thermoluminescence Dosimetry, Nuclear Instrument and Methods in Physics Research A 244 (1986) 556-564

Horowitz Y S, Editorial – Fading in LiF: Mg, Ti, Radiation Protection Dosimetry, 32 (1990) 147

Horowitz Y S and Yossian D, Computerised glow curve deconvolution: Application to thermoluminescence Dosimetry, Radiation Protection Dosimetry 60 (1995) 1-114

Horowitz Y S, Thermoluminescence and thermoluminescent dosimetry, CRC Press Inc. (2000), Florida

Horowitz Y S and Moscovitch M, Highlights and Pitfalls of 20 Years of Application of Computerised Glow Curve Analysis to Thermoluminescence Research and Dosimetry, Radiation Protection Dosimetry 153 (2013) 1-22

Huntley D J, An explanation of the power-law decay of luminescence, Journal of Physics Condensed Matter 18 (2006) 1359-1365

Huzimura R, Asahi K and Takenaga M, An ESR Study of Thermoluminescent Processes in $CaSO_4$ Phosphors, Nuclear Instruments and Methods 175 (1980) 8-9

ICRP, Principles for handling emergency and Accidental Exposures of Workers, Publication 28, Annals of ICRP 2 (1) (1978), Oxford

Ingham J D and Lawson D D, Thermoluminescence, potential applications in forensic Science, Journal of Forensic Science 18 (1973) 217-225

Isukapalli S S, Ph.D Thesis, Uncertianty analysis of transport transformation models (1999), New Jersey

Jain M, Guralnik B and Andersen M T, Stimulated luminescence emission from localized recombination in randomly distributed defects, Journal of Physics D: Applied Physics 24 (2012) 385402

Joentgen A, Mikenina L, Weber R, Zeugner A and Zimmermann H J, Automatic fault detection in gearboxes by dynamic fuzzy data analysis, Fuzzy sets and systems 105 (1999) 123-132

Johnson P D and Williams F E, Energy Levels and Rate Processes in the Thallium Activated Potassium Chloride Phosphor, Journal of Chemical Physics 20 (1952) 124-128

Jonscher A K and de Polignac A, The time dependence of luminescence in solids, Journal of Physics C: Solid State Physics 17 (1984) 6493-6519

Kazakis N A, Tldecoxcel: a dynamic excel spreadsheet for the computerized curve deconvolution of TL glow curves into discrete energy and/or continuous energy distribution peaks, Radiation protection dosimetry 187 (2019) 154-163

Kao K C and Hwang W, Electrical Transport in Solids, Pergamon Press (1981), Oxford

Karmakar M, Bhattacharyya S, Sarkar A, Mazumdar P S and Singh S D, Analysis of Thermoluminescence Glow Curves Using Derivatives of Different Orders, Radiation Protection Dosimetry 175 (2017) 493-502

Keating P N, Thermally Stimulated Emission and Conductivity Peaks in Case of Temperature Dependent Trapping Cross Section, Proceeding of Physical Society 78 (1961) 1408-1415

Kelly P and Braunlich P, Phenomenological Theory of Thermoluminescence, Physical Review B 1 (1970) 1587-1595

Kelly P, Laubitz M J and Braunlich P, Exact solutions of kinetic equations governing Thermally Stimulated Luminescence and Conductivity, Physical Review B, 4 (1971) 1960-1968

Kieffer F, Meyer C and Rigaut J, Is isothermal deferred luminescence in organic glasses due to electron tunnelling? Chemical Physics letters 11 (1971) 359-361

Kiisk V, Deconvolution and simulation of thermoluminescence glow curves with Mathcad, Radiation Protection Dosimetry 156 (2013) 261-267

Kirkpatrick S, Gelatt C D and Vecci M P, Optimization by simulated annealing, Sci. New Ser. 220 (1983) 671-680

Kitis G, Gomez-Ros J M and Tuyn J W N, Thermoluminescence glow-curve deconvolution functions for first, second and general orders of kinetics, Journal of Physics D: Applied Physics 31 (1998) 2636-2641

Kitis G and Gomez Ros J M, Thermoluminescence glow-curve deconvolution functions for mixed order of kinetics and continous trap distribution, Nuclear Instruments and Methods in Physics Research A 440 (2000) 224-231

Kitis G, Chen R, Pagonis V, Carinou E and Kamenopoulou V, Thermoluminescence under exponential heating function: I. Theory, Journal of Physics D: Applied Physics, 39 (2006) 1500-1507

Kitis G, Chen R, Pagonis V, Carinou E, Ascounis P and Kamenopoulou V, Thermoluminescence under exponential heating function: II. Glow curve deconvolution of experimental glow curve, Journal of Physics D: Applied Physics, 39 (2006) 1508-1514

Kitis G, Carinou E and Askounis P, Glow-curve-de-convolution analysis of TL glow-curve from constant temperature hot gas TLD reader, Radiation Measurements 47 (2012) 258-265

Kitis G and Vlachos N D, General semi analytical expression for TL, OSL and other luminescence stimulation modes derived from OTOR model using Lambert W function, Radiation Measurements 482 (2013) 47-54

Kitis G and Pagonis V, Analytical solution for stimulated luminescence emission from tunnel recombination in random distribution of defects, Journal of luminescence 137 (2013) 109-115

Kitis G and Pagonis V, Localized transition models in luminescence: a reappraisal, Nuclear instruments and methods in Physics Research B 432 (2018) 13-19

Kitis G, Polymeris G S and Pagonis V, Stimulated luminescence emission: From phenomenological models to master analytical equations, Applied Radiation and Isotopes 153 (2019) 108797

Kittel C, Introduction to Solid State Phys., John Wiley(1953), New York

Klasens H A, Transfer of Energy Between Centres in Zinc Sulphide Phosphors, Nature 158 (1946) 306-307

Koza J R, Genetic Programming, On the programming of computers by means of natural selection, The MIT Press (1992), Cambridge

Kumar M, Kher R K, Bhatt B C and Sunta C M, Thermally stimulated luminescence arising simultaneously from localized and delocalized recombination processes, Journal of Physics D: Applied Physics 39 (2006) 2670-2679

Lakshmanan A R, Chandra B and Bhatt R C, Gamma Radiation Induced Sensitization in $CaSO_4$: Dy TLD Phosphor, Nuclear Instruments and Methods 153 (1978) 581-588

Lakshmanan A R, Bhatt R C and Supe S J, Mechanism of nonlinearity in response characteristics of thermoluminescent dosimeter, Journal of Physics D.: Applied Physics 14 (1981) 1683-1706

Lakshmanan A R, Mechanism of non linearity in the response characteristics of thermoluminescence dosimeter: a further comment, Journal of Physics D: Applied Physics 15 (1982) L189-L193

Lakshmanan A R, Shinde S S and Bhatt R C, A Comparative Study of some $CaSO_4$ Thermoluminescent Phosphors for Radiation Dosimetry, Radiation Protection Dosimetry, 16 (1986) 237-241

Lakshmanan A R, Shinde S S, Bhatt R C and Supe S J, Grain size and Dy Concentration Effect in Thermoluminescent $CaSO_4$: Dy Radiation Protection Dosimetry 22 (1988) 173-177

Lakshmanan A R, Photoluminescence and thermostimulated luminescence processes in rare-earth-doped $CaSO_4$ phosphors, Progress in Material Science 44 (1999) 1-187

Lampert M A and Mark P, Current injections in Solids, Academic Press (1970), New York

Land P L, Equations for thermoluminescence and thermally stimulated current as derived from simple models, Journal of physics and chemistry of solids 30 (1969) 1693-708

Lapraz D, Goyet D, Gerome V, Iacconi P, Prevost H, Gasiot J and Baumer A, UV emissions in thermostimulated luminescence of $CaSO_4$: Dy^{3+}. Influence of host $CaSO_4$ lattice, Dy^{3+} concentration, and TM^{3+} codoping, physica status solidi 153 (1996) 239-247

Lawrence P W, Corless R M and Jeffrey D J, Algorithm 917: Computer double precision evaluation of Wright ω function, ACM Trans. Math. Softw. 38 (2012) 1-17

Lax M, Sascade Capture of Electrons in Solids, Physical Review 119 (1960) 1502-1504

Levenberg K, A method for the solution of certain non-linear problems in least squares, Quarterly of Applied Mathematics 2 (1944) 164-168

Levy P W, Thermoluminescence Kinetics in Material Exposed to the Low Doses Applicable to Dating and Dosimetry, Nuclear tracks and Radiation measurement 10 (1985) 547-556

Levy P. W. in The Encyclopedia of physics, 2nd edition, VCH Publication Inc. (1991), New York 1264

Lewandowski A C and Mckeever S W S, Generalized description of thermally stimulated processes without the quasiequilibrium approximation, Physical Review B, 43 (1991) 8163-8178

Lewandowski A C, Markey B G and Mckeever S W S, Analytical description of thermally stimulated luminescence and conductivity without quasiequilibrium approximation, Physical Review B 49 (1994) 8029-8047

Llamas H F and Tapia C G, Thermoluminescence glow curve deconvolution function by continued fraction for different order of kinetics, Radiation Effects and defects in solids 168 (2013) 48-60

Mandowski A, Semi localized transitions model for thermoluminescence, Journal of Physics D: Applied Physics 38 (2005) 17-21

Marquardt D W, An algorithm for Least-Squares Estimation of Nonlinear Parameters, Journal of the Society for Industrial and Applied Mathematics, 11 (1963) 431-441

Mathews P M and Venkatesan K, A textbook of Quantum Mechanics, Tata Mcgraw Hill (1976), New Delhi

Mathews R J and Stoebe T G, Thermoluminescent spectra and optical absorption in CaSO4: Dy, Journal of Physics C: Solid State Physics 15 (1982) 6271-6280

Maxia V, Nonequilibrium thermodynamics of the thermoluminescent process, Physical Reviwe B, 17 (1978) 3262-3268

Maxia V, Nonequilibrium thermodynamics of luminescent processes in solids, Physical Reviwe B, 21 (1980) 749-759

May C E and Partridge J A, Thermoluminescence kinetics of Alpha-Irradiated Alkali Halides, Journal of Chemical Physics 40 (1964) 1401-1409

Mcdougall D J, Thermoluminescence of geological material, Academic Press (1968), New York

Mckeever S W S, Thermoluminescence of solids, Cambridge University Press (1983), Cambridge

Mckeever S W S, Rhodes J F, Mathur V K, Chen R, Brown M D and Bull R K, Numerical solutions to the rate equations governing the simultaneous release of electrons and holes during thermoluminescence and isothermal decay, Physical Review B 32 (1985) 3835-3843

Mckeever S W S, Markey B G and Lewandowski A C, Fundamental Processes in the Production of Thermally Stimulated Luminescence, Nuclear Tracks and Radiation Measurements 21 (1993) 57-64

Mckeever S W S and Chen R, Luminescence models invited review paper, Special issue on luminescence dating, Radiation Measurements 27 (1997) 625-661

Mckinley A F, Bartlett D T and Smith P A, The development of photo-transferred (PTTL) technique and its application to routine re-assessment of absorbed dose in NRPB automated personal dosimetry system, Nuclear Instruments and Methods 175 (1980) 57-59

McLachalan G J and Krishnan T, The EM algorithm and Extensions, Wiley (1997), New York

McLachlan G and Peel D, Finite mixture models, John Wiley and sons Inc. (2004), USA

Medlin W L, Decay of Phosphorescence from a Distribution of Trapping levels, Physical Review 123 (1961) 502-509

Misra S K and Eddy N W, IFOM, a formula for universal assessment of goodness-of-fit of gamma ray spectra, Nuclear Instruments and Methods 166 (1979) 537-540

Mohan N S and Chen R, Numerical curve fitting for calculating glow parameters, Journal of physics D: Applied Physics (1970) 3 243-247

Morgan M D and Stoebe T G, Optical absorption and luminescent processes in thermoluminescent $CaSO_4$: Dy, Journal of Physics: Condensed Matter 1 (1989) 5773-5781

Moscovitch M, Horowitz Y S and Oduko J, LiF Themoluminescence Dosimetry via Computerised First Order Kinetics Glow Curve Analysis, Radiation Protection Dosimetry 6 (1984) 157

Moscovitch M, Automatic Method for Evaluating Elapsed Time Between Irradiation and Readout in Lif-TLD, Radiation Protection Dosimetry 17 (1986) 165-169

Moscovitch M, Kaufman M M, Rodgers J E and Niroomand-Rad A, Ultra-Low Dose (100 nGy – 100 μGy) Response of Alfa-Al_2O_3: C, Radiation Protection Dosimetry 47 (1993) 173-176

Mott N F and Gurney R W, Electronic processes in ionic crystals, 2^{nd} edition, Oxford University Press (1948), London

Mott N F and Davies E A, Electronic processes in non crystalline material, 2^{nd} edition, Clarendon Press (1979), Oxford

Murthy K B S, Ph.D thesis, University of Gujarat, BARC, Mumbai (1982)

Nambi K S V, Bapat V N and Ganguly A K, Thermoluminescence of $CaSO_4$ doped with rare earth, Journal of Physics C: Solid State Physics 7 (1974) 4403-4415

Nambi K S V, Thermoluminescence: Its understanding and applications (1977), Brasil

Nambi K S V and Bapat V N, Valency conversions in rare-earth ions of gamma irradiated $CaSO_4$ phosphors, Journal of Physics C: Solid State Physics 13 (1980) 1555-1557

Oatley D, Hudson G and Plato P, Projected Response of Panasonic Dosimeters to Submersion in and Distant Exposure by 133Xe, Health Physics 41 (1981) 513-525

Oliveri E, Fiorella O and Mangia M, High dose behaviour of $CaSO_4$: Dy thermoluminescence phosphors as deduced by continous model for trap depths, Nuclear instruments and methods 154 (1978) 203-205

Opanowicz A, On the kinetic order of thermoluminescence in insulating crystals, physica status solidi (a) 116 (1989) 343-348

Opanowicz A, Effect of initial trap occupancy on thermoluminescence characteristics of insulating crystal, physica status solidi (a) 130 (1992) 207-217

Pagonis V, Mian S M and Kitis G, Fit of First Order Thermoluminescence Glow Peaks using the Weibull Distribution Function, Radiation Protection Dosimetry 93 (2001) 11-17

Pagonis V and Kitis G, Fit of second order Thermoluminescence glow peaks using the logistic distribution function, Radiation Protection Dosimetry 95 (2001) 225-229

Pagonis V, Kitis G, On possibility of using commercial software packages for thermoluminescence glow curve deconvolution analysis, Radiation Protection Dosimetry 101 (2002) 93-98

Pagonis V, Evaluation of activation energies in the semi localized transition model of thermoluminescence, Journal of Physics D: Applied Physics 38 (2005) 2179-2186

Pagonis V, Kitis G and Furetta C, Numerical and Practical exercises in thermoluminescence, Springer (2006), USA

Peng J, Dong Z and Han F, tgcd: An R package for analyzing thermoluminescence glow curves, SoftwareX (2016) 112-120

Peng J, Kitis G, Sadek A M, Asal E C K and Li Z, Thermoluminescence glow curve deconvolution using analytical expressions: A unified presentation, Applied Radiation and Isotopes 168 (2021) 109440

Piesch E, Applied thermoluminescence dosimetry, (1981), Adam Hilger, Bristol

Pla C and Podgorsak E B, A computerized TLD system, Medical Physics 10 (1983) 462-466

Puchalska M and Bilski P, GlowFit – a new tool for thermoluminescence glow curve deconvolution, Radiation Measurements 41 (2006) 659-664

Randall J T and Wilkins M H F, Proceedings of Royal Society London 184 (1945a) 366-389

Randall J T and Wilkins M H F, Proceedings of Royal Society London 184 (1945b) 390-407

Rasheedy M S, On the general-order kinetics of the thermoluminescence glow peak, Journal of Physics: Condensed Matter 5 (1993) 633-636

Reddy S S, Chauhan N, Nagabhushana K R and Singh F, TL/OSL properties of beta irradiated Al2O3: Tm3+ phosphor synthesized by microwave combustion method, Material Research Bulletin, 104 (2018) 236-243

Rickayzen G, On the theory of the thermal capture of electrons in semi-conductors, Proceedings of Royal Society of London (1957) 480-494

Riehl N, Tunnel Luminescence and Infrared Stimulation, Journal of Luminescence 1-2 (1970) 1-16

Rudlof G, Becherer J and Glaefeke H, Behaviour of fractional glow technique with first-order detrapping processes, trap distribution in energy or frequency factor, physica status solidi (a) 49 (1978) K121-K124

Sadek A M, Eissa H M, Basha A M and Kitis G, Development of peak fitting and peak shape methods to analyse thermoluminescence glow curves generated with exponential heating function, Nuclear Instruments and methods in Physics Research B 330 (2014) 103107

Sadek A M, Eissa H M, Basha A M and Kitis G, Properties of thermoluminescence glow peaks simulated by interactive multiple trap system (IMTS) model, Physics Status Solidi B 252 (2014) 721-729

Sadek A M, Eissa H M, Basha A M, Carinou E, Askounis P and Kitis G, The deconvolution of thermoluminescence glow-curve using general expression derived from one trap-one recombination (OTOR) level model, Applied radiation and isotopes 95 (2015) 214-221

Sadek A M and Kitis G, A critical look at the kinetic parameter values used in simulating the themoluminescence glow curve, Journal of luminescence 183 (2017) 533-541

Sahai M K, Bakshi A K and Datta D, Study of Residual TL of $CaSO_4$: Dy-Based Thermoluminescence Dosimeter, Radiation Protection Dosimetry 177 (2017) 342-347

Sahai M K, Bakshi A K and Datta D, Revisit to power law decay of luminescence, Journal of luminescence 195 (2018) 240-246

Sahai M K, Bakshi A K and Datta D, Anomalous fading correction for dosimetry at small time scales, Radiation Physics and Chemistry 158 (2019) 137-142

Sakurai T, A new method for numerical analysis of thermoluminescence glow curves, Journal of physics D: Applied physics 28 (1995) 2139-2143

Sammaknejad N, Zhao Y and Huang B, A review of the Expectation Maximization algorithm in data-driven process identification, Journal of Process Control 73 (2019) 123-136

Sature K R, Patil B J, Dahiwale S S, Bhoraskar V N and Dhole S D, Development of computer code for deconvolution of thermoluminescence glow curve and DFT simulation, Journal of luminescence 192 (2017) 486-495

Saunders I J, The thermally stimulated luminescence and conductivity of insulators, Journal of Physics C: Solid State Physics 2 (1969) 2181-2198

Schmidt K, Linemann H and Giessing R, Proceedings of 4th International Conference on Luminescence Dosimetry (1974) Krakow

Schon M, Z. Physik 119 (1942) 463-471

Seitz F, Modern theory of solids, McGraw-Hill (1940), New York

Shenker D. And Chen R, Numerical curve fitting of general order kinetics glow peaks, Journal of physics D: Applied physics (1971) 4 287-291

Shenker D and Chen R, Numerical Solution of Glow Curve Differential Equations, Journal of Computational Physics, 10 (1972) 272-283

Shinde S S and Shastry S S, Relative Thermoluminescence Response of $CaSO_4$: Dy to Alpha and Gamma Rays, International Journal of Applied Radiation and Isotopes 30 (1979) 75-78

Shinde S S, Lakshmanan A R, Bhatt B C and Bhatt R C, Photo Transfer Thermoluminescence in CaSO4: Dy – Grain size effect, Nuclear Instruments and Methods in Physics Research B 31 (1988) 592-596

Sidran M, Proceedings of 2nd International Conference of Luminescence Dosimetry, Gatlinburg (1969) 883

Singh T B, Rey L and Gartia R K, Application of PeakFit software in thermoluminescence studies, Indian Journal of pure and applied physics 49 (2011) 297-302

Singh L L and Gartia R K, Theoretical derivation of a simplified form of the OTOR/GOT differential equation 59 (2013) 160-164

Singh L L and Gartia R K, Glow curve deconvolution of thermoluminescence glow curves in the simplified OTOR equation using Hybrid Genetic Algorithm, Nuclear Instruments and Methods in Physics Research B 319 (2014) 39-43

Singh L L and Gartia R K, Derivation of a simplified OSL OTOR equation using Wright Omega function and its applications, Nuclear Instruments and Methods in Physics Research B 346 (2015) 45-52

Souza J H, da Rosa L A R and Mauricio C L P, On the Themoluminescence Glow Curve of $CaSO_4$: Dy, Radiation Protection Dosimetry 47 (1993) 103-106

Sprunck M, Regulla D and Fill U, TL measurements with computerized glow curve analysis in clinical dosimetry, Radiation Protection Dosimetry 66 (1996) 269-271

Srivastava J K, and Supe S J, Gamma radiation induced changes in the glow curve of $CaSO_4$: Dy tld phosphor, Radiation Effects 45 (1979) 13-18

Srivastava J K, and Supe S J, Thermoluminescence processes in $CaSO_4$: Dy. Dependence on stopping power, Journal of Physics D: Applied Physics 13 (1980) 2337

Srivastava J K, and Supe S J, Trap distribution analysis for thermoluminescence of $CaSO_4$: Dy, Journal of physics D: Applied Physics 16 (1983) 1813-1818

Srivastava J K, Supe S J and Bhatt R C, Reversible and Irreversible Effect of γ and α Radiation Damage on Thermoluminescence of $CaSO_4$: Dy, Phys. Stat. Sol. (a) 124 (1991) 401-416

Srivastava J K, Bhatt B C and Supe S J, Thermoluminescence Characteristics of $CaSO_4$ doped with Dy and Cu, Radiation Protection Dosimetry 40 (1992) 271-274

Stadmann H and Wilding G, Glow curve deconvolution for routine readout of LiF: Mg, Ti thermoluminescent detector, Radiation measurements 106 (2017) 278-284

Stoebe T G and Morgan M D, In Horowitz Y S Editor, Thermoluminescence and thermoluminescence Dosimetry, CRC (1984), New York

Sunta C M, Kumar M, Kher R K and Bhatt B, Thermoluminescence emission from localized recombination model, Journal of Physics D: Applied Physics 39 (2006) 4557-4562

Tachiya M and Mazumdar A, Kinetics of geminate-ion recombination by electron tunnelling, Chemical Physics Letters 34 (1975) 77-79

Tatake V G, Proceedings of national symposium on thermoluminescence and its applications, Kalpakkam, (1975) 262

Thomas D G, Hopfield J J and Augustyniak W M, Kinetics of Radiative Recombination at Randomly Distributed Donors and Acceptors, Physical Review 140 (1965) A202-A220

Tomita A and Tsutsumi K, Emission Spectra of Thermoluminescence in $CaSO_4$, Japanese Journal of Applied Physics, 17 (1978) 453-454

Tyler S and Mckeever S W S, Anomalous fading of thermoluminescence in oligoclase, International Journal of Radiation Applications and Instrumentation. Part D. Nuclear Tracks and Radiation Measurements 14 (1988) 149-154

van Laarhoven P J M and Aarts E H L, Simulated Annealing: Theory and applications, Reidel Publishing Company (1987), Dordrecht

van Dijk J W E and Julius H W, Glow Curve Analysis for Constant Temperature Hot Gas TLD Readers, Radiation Protection Dosimetry 47 (1993) 479-482

van Dijk J W E, Thermoluminescence glow curve deconvolution and its statistical analysis using the flexibility of spreadsheet programs 119 (2006) 332-338

Vana N, Schoner W, Fugger M, and Akatov Y, Absorbed Dose Measurement and LET Determination with TLDs in Space, Radiation Protection Dosimetry 66 (1996) 145-152

Visocekas R, Ceva T, Marti C, Lefaucheux F and Robert M C, Tunneling processes in afterglow of calcite, physica status solidi (a) 35 (1976) 315-327

Visocekas R, Nuclear Tracks and Radiation Measurements, Tunnelling Radiative recombination in labradorite: Its association with anomalous fading of luminescence 10 (1985) 521-529

Visocekas R, Comparision between tunnelling afterglows following alpha or beta irradiations, International Journal of Radiation Applications and Instrumentation. Part D. Nuclear Tracks and Radiation Measurements, 14 (1988) 163-168

Visocekas R, Spooner N A, Zink A and Blank P, Tunnel afterglow, fading and infrared emission in thermoluminescence of feldspars, Radiation Measurement 23 (1994) 371-385

Wang T K, Hsu P C, Weng P S, Feasibility Study of Using $CaSO_4$: Dy Phosphor for Simulation Estimation of Exposure and Time Elapsed Post-Exposure, Radiation Protection Dosimetry 18 (1987) 157-161

Watanabe S, Properties of a CaSO4: Mn Phosphor under Vacuum Ultraviolet Excitation, Phys. Rev. 83 (1951) 785-791

Wiener N, The Homogeneous Chaos, American J. Of Mathematics 60 (1938) 897-936

Wright E M, Solution of the equation $ze^z = a$, Bulletin of American Mathematical Society 65 (1959) 89-93

Xiu D and Karniadakis G M, The Wiener—Askey polynomial chaos for stochastic differential equations, Society for Industrial and Applied Mathematics 24 (2002) 619-644

Zadeh L A, Fuzzy Sets, Information and control 8 (1965) 338-353

Zettili N, Quantum mechanics: Concepts and applications, John Wiley (2001), New York

Thesis Highlight

Name of the Student: Manish Kumar Sahai
Name of the CI/OCC: Bhabha Atomic Research Centre **Enrolment No.: PHYS01201604010**

Thesis Title: Uncertainty modeling of thermoluminescence glow curve and development of deconvolution technique to resolve TL peak

Discipline: Physical Sciences **Sub-Area of Discipline:** Thermoluminescence

Date of viva voce: 05/02/2021

The phenomenon of themoluminescence (TL) is emission of light when a pre exposed sample is given thermal stimulus. On exposure charge carriers (electron hole pairs) are generated. While translating in delocalized energy levels, small fraction of them is trapped in defect centers. Sample stays in this meta stable state for fairly long period of time depending upon material parameters. On getting thermal stimulus trapped charge carriers are excited to respective delocalized energy levels. Further, while moving in delocalized energy levels eventually recombine with opposite charge carrier trapped at defect centers and produce luminescence. Figure (left, top) gives the figure of basic apparatus for recording TL. Figure (left, bottom) illustrates the mechanism explained.

But if trapping sites of charge carrier and recombination centers are spatially close, phenomenon of tunneling is possible due to which we may get continuous signal since exposure. This is called afterglow. The phenomenon of afterglow is known to follow power law decay with exponent ranging from 0.5 to 2.0. The full range of exponent could not be explained theoretically, region behind, the problem was always approached with a rectangular potential barrier between trap and recombination center. We considered non rectangular potential barrier between trap and recombination center and successfully explained full experimental range of exponent. The final expression we obtained for TL phenomenon can be broken into time dependent (G2) and time independent (G1) parts. The time dependent part translates on the time independent part as shown in figure (right, (A) and (B)). Using this we could explain the non linearity in afterglow. Figure (right, (C) and (D)) are spatial integration of figure (right, (A) and (B) respectively) and figure (right, (E) and (F)) illustrates the afterglow shapes in the respective cases.

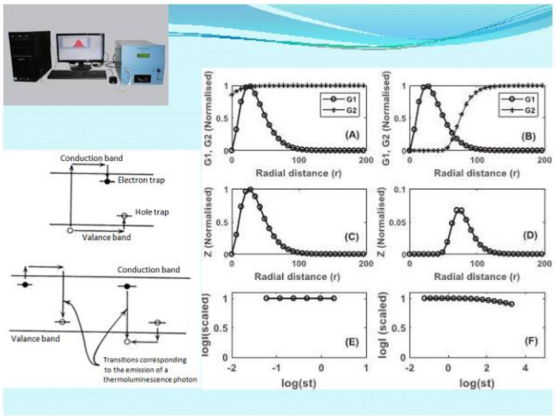

Figure 1. Basic TL apparatus (left, top); Mechanism of TL (left, bottom); Explanation of non linearity in afterglow (right)

The parametric uncertainty analysis of these models is a gray area in TL literature. We tried to throw light on this area in this dissertation and established that the Temperature vs. uncertainty graph for basic delocalized TL model has a typical shape with two peaks. The typical shape is independent of parameters in the model and the uncertainty in them.

Further, a realistic material will never have one trap and one recombination site. There will be multiple sites and hence the experimental TL signal will be a convolution of TL from single sets. Hence, it is interesting to develop and new methodology to deconvolve the composite TL signal. It is mandatory for understanding the phenomenon and extracting various benefits out of the phenomenon. We developed a mixture model and Bayes' theorem based methodology for the deconvolution of TL signal.